ISSN 2463-6029 (Print)
ISSN 2350-3432 (Online)

Modifying hydrological regime and catchment land use to improve water quality in Lake Waikare: Modelled insights

ERI REPORT NUMBER 174

by

Matthew J. Prentice and Deniz Özkundakci

A client report prepared for

Waikato Regional Council

2025

Environmental Research Institute – Te Tumu Whakaora Taiao
Division of STEM,
University of Waikato, Private Bag 3105,
Hamilton 3240, New Zealand

THE UNIVERSITY OF WAIKATO
Te Whare Wānanga o Waikato

Te Tumu Whakaora Taiao
Environmental
Research Institute
THE UNIVERSITY OF WAIKATO

Cite report as:

Prentice M.J., & Özkundakci D. 2025. Modifying hydrological regime and catchment land use to improve water quality in Lake Waikare: Modelled insights. ERI Report 174, a client report prepared for Waikato Regional Council. Environmental Research Institute – Te Tumu Whakaora Taiao, Division of STEM, University of Waikato, Hamilton, New Zealand. 66 pp. DOI: doi.org/10.15663/ERI.Report.174, ISSN 2463-6029 (Print), ISSN 2350-3432 (Online)

Cover picture:

Lake Waikare by David Schmale III, Viginia Tech, USA.

Reviewed by:

Grant Tempero

Senior Research Officer

University of Waikato

Approved for release by:

Charles Lee

Director

Environmental Research Institute

EXECUTIVE SUMMARY

Effective management of eutrophication in large, shallow, lakes is particularly challenging, especially in catchments dominated by agricultural activities. These challenges are further exacerbated in lakes that have undergone significant hydrological and biogeochemical modification. In these systems, effective hydrological management strategies may involve increasing discharge rates to promote flushing and modifying lake depth to reduce the effects of wind-induced sediment resuspension, while effective biogeochemical modification may involve improving catchment management practices to reduce external nutrient loading. In this study, we present a modelling investigation of Lake Waikare, Waikato, New Zealand; a large (surface area: 34 km^2), shallow (mean depth: 1.2 m), hypereutrophic lake that has experienced significant hydrological modification and water quality deterioration since the early 1900s.

We applied a process-based modelling approach to investigate the effects of changes in the hydrodynamic regime, both in isolation and in combination with hypothetical catchment land use changes, on water quality in Lake Waikare. Specifically, the study explored scenario simulations involving altered lake level dynamics, changes in Te Onetea inflow discharge rate, and modifying catchment nitrogen (N) and phosphorus (P) loading, thus enabling a better understanding of the potential trade-off between existing flood protection measures and hypothetical water quality remediation efforts resulting from changes in lake hydrology and catchment loading. A further aim was to support the identification of adaptive management strategies that could help mitigate potential conflicts and maximise the overall benefits to both Lake Waikare and the broader flood protection scheme. To achieve this, we configured and calibrated a three-dimensional coupled hydrodynamic-ecological model (Aquatic Ecosystem Model 3D; AEM3D) of the lake, incorporating two phytoplankton groups and suspended solid classes, and simulated twelve scenarios over a four-year period, from July 2017 through June 2021.

The twelve scenarios investigated in this study revealed that no simulated management strategy for Lake Waikare, whether implemented individually or in combination, led to improvements in water quality exceeding 26% for total N, 29% for total P, 33% for Secchi disk depth, and 6% for chlorophyll *a*. However, given the hypertrophic nature of the lake, such improvements are by no means trivial and equate to reductions of up to 0.810 mg L^{-1} for TN, 0.034 mg L^{-1} for TP, 5.3 µg L^{-1} for chlorophyll *a*, and improvements of 0.07 m for Secchi disk depth. Among the management measures applied individually, hydrological modification by raising the minimum and maximum lake levels produced the greatest overall improvement in water quality. This benefit was further enhanced when combined with reducing catchment nutrient loading and maximising Te Onetea inflow discharge rate. Additionally, scenario testing helped to demonstrate the relative influence of the hydrological regime and catchment land use as key drivers of water quality decline, thereby supporting the identification of more targeted management strategies. Notably, scenario testing revealed that broad-scale improvements in water quality, such as improved light conditions (i.e., increased Secchi disk depth) and small reductions in N and P concentrations, may promote a shift toward greater cyanobacterial dominance. These findings highlight the complexities of managing lakes that have been heavily modified both hydrologically and biogeochemically, and underscore the value of detailed modelling in guiding effective and informed management decisions.

TABLE OF CONTENTS

LIST OF TABLES

LIST OF FIGURES

LIST OF ABBREVIATIONS & ACRONYMS

AEM3D	Aquatic Ecosystem Model
CC	Cloud cover
DO	Dissolved oxygen
DOC	Dissolved organic carbon
DON	Dissolved organic nitrogen
DOP	Dissolved organic phosphorus
DRP	Dissolved reactive phosphorus
IN_{Cyan}	Cyanobacteria internal nitrogen
IN_{Oth}	Other-phytoplankton internal nitrogen
IP_{Cyan}	Cyanobacteria internal phosphorus
IP_{Oth}	Other-phytoplankton internal phosphorus
LWWFCS	Lower Waikato-Waipā Flood Control Scheme
MAE	Mean absolute error
N	Nitrogen
NH_4	Ammonium
NNN	Nitrate-Nitrite-Nitrogen
NO_3	Nitrate
P	Phosphorus
PO_4	Phosphate
POC	Particulate organic carbon
PON	Particulate organic nitrogen
POP	Particulate organic phosphorus
RMSE	Root mean squared error
SSOL1	Suspended Solids #1 (i.e., Clay)
SSOL1	Suspended Solids #2 (i.e., Silt)
SWR	Shortwave radiation
TN	Total nitrogen
TP	Total phosphorus
TSS	Total suspended solids
UoW	University of Waikato
VSS	Volatile suspended solids
WRC	Waikato Regional Council

1 INTRODUCTION

1.1 Project Scope

Waikato Regional Council (WRC) commissioned modelling and analysis of Lake Waikare to support management decisions aimed at improving water quality. Following initial discussions between WRC and University of Waikato (UoW) in August 2023, a project proposal presenting three modelling options was submitted. WRC selected the most comprehensive option: a fully calibrated and configured hydrodynamic-ecological model. This study is directed by the initial project understanding and objective and the most comprehensive option outlined in 'Modelling options with increasing complexity' of the Project Proposal dated 25 August 2023 (modified to past tense, and reflect the final outcome):

Project understanding and objective

WRC commissioned a hydrodynamic-ecological modelling project for Lake Waikare. The model was applied to inform implementation of lake management actions and to aid the development of achievable water quality targets for the lake, to in turn inform future policy formulation. WRC expected that halting the ongoing water quality decline in Lake Waikare and meeting aspirational community targets will be costly and challenging given its role in the wider Lower Waikato Basin flood protection scheme. A modelling approach was designed to provide the necessary insights and strategies to optimise resource allocation, prioritise interventions, and develop effective management plans that strike a balance between safeguarding the vital flood protection scheme and improving water quality in Lake Waikare.

We developed a 3D hydrodynamic-ecological model for Lake Waikare, to enable scenario testing aimed at identifying the most effective management interventions for improving water quality. Prior to scenario testing a workshop was convened with key staff at WRC to refine the desired set of interventions to be assessed and the metrics to be used to quantify the appropriateness of the interventions. Following the completion of the modelling scenarios an online meeting was convened between relevant parties at WRC and UoW to discuss the results and finalise the report.

The modelling project was guided by the following research questions:

1. How can the hydrodynamic water quality model effectively integrate data on nutrient loading, sediment dynamics, and hydrological processes to accurately simulate the interactions between the lake's water quality and its role within the Lower Waikato Basin flood protection scheme?
2. What are the most critical factors influencing the water quality decline in Lake Waikare, and how can the model be designed to simulate various management scenarios that address these factors while considering the cost implications and feasibility of achieving different water quality targets?
3. How can the developed model be used to evaluate trade-offs between flood protection measures and water quality remediation efforts, and what adaptive management strategies can be identified to mitigate potential conflicts and maximise the overall benefits to both Lake Waikare's ecosystem and the wider flood protection scheme?

Outcomes of this modelling project should provide WRC valuable insight into determining the most effective intervention(s) to effect an improvement in water quality in Lake Waikare. Project outcomes could feasibly be coupled with costings of the proposed interventions to inform the most cost-effective measures.

1.2 Background

Lake Waikare (37°26'08.5"S 175°12'00.7"E) is a large-shallow warm-polymictic lake in the lower Waikato region of New Zealand. The lake was once part of a hydraulically linked lake–wetland complex that included Lakes Kopuera, Ohinewai, Rotokawau, and the Whangamarino Wetland. Seasonal fluctuations in water levels of up to 2.71 m contributed to dynamic littoral habitats and periodically inundated marginal wetlands. While historical water quality data are limited, water quality inferred from historical accounts and regional comparisons with similar systems suggest a substantially less eutrophic state than that observed today.

Over the past 150 years, Lake Waikare has undergone a marked transition from a relatively natural, to a heavily modified, hypertrophic lake, driven by dramatic changes to its catchment land use and hydrological regime. Beginning in the 1860s, this involved drainage of much of the low-lying catchment area and subsequent conversion from native forested land to sheep farming land (Lawrence & Ridley, 2018). From the 1920s through the 1940s, this included conversion of much of the catchment's hill country land from native forested land to pine forested land (Lawrence & Ridley, 2018). Beginning in the 1920s, this was related to conversion of much of the low-lying sheep farming land to more intensive beef and cattle farming (Lawrence & Ridley, 2018). In 1982, following decades of flooding, and in particular the 1953, 1956, and 1958 events, this included the completion and full implementation of the Lower Waikato-Waipā Flood Control Scheme (LWWFCS) which resulted in the mean lake level being reduced by ~1 m and the lake level fluctuation being reduced from 2.71 m to 0.35 m (Reeves et al., 2002).

The aforementioned modifications have contributed to a substantial decline in water quality. Aerial photographs dating back to the 1940s suggest extensive land clearance and subsequent conversion in the Matahuru sub-catchment led to substantial increases in turbidity in the lake. Anecdotal reports note reduced water level fluctuation as a result of the LWWFCS led to the loss of approximately 840 ha of surrounding seasonally inundated wetland area, with broader estimates suggesting a 67% reduction in wetland extent since 1963 (Reeves et al., 2002). Anecdotal evidence also indicates additional and sustained turbidity in the lake is driven by resuspension of internal sediment stores derived from the catchment resulting from the reduced water level in the lake (dictated by the LWWFCS) which increased the effect of wind induced turbulence (Reeves, et al., 2002). These changes and their effect on light attenuation have been implicated as the primary driver for the decline in submerged aquatic vegetation in the lake (Reeves, et al., 2002), with a phytoplankton bloom in the late 1970s thought to have initiated the final collapse of the lake's already stressed submerged aquatic vegetation (Dean-Speirs et al., 2014).

Currently the lake is classified as hypereutrophic, reflecting extreme nutrient enrichment and persistent poor water quality. The lake has been listed among a suite of lakes across New Zealand that had lost all submerged vegetation by the late 1970s (first native species and later the exotic *Egeria densa*), with current elevated sediment resuspension and thus low light availability inhibiting macrophyte recovery (Lawrence & Ridley, 2018). In addition, populations of invasive benthic fish species such as catfish (*Ameiurus nebulosus*), koi carp (*Cyprinus rubrofuscus*), and rudd (*Scardinius erythrophthalmus*) now dominate the fish biomass in the lake (Dean-Speirs et al., 2014). These species are known to disrupt sediments, reduce water clarity, and exacerbate eutrophic conditions (Lawrence & Ridley, 2018). Moreover, the lake is so eutrophied, it has been suggested that flow derived from the Waikato River drives a reduction in turbidity through a flushing effect (Lawrence & Ridley, 2018).

Lake ecosystem models are highly parametrised numerical models which can simulate the interactions between various physical, chemical, and biological components within the system (Bruce et al., 2006). They may also be applied for scenario testing to better understand, project, and manage the systems response to hypothetical changes in forcing factors such as nutrient loadings, meteorology, and a variety of interventions. These numerical models typically take the form of a 1-dimensional (1-D) (e.g., General Lake Model; GLM; Hipsey et al., 2019) or 3-dimensional (3-D) (e.g., Aquatic Ecosystem Model; AEM3D; Hodges & Dallimore, 2018) hydrodynamic model which may or may not be coupled to an ecological model (or module; Hodges et al., 2000). Hydrodynamic models allow fine-resolution simulation of the temporal and spatial behaviour of physical properties (e.g., water density and temperature) in waterbodies subject to environmental forcing by inflows, outflows, surface heat fluxes, and wind stress (Hodges & Dallimore, 2018). In addition, these models when coupled to an ecological model allow for additional fine-resolution simulation of an array of chemical and biological variables, and an assessment of interactions amongst variables, for example, nutrients and phytoplankton dynamics (Chan & Hamilton, 2001). Consequently, when accurately configured and calibrated, these highly parameterised coupled hydrodynamic-ecological models present a powerful means to quantify the impact of various restoration and prevention measures, and in the case of this present study changes to the hydrological regime and catchment land use.

1.3 Aims and objectives

The aim of this study was to apply a process-based modelling approach to investigate the effects of changes in the hydrodynamic regime, both in isolation and in combination with hypothetical catchment land use changes on water quality in Lake Waikare. Specifically, the study sought to explore scenario simulations involving raising the lake water level, maximising Te Onetea inflow discharge rate, and reducing catchment nitrogen (N) and phosphorus (P) loading to better understand the potential of these interventions in supporting water quality remediation in the lake. This was accomplished through the configuration and calibration of a three-dimensional coupled hydrodynamic-ecological model (AEM3D) of Lake Waikare, followed by scenario testing.

2 STUDY SITE

Lake Waikare (37°26'08.5"S 175°12'00.7"E) is a large-shallow warm-polymictic lake in the Waikato, New Zealand (Figure 1). The climate of the region is temperate, with monthly median rainfall of ~80 mm in summer (December–February) and ~119 mm in winter (June–August) (Ruakura 2 Ews [26117], 2003–2023, NIWA, New Zealand). The lake has a direct catchment area of 210.5 km^2, including 106.3 km^2 as part of the Matahuru sub-catchment (River Environment Classification New Zealand, 2010). Catchment land use is primarily dry stock (predominantly sheep and beef) and dairy (Lawrence & Ridley, 2018). Inflow is primary from regulated flow from the Waikato River, via Te Onetea Stream, and unregulated flow via the Matahuru Stream. Inflow is also received from 24-plus minor tributaries and as treated wastewater from the Te Kauwhata Wastewater Treatment Plant (WWTP). Outflow is primarily via regulated release from the Northern Outlet Control Gate (NOCG), with unregulated release from an adjacent Fish Pass Culvert. These flows both enter the Pungarehu Canal which drains into the Whangamarino Wetland.

The lake operates as a flood storage reservoir, as part of the Lower Waikato-Waipa Flood Control Scheme (LWWFCS), and lake level (i.e., surface elevation) is strictly managed within a vertical range of ~0.3 metres (Lawrence & Ridley, 2018). At its median surface elevation (5.55 m Moturiki datum; from 1 January 2014 through 31 December 2023; WRC, unpub.), the lake has a volume of 38,460 ML, area of 34.56 km^2, and mean and maximum depths of 1.11 and 1.60 m, respectively. The lake's morphometry comprises a larger and marginally deeper northern basin (mean and max depths of 1.14 and 1.59 m, respectively; lake surface elevation at 5.55 m Moturiki datum) and smaller and marginally shallower southern basin (mean and max depths of 1.00 and 1.35 m, respectively). The lake intermittently diurnally stratifies throughout the year, with the majority of stratification events taking place during summer.

The lake is classified as hypertrophic, with mean total nitrogen (TN) concentration of 4.0±1.7 mg L^{-1}), total phosphorus (TP) concentration of 0.17±0.5 mg L^{-1}, chlorophyll *a* concentration of 176±139 µg L^{-1} and Secchi depth of 18±9 cm µg L^{-1} (mean ± standard deviation; 1 January 2014 through 31 December 2023; WRC, unpub.). The poor water clarity in the lake is a result of high absorption and scattering resulting from high concentrations of humic substances, inorganic sediment, and algal biomass (Lawrence & Ridley, 2018; Reeves et al., 2002). The lake is typically low in bioavailable N (dissolved inorganic N; DIN) and bioavailable P (dissolved reactive P; DRP), with mean concentrations of 0.153±0.326 mg L^{-1} (4.0% of TN) and 0.004±0.000 mg L^{-1} (2.7% of TP), respectively (1 January 2014 through 31 December 2023; WRC, unpub.). The phytoplankton community is dominated by chlorophytes, cyanobacteria, and diatoms, with mean biovolumes of 35.7, 25.0, 9.9 of mm^3 L^{-1}, respectively (mean; 1 January 2014 through 31 December 2023; WRC, unpub.). Dominant cyanobacteria species include *Planktolyngbya*, *Cylindrospermopsis*, *Limnothrix* and *Aphanizomenon*, of which some are also well-known toxin producers. The chlorophyte *Monoraphidium* sp. forms infrequent large-scale blooms that have attracted considerable media coverage and public concern since the first recorded event in autumn 2014. These blooms typically occur in late summer or early autumn and are characterised by the distinctive red appearance in the lake, attributed to zeaxanthin, one of the most common carotenoids in nature. While bloom events can be intense, they are often interspersed with several years of low *Monoraphidium* sp. abundance. Despite their visual prominence and public impact, the ecological drivers of bloom variability in Lake Waikare, and the broader ecology of *Monoraphidium* sp. within the Waikato lakes, remain poorly understood.

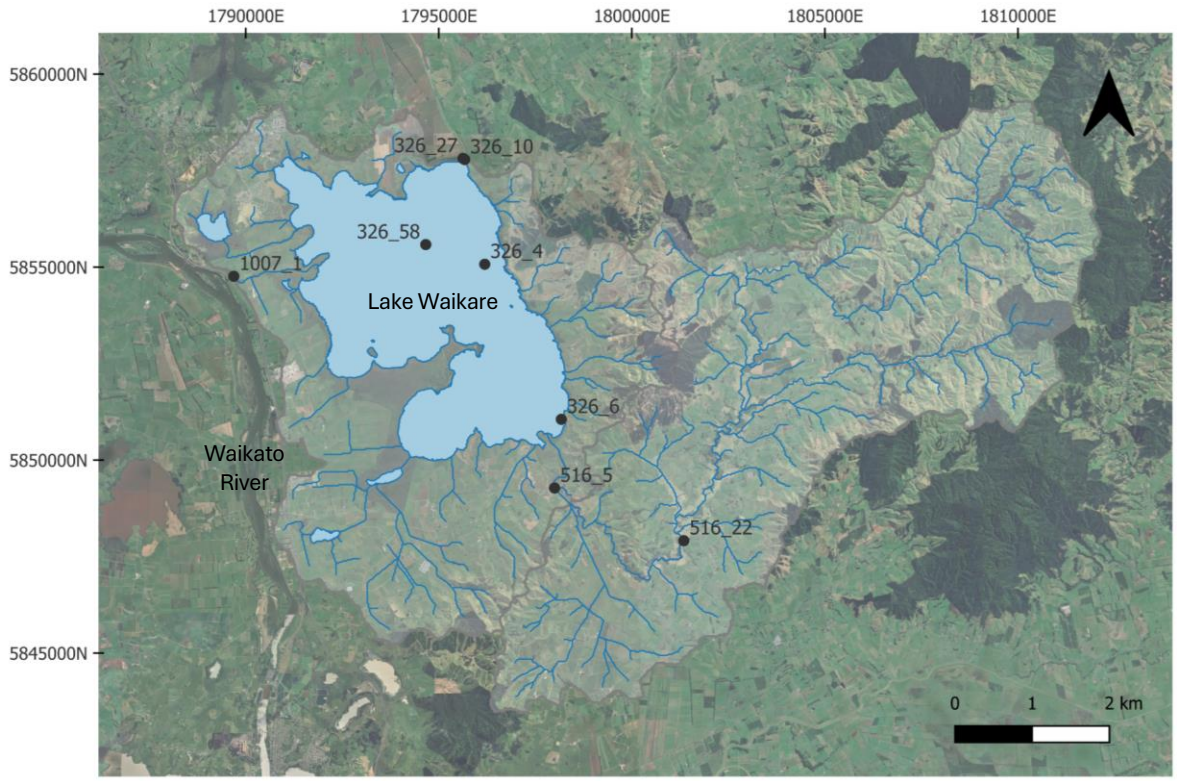

Figure 1: Lake Waikare study site. Lakes determined as shapefiles from Freshwater Ecosystems of New Zealand (FENZ) 'Lakes' November 2024; Catchment shapes (grey lines) generated from shapefiles from River Environment Classification Catchment Order 2–5 (2010); rivers determined as shapefiles from River Environment Classification New Zealand (2010). N.b. Te Onetea (1007_1) denotes the controlled inflow from and outflow to the Waikato River; Catchment separated Matahuru and non-Matahuru sub-catchments. For site descriptions see companion Table 1.

3 METHODS

3.1 Data sources

Bathymetric data were collected from a comprehensive bathymetric survey using depth soundings in 2014, by Discovery Marine Ltd. (Hydrographic & Coastal Management Services New Zealand). Surrounding topographical data were collected from a topographic survey using LIDAR in 2024, by Landpro Ltd. Water level measurements (326_6), for 1 May 2006 through 31 December 2023, were provided by WRC. Meteorological data, including air temperature, atmospheric pressure, rainfall, relative humidity, shortwave radiation (SWR), and wind speed and wind direction, for 1 May 2006 through 31 December 2023, were provided by The National Institute of Water and Atmospheric Research (NIWA), New Zealand, and MetService, New Zealand. Meteorological sites included NIWA Site 26117 (Ruakura 2 Ews; 1-h resolution), NIWA Site 2006 (Pukekohe Ews; 1-h resolution), MetService Site 1770 (Rotorua Aero Aws, 1-h resolution), and NIWA Virtual Climate Station Network (VCSN) Site 27116. In addition, air temperature, relative humidity, SWR, and wind speed and wind direction were generated from an onsite meteorological station (326_58) provided by WRC, this data however was inconsistent and patchy.

Table 1 Summary of WRC sampling sites applied in this study, including their application and sample resolution.

Location Key	Site name	Station name	Latitude	Longitude	Application (Resolution)
326_4	Lake Waikare	Epilimnion	-37.4304	175.2174	Water quality & Phytoplankton (~Monthly)
326_6	Lake Waikare	Lake Rd	-37.4662	175.2409	Water level (5-min)
326_10	Lake Waikare	Northern Outlet Control Gate (NOCG)	-37.4061	175.2108	Discharge (Daily)
326_27	Lake Waikare	Fish Pass Culvert	-37.4058	175.2103	Discharge (5-min)
326_58	Lake Waikare	Lake Waikare Buoy	-37.4261	175.2000	Meteorology (15-min); Water temp (15-min)
516_5	Matahuru Stm	Waiterimu Road Below Confluence	-37.4822	175.2394	Discharge (Daily)
516_22	Matahuru Stm	Myjers Farm Bridge	-37.4938	175.2776	Water quality (~Monthly)
1007_1	Te Onetea Stm	Rangiriri	-37.4346	175.1440	Discharge (Daily); Water quality – Event (Sub-daily)
1131_77	Waikato River	Huntly-Tainui Br	-37.5662	175.1543	Water quality (~Monthly)
1131_91	Waikato River	Mercer Br	-37.2813	175.0467	Water quality (~Monthly)
3021_2	Northern Outlet Canal	Farm Bridge	-37.3652	175.1837	Discharge (15-min)

Te Onetea Stream at Rangiriri (1007_1) and Matahuru Stream at Waiterimu Road Below Confluence (516_5) flow data for 1 January 2007 through 30 June 2023 were provided by WRC. Te Kauwhata WWTP (daily resolution) flow data for 1 July 2016 through 30 June 2020 were provided by WRC. Northern Outlet Control Gate flow data (326_10) for 1 January 2007 through 30 June 2023, and Northern Outlet Canal (a.k.a. Pungarehu Canal; 3021_2) for 22 October 2015 through 15 June 2023, were provided by WRC. Fish Pass Culvert flow data (326_27), for 1 July 2022 through 27 July 2023, were provided by WRC.

Waikato River at Huntly (1131_77), Waikato River at Mercer (1131_91), and Matahuru Stream at Myjers Farm Bridge (516_22) water quality data for 1 December 2006 through 31 July 2023 were provided by WRC. Te Kauwhata WWTP (~monthly resolution) water quality data (TN, TP, and TSS only) for 1 July 2016 through 30 June 2020 were provided by WRC. Water quality data for Matahuru,

Moana, Ohinewai, Onekura, Papaatawhai, and White streams (~fortnightly resolution), for 26 January 2017 through 12 January 2018, were provided by A. Hopkins (Unpub.). In addition, high resolution storm/event flow sampling of Matahuru Stream at Waiterimu Road Below Confluence (516_5; Hughes (2018)), capturing several events from 8 March 2017 through 8 September 2017, was provided by WRC.

In-lake water quality data (326_4) for 1 December 2006 through 31 July 2023, were provided by WRC. Water quality data included temperature, dissolved oxygen (DO), pH, specific conductivity, dissolved reactive P (DRP), TP, ammonium (NH_4), nitrate-nitrite-nitrogen (NNN), TN, turbidity, volatile suspended solids (VSS), total suspended solids (TSS), and chlorophyll *a*. Phytoplankton assemblage and count and biovolume data (with some gaps – notably three data points from January 2015 through June 2018) in Lake Waikare (326_4) for May 2006 through July 2023, were provided by WRC.

3.2 Modelling

3.2.1 Model description

The Aquatic Ecosystem Model (AEM3D; v 1.1.2; Hodges & Dallimore, 2018) was used to simulate the hydrodynamics in Lake Waikare. AEM3D is a 3-dimensional hydrodynamic-ecological model that simulates the temporal and spatial behaviour of stratified waterbodies subject to environmental forcing (inflows, outflows, surface heat fluxes, and wind stress). The 3-D nature of the AEM3D lends itself well to simulating complex spatially variable systems. The hydrodynamic module is based on the Estuary and Lake Computer Model (ELCOM) which has been applied to lakes from a range latitudes and markedly different morphometries (Chung et al., 2009; León et al., 2005; Romero et al., 2004). The model applies the unsteady Reynolds-averaged Navier-Stokes equations for incompressible flow, with a Boussinesq approximation for density differences and a hydrostatic assumption for pressure (Hodges et al., 2000). The hydrodynamic algorithms are based on the Euler-Lagrange method for advection of momentum, and a conservative ULTIMATE QUICKEST (Leonard, 1991) approach for active (e.g., temperature) and passive (e.g., tracer) scalar transport (Hodges et al., 2000; Romero et al., 2004).

3.2.2 Model set-up

The model was configured to run at a 100-m^2 horizontal grid and uniform 1-m vertical layer, on a 2-min timestep, in trade-off between model resolution and runtime. The hydrodynamic model was configured with a photosynthetic active radiation (PAR) extinction coefficient (Kd(PAR)) of 11 and near infrared radiation (NIR) extinction coefficient (Kd(NIR)) of 7.5. The full hydrodynamic-ecological model was configured with a base Kd(PAR) of 0.4, and base Kd(NIR) of 7.5 (as, unlike PAR, the ecological model does not consider the effect of particulates on NIR attenuation). In lieu of adequate data quantifying the particulate N and P fractions, the hydrodynamic-ecological model was configured to not simulate particulate inorganics or refractory particulate organics (i.e., only labile particulate organics). Consequently, particulate organic N and P can be considered particulate N and P. In addition, the hydrodynamic-ecological model was configured to include two phytoplankton groups, cyanobacteria (summer-adapted) and other (and other; winter-adapted), with growth and respiration functions for salinity, silica, and photoinhibition disabled for both groups. Atmospheric deposition of N and P was explicitly incorporated, made possible by its recent incorporation within the AEM3D model. Light, oxygen, N, P, and organic matter were parameterised as presented in Table 2, and the phytoplankton groups parameterised as presented in Table 3.

Table 2 Configuration of light, oxygen, nitrogen, phosphorus, and organic matter for the ecological model.

Parameter	Unit	Value
Light		
UVA base extinction coefficient	m^{-1}	1.5
UVB base extinction coefficient	m^{-1}	2.5
NIR base extinction coefficient	m^{-1}	7.5
PAR base extinction coefficient	m^{-1}	0.4
Oxygen		
DO sediment flux temperature multiplier	Dimensionless	1.05
DO sediment flux coefficient	g m^{-2} day^{-1}	2.25
DO sediment flux O_2 half-saturant constant	mg L^{-1}	0.25
Nitrogen		
Sediment parameters		
NH_4 sediment flux temperature multiplier	Dimensionless	1.05
NH_4 sediment flux coefficient	g m^{-2} d^{-1}	0.13
NH_4 sediment flux O_2 half-saturation constant	mg L^{-1}	1.0
NO_3 sediment flux temperature multiplier	Dimensionless	1.05
NO_3 sediment flux coefficient	g m^{-2} d^{-1}	-0.0
NO_3 sediment flux O_2 half-saturation constant	mg L^{-1}	2.75
Water-column parameters		
Nitrification temperature multiplier	Dimensionless	1.08
Nitrification coefficient	d^{-1}	0.1
Nitrification O2 half-saturation constant	mg L^{-1}	0.5
Denitrification temperature multiplier	Dimensionless	1.08
Denitrification coefficient	d^{-1}	0.08
Denitrification O2 half-saturation constant	mg L^{-1}	0.5
Mineralisation temperature multiplier	Dimensionless	1.08
Mineralisation coefficient	d^{-1}	0.08
Mineralisation O2 half-saturation constant	mg L^{-1}	1.5
Phosphorus		
Sediment parameters		
PO_4 sediment flux temperature multiplier	Dimensionless	1.05
PO_4 sediment flux coefficient	g m^{-2} d^{-1}	0.008
PO_4 sediment flux O_2 half-saturation constant	mg L^{-1}	1.0
Water-column parameters		
Mineralisation temperature multiplier	Dimensionless	1.08
Mineralisation coefficient	d^{-1}	0.03
Mineralisation O_2 half-saturation constant	mg L^{-1}	1.5
Organic matter (OM)		
OM density	kg m^{-3}	1050
OM diameter	m	1.25E-05
OM settling model	-	STOKES
OM critical shear	N m^2	2.00E-03
OM resuspension rate	g m^2 d^{-1}	4.00E-03
OM resuspension half-saturation	g m^2	1.0
Decomposition temperature multiplier	Dimensionless	1.08
Decomposition coefficient	d^{-1}	0.002
Decomposition O_2 half-saturation constant	mg L^{-1}	1.5
OM light attenuation	m^{-1}	0.02
Suspended Solids #1 – Clay (SSOL1)		
SSOL1 density	kg m^{-3}	2650
SSOL1 diameter	m	1.00E-06
SSOL1 settling model	-	STOKES
SSOL1 critical shear	N m^2	2.00E-05
SSOL1 resuspension rate	g m^2 d^{-1}	25
SSOL1 resuspension half-saturation	g m^2	1.0
SSOL1 light attenuation	m^{-1}	0.12
Suspended Solids #2 – Silt (SSOL2)		
SSOL2 density	kg m^{-3}	2650
SSOL2 diameter	m	1.00E-05
SSOL2 settling model	-	STOKES
SSOL2 critical shear	N m^2	1.50E-02
SSOL2 resuspension rate	g m^2 d^{-1}	2775
SSOL2 resuspension half-saturation	g m^2	1.0
SSOL2 light attenuation	m^{-1}	0.08

Table 3 Configuration of phytoplankton groups for the ecological model.

Parameter (as key string)	Unit	Value	
		Cyanobacteria	Other
General parameters			
Minimum biomass	µg chl *a* L^{-1}	0.1	0.1
Carbon: Chl *a* ratio	Dimensionless	40	40
Sediment decay rate	d^{-1}	0.5	0.5
Units	-	chla*	chla*
Salinity growth function type	-	NONE	NONE
Salinity respiration function type	-	NONE	NONE
Growth parameters			
Growth coefficient	d^{-1}	0.70	1.30
Growth initial light curve slope	µmol m^{-2} s^{-1}	80	5
Growth temperature multiplier	Dimensionless	1.05	1.05
Growth temperature – standard	°C	18	16
Growth temperature – optimum	°C	32	26
Growth temperature – maximum	°C	39	36
P: Chl *a* ratio – minimum	mg P mg chl a^{-1}	0.19	0.21
P: Chl *a* ratio – maximum	mg P mg chl a^{-1}	0.75	0.51
P uptake rate – maximum	mg P mg chl a^{-1} d^{-1}	0.988	0.748
P growth half saturation constant	mg P L^{-1}	0.007	0.006
N: Chl *a* ratio – minimum	mg N mg chl a^{-1}	4.0	4.0
N: Chl *a* ratio – maximum	mg N mg chl a^{-1}	6.0	6.0
N uptake rate – maximum	mg N mg chl a^{-1} d^{-1}	2.948	3.348
N growth half saturation constant	mg N L^{-1}	0.028	0.035
Loss parameters			
Respiration coefficient	d^{-1}	0.049	0.091
Respiration temperature multiplier	Dimensionless	1.05	1.05
Mortality coefficient	d^{-1}	0.0105	0.0195
Excretion coefficient	d^{-1}	0.0105	0.0195
Other parameters			
Migration type	-	CONSTANT	CONSTANT
Settling velocity	m s^{-1}	5.30E-08	2.30E-07
Density	kg m^{-3}	990	980
Diameter	m	1.50E-04	8.00E-06
Light attenuation	m^{-1}	0.014	0.014

*units were stipulated as chla, however an error in the base model release meant the unit 'chla' was actually being read as C (Carbon). Consequently, P_max_uptake_rate and N_max_uptake_rate are input in the model as one fortieth of that shown in the table above.

Lake geometry

Lake geometry input was compiled in the pre-processor model, and included input relating to 1) lake bathymetry, 2) inflow and outflow boundary conditions, and 3) update boundary conditions boundary conditions. Lake bathymetry was input as a 3-dimensional cartesian mesh, with uniform cell spacing of 100 m in each of the horizontal dimensions (x and y) and at 1 m in the vertical dimension (z). Lake bathymetry was generated in QGIS v. 3.16.14 (QGIS.org, 2023) by resampling data from the bathymetric and LIDAR surveys. The extent of the lake was clipped at 5.6 m Moturiki datum. To enable simulations above this height (and up to 6.8 m Moturiki datum) an artificial cell with a height of 6.8 m Moturiki datum added at the edge of the lake. It is acknowledged that there would be some local flooding not captured under this configuration. However, maintaining lake boundary at 5.6 m Moturiki datum as a pragmatic choice was based on uncertainties around the exact extent of the potential flooded area (per 10 m^2 grid cell resolution), properties of the lake bottom sediment during flooding in areas that were, for example, pasture, and complexities in adjusting the surface runoff derived from each sub-catchment flow when partially inundated with water.

Inflow and outflow boundary conditions (as flow direction and x, y, and z placement within the bathymetric grid) were stipulated for 28 inflows, and 2 outflows. Inflows included the Te Onetea Stream inflow (positive values inflow, and negative values outflow), Matahuru Stream inflow, 24 ungauged inflows (i.e., all inflows representing sub-catchments ≥ 0.5% of the Matahuru catchment area), Te Kauwhata WWTP inflow, and a residual inflow (for balancing of the water budget; positive values inflow, and negative values outflow). Outflows included the NOCG outflow, and Fish Pass Culvert outflow. In addition, a third residual outflow was added for balancing of the water budget, with positive values outflow, and negative values inflow.

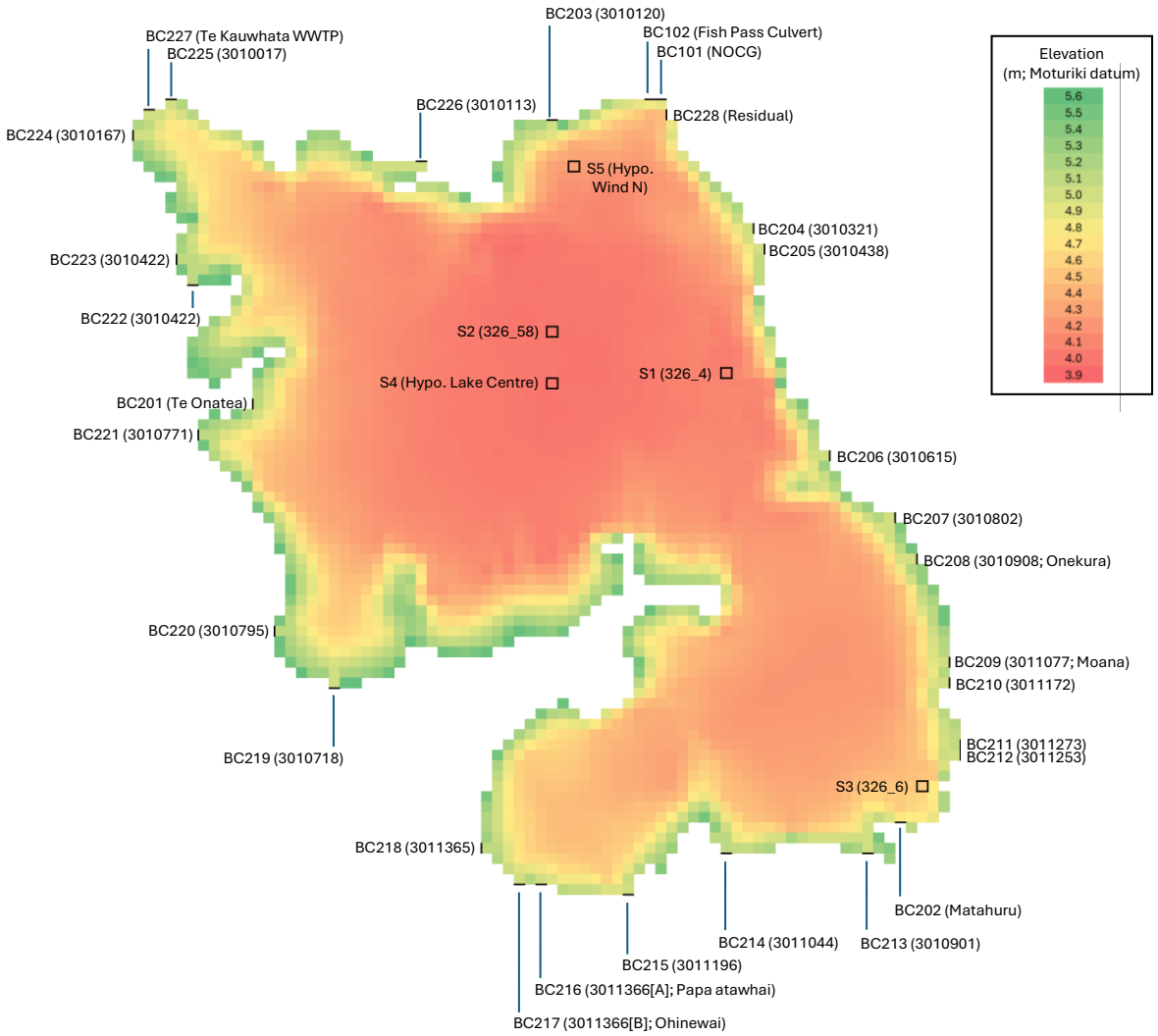

Figure 2: X and Y model grid of Lake Waikare, demonstrating lake bathymetry, sites (SX), and in- (BC2XX) and out- (BC1XX) flow boundary conditions (BC). Numbers in parentheses for BC 203 through 226 relate to NZReach numbering system; Artificial cell at 6.8 removed for viewing purposes; Hypo. = hypothetical.

Meteorology

In lieu of a long-term on-lake meteorological data set, long-term meteorological data was derived directly or indirectly, as follows:

First, rainfall and atmospheric pressure were derived daily from the hypothetical meteorological VCSN Site 27116, and SWR, and subsequently cloud cover (CC), and wind direction were determined as that measured from a nearby meteorological station (NIWA Site 26117; Ruakura 2 Ews). CC was determined from SWR (Luo et al., 2010), using a 10-year subset (2013–2023) of measured CC and SWR data collected from MetService Site 1770 (Rotorua Aero Aws; Prentice & Özkundakci, 2024), given as (Equation 1):

$$CC = \left(-1.4859 \cdot {O_{SWR}}^2\right) + (2.4098 \cdot O_{SW}) \quad (1)$$

where CC is cloud cover, and O_{SWR} is the (cloud)obstructed fraction of SWR. O_{SWR} is given as (Equation 2):

$$O_{SW} = 1 - \left(\frac{M_{SWR}}{CS_{SWR}}\right) \quad (2)$$

where M_{SWR} is the measured SWR, and CS_{SWR} is the theoretical "clear-sky" SWR (i.e., SWR under cloud-free conditions). CS_{SWR} was determined using the BIRD Clear Sky model (Bird & Hulstrom, 1981; Myers, 2012), and parametrised per Table 4, Ruakura. CC was input daily and applied uniformly across all horizontal grids.

Table 4 Configuration for BIRD Clear Sky Model.

Parameter	Unit	Ruakura	Pukekohe	Rotorua	Reference
Latitude	decimal degrees	-37.77389	-37.20637	-38.0398	N/A
Longitude	decimal degrees	175.30517	174.86384	176.3465	N/A
Time zone	GMT offset	12	12	12	N/A
Pressure	mB	1012.12	1007.49	982.01	MetService/NIWA
Ozone	cm	0.296	0.296	0.296	Luo et al. (2010)
Total Colum Water Vapour	cm	1.5	1.5	1.5	Default
Aerosol Optical Depth	cm	0.0254	0.0254	0.0254	Luo et al. (2010)
Aerosol Optical Depth	cm	0.0290	0.0290	0.0290	Luo et al. (2010)
Ba	Dimensionless	0.85	0.85	0.85	Default
Albedo	Dimensionless	0.2	0.2	0.2	Default

Second, locally specific variables, i.e., air temperature, relative humidity, wind, were derived from a nearby meteorological station (NIWA Site 26117; Ruakura 2 Ews) and statistically transformed, at varying levels, to best represent the shorter-term and patchy on-lake measurements (LimnoTrack Waikare Automated Profiler). This was achieved using a two-year dataset comparing like-for-like measurements at the two stations, with a complete two-year period used to ensure proper weighting of seasonal effects. To account for diurnal variation, this was conducted separately for each hour of the day. With the longest-consistent on-lake meteorological record spanning 23 May 2017 through 11 May 2019, the representative two-year period was determined as that from 23 May 2017 through 11 May 2019 with the period from 12 May 2019 through 22 May 2019 filled by that collected in the previous year. Air temperature and relative humidity were determined as:

$$X_{NIWA\_sacled} = \frac{X_{NIWA} - \mu_{NIWA}}{\sigma_{NIWA}} \cdot \sigma_{LT} + \mu_{LT} \quad (3)$$

where X_{NIWA_scaled} represents the NIWA-derived value scaled to the LimnoTrack-derived value, X_{NIWA} the NIWA value, μ_{NIWA} the NIWA mean across the 18 years from 1 January 2006 through 31 December 2023, σ_{NIWA} the NIWA standard deviation across the 18 years from 1 January 2006 through 31 December 2023, μ_{LT} the theoretical LimnoTrack mean across the 18 years from 1 January 2006 through 31 December 2023, σ_{LT} the theoretical LimnoTrack standard deviation across the 18 years from 1 January 2006 through 31 December 2023. In the absence of having 18-years of LimnoTrack data, μ_{LT} and σ_{LT} were given as:

$$\mu_{LT} = \mu_{LT\_2} \cdot \left(\frac{\mu_{NIWA}}{\mu_{NIWA\_2}} \right) \tag{4}$$

where μ_{LT_2} is the LimnoTrack mean across the 2-year period, μ_{NIWA_2} is the NIWA mean across the 2-year period.

and σ_{LT} were given as

$$\sigma_{LT} = \sigma_{LT\_2} \cdot \left(\frac{\sigma_{NIWA}}{\sigma_{NIWA\_2}} \right) \tag{5}$$

where σ_{LT_2} is the LimnoTrack standard deviation across the 2-year period, σ_{NIWA_2} is the NIWA standard deviation across the 2-year period. This scaling assumes that NIWA and LimnoTrack data scale consistently and was considered the most appropriate method to represent site specific data over prolong periods.

Wind speed was determined as per air temperature and relative humidity, but required a subsequent transformation. This transformation was based on preliminary analysis, which revealed the two datasets (while having identical means and standard deviations) had very different frequency distributions. To account for this, data at each site was sorted into 5-percentile bins and the mean determined in each bin, then the resultant scaling factor for each bin applied to ensure similar frequency distributions across the two datasets (Figure 3).

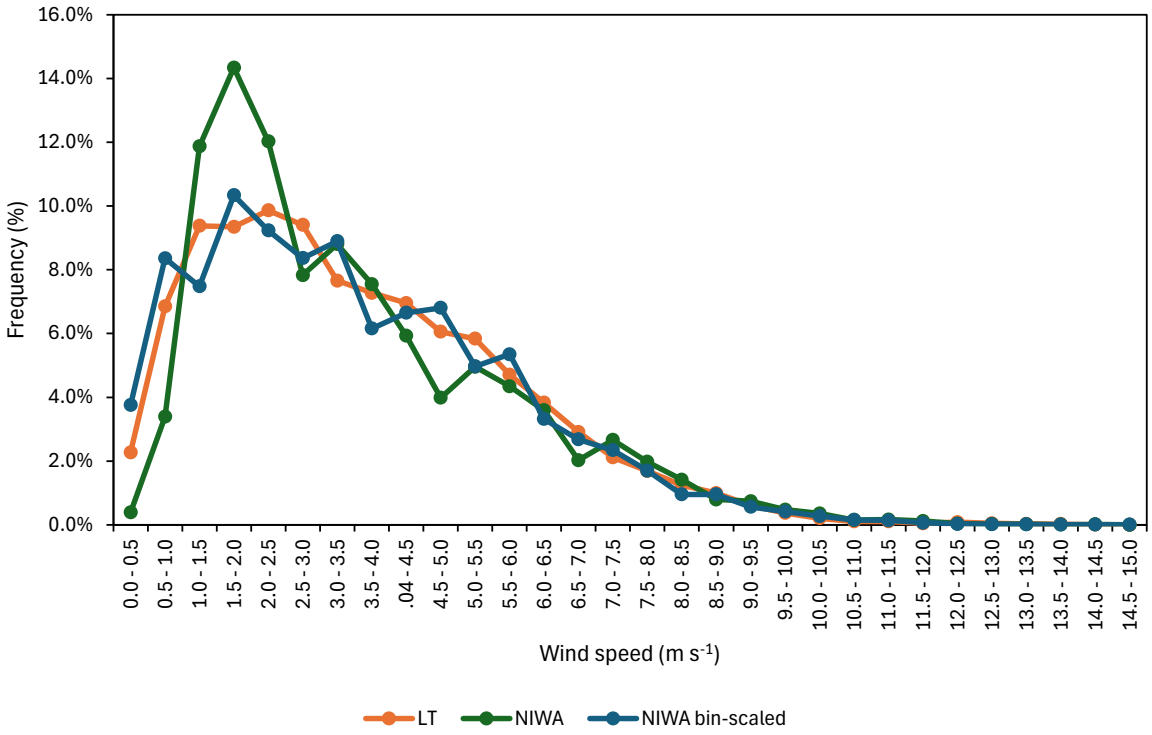

Figure 3: Frequency distribution of wind speed data at 2 m, for LimnoTrack (LT), NIWA, and NIWA data following frequency distribution alignment.

The NIWA Site 26117 (Ruakura 2 Ews) used as direct or indirect input as described above, had missing data infilled in the first instance by NIWA Site 2006 (Pukekohe Ews), and in the second instance (i.e., where data was missing at both NIWA sites 26117 and 2006) by MetService Site 1770 (Rotorua Aero Aws). QAQC—in comparing daily data to the mean value on a given day and time over the entire data set for a given site—identified suspect sequences in the Ruakura relative humidity (1 December 2012 through 17 February 2014) and SWR (10 December 2013 through 25 December 2013; and 6 March 2018 through 8 April 2018) datasets that warranted their removal. In addition, QAQC—in comparing measured SWR data to theoretical clear sky SWR data for a given site—identified sensor drift in SWR at all three sites, and in particular the two NIWA sites. To amend this, a correction factor (F) was given as:

$$F(w) = median\{F_w(w') \mid w' \in [w-12, w+12]\} \quad (6)$$

where F is the scaling factor determined as the median F_w across 25 weeks, including 12 weeks before and after the given week w, and F_w is the maximum factor within a given week, given as:

$$F_w(w) = max\{F_d \mid d \in week\ w\} \quad (7)$$

where F_d is the factor on a given day, given as

$$F_d = \frac{M_{1300}(d)}{T_{1300}(d)} \quad (8)$$

where M_{1300}(d) is the measured value at 1300 hrs on day d, and T_{1300}(d) is the theoretical maximum BIRD value at 1300 hrs on day d. The final step involved applying the scaling factor *F* determined for a given week to each day within the given week *w*. Data at each site was then scaled by mean, using data common across all three sites, to that measured at the primary site (26117).

Air temperature, relative humidity, SWR, wind speed and wind direction were input hourly and applied uniformly across all horizontal grids (Appendix 1; Appendix 2). Rainfall and atmospheric pressure were input daily and applied uniformly across all horizontal grids (Appendix 1; Appendix 2).

Inflow and outflow volume

The Te Onetea Stream (positive values inflow, and negative values outflow) and Matahuru Stream inflow were input daily, with missing values linearly interpolated (Appendix 3). Twenty-four minor ungauged flows were included, based on areas given per River Environment Classification New Zealand (2010; Appendix 4). These included all sub-catchments with areas > 0.5% of the Matahuru catchment, not included as part of a monitored flow (i.e., NZReach 3010655 was excluded as it was included in the monitored Te Onetea flow). In addition, the NZReach 3011366 catchment, was apportioned across Papaatawhai (57.3%) and Ohinewai (42.7%), per the mean flow rates as measured by A. Hopkins at each site. The 24 minor flows, were given as:

$$Q_X = Q_M \cdot \left(\frac{A_X}{A_M}\right) \cdot S \quad (9)$$

where Q_X is the modelled flow for a given minor flow, Q_M is the measured flow at Matahuru Stream, A_X is the surface area of the sub-catchment for the given minor flow, and A_M is the surface area of the sub-catchment of the Matahuru flow. A_X was determined as the catchment area associated with the given stream in the 'River Environment Classification New Zealand', A_M determined per Lawrence and Ridley (2018), and *S* is a scaling factor applied to apportion sub-catchments (with areas < 0.5% of the Matahuru catchment) not explicitly included. The scaling factor was given as:

$$S = \frac{A_{CW} - A_{CM} - A_{LW} - A_{CX}}{A_{CY} - A_{CX}} \quad (10)$$

where A_{CW} is the area of the entire Waikare catchment, A_{CM} is the area of the Matahuru sub-catchment, A_{LW} is the area of Lake Waikare, A_{CX} is the area of NZReach 3010655 (i.e., the sub-catchment included within the monitored Te Onetea flow), and A_{CY} is the total area covered by the 24 minor flows. Te Kauwhata WWTP inflow were input as daily, with measured values between 1 July 2016 and 30 June 2020 linear interpolated, and in lieu of no data from 1 July 2007 through 1 July 2016 and 1 July 2020 through 30 June 2023 values for a given and of the year were entered as the mean value of known data for the given day of the year (Appendix 3).

Northern Outlet Control Gate outflow (326_10) were input daily, with missing data first modelled from a linear relationship (R^2 = 0.96) between measured discharge > 0.1 m s^{-1} at the NOCG and the

Northern Outlet Canal (3021_2), and second by linear interpolation. Fish Pass Culvert flow was input daily, as determined by a 4th order polynomial relationship (R^2 = 1.00) between measured lake height and discharge for the period of 1 July 2022 through 27 July 2023. Fish Pass Culvert flow values below 5.4 m Moturiki datum were input as zero (Appendix 3).

The residual term of the water balance was assigned to the residual inflow, with positive values inflow and negative values outflow (Appendix 3). The water balance was calculated at a daily timestep, with the residual given as:

$$Q_{Res} = (Q_{In} - Q_{Out}) + \Delta S \tag{11}$$

where Q_{Res} is mean daily ungauged inflow ($m^3\ s^{-1}$); Q_{In} is the total daily inflow ($m^3\ s^{-1}$) derived from known surface inflows and rainfall onto the lake surface; Q_{Out} is the total daily outflow derived from known surface outflows and evaporation; ΔS is mean daily rate of change in lake storage ($m^3\ s^{-1}$) due to water level change. To reduce the impact of wind set up (of which preliminary scenarios indicated were substantial) in the calculation of the residual, the water level height was determined as the 3-day mean of the lake height at midnight, which was determined as the median lake height value between midnight and midday (i.e., when WS was typically lowest, and lake level least variable) on a given day and in turn linearly interpolated to midnight. The residual term was then applied as a 15-day mean. Evaporation was calculated based on Fischer et al. (1979), per Hodges and Dallimore (2013):

$$E = A\left(\frac{\frac{-0.622}{P} C_L\, \rho_a\, L_E U (e_a - e_s)(T_{surf})}{L_v}\right) \tag{12}$$

Where E is evaporation ($m\ s^{-1}$); A is the area of the lake (m^2); C_L is the latent heat transfer coefficient for wind speed (0.0013); ρ_a is air density ($kg\ m^{-1}$); L_E is the latent heat of evaporation of water (2,453,000 J kg^{-1}); U is measured wind speed ($m\ s^{-1}$); e_a is the vapour pressure of the air (Pa); e_s is the saturated vapour pressure of the air (Pa) corresponding to the lake water surface temperature (°C); P is the atmospheric pressure (Pa); L_v is the latent heat of vaporisation (2,260,000 J kg^{-1}); and T_{surf} is the surface water temperature (°C) given as 1.1157x + 1.5075 (R^2 = 0.92), where x is the 6-day mean of air temperature. This relationship provided the best fit (i.e., highest R^2) of seven models relating data as measured at 0.05 m depth by the onsite automated sampling station against the 1- through 7-day mean of air temperature. e_s was calculated by the Magus–Tetens formula per Hodges and Dallimore (2013):

$$e_s(T_{0.05}) = 100 \exp\left[2.3026\left(\frac{7.5\, T_{0.05}}{T_{0.05} + 237.3}\right) + 0.758\right] \tag{13}$$

To ensure a simulated water level matched the measured water level, the water balance was adjusted over three iterations. First, as that described above. Second, by replacing evaporation in '1' with simulated evaporation values determined at the middle of the northern basin (Site 4 [Hypothetical station Lake Centre]) across individual hydrological year hydrodynamic-only simulations. This was achieved by running a suite of single limnological year (plus 1-month spin up) hydrodynamic-model only simulations. Third, adjusting evaporation in '2' to account for long term loss/gain in the water balance (c.f., measured data) across a full (from 1 June 2017 through 30 June 2021) simulation, as:

$$X = \frac{E_{4\_y} - \Delta WB_{4\_y}}{E_{4\_y}} \quad (14)$$

Where X is the evaporation adjustment factor, E_{4_y} is the total evaporation flux (m^3) over 4 years from 1 June 2017 through 31 May 2021, and ΔWB_{4_y} is the total change in water balance (m^3) over 4 years from 1 June 2017 through 31 May 2021.

Inflow water quality

Water temperature for each inflow was determined daily by modelling measured temperatures for a given site against 1- through 7-day mean air temperatures (Appendix 3). Here, the model for a given inflow was determined from the best fit (i.e., highest R^2) out of the seven models. Te Onetea Stream inflow temperature was given as 0.9474x + 3.494 (R^2 = 0.90), where x is the 7-day mean of air temperature. Measured temperature for Te Onetea was determined as the mean of that measured at Waikato River at Huntly (1131_77), and Waikato River at Mercer (1131_91). These sites were chosen owing to there being more consistent and complete data than the site of Rangiriri Bridge, and the mean of the two sites minimising the influence of temperature pollution associated with the Huntly Power station. Matahuru inflow temperature was given as 0.8617x + 3.1136 (R^2 = 0.92), where x is the 3-day mean of air temperature. The 24 minor inflows were given as that determined for Matahuru inflow, and the Te Kauwhata WWTP inflow that determined for Te Onetea inflow.

Te Onetea water quality (except for temperature) was determined daily by linear interpolation of ~monthly samples taken from the Waikato River at Huntly (1131_77; Appendix 3). Matahuru Stream water quality (except for temperature) was determined daily using the 'local minimum' hydrograph separation method of Pettyjohn and Henning (1979), per the 'SepHydro - Hydrograph Separation Tool' (www.sephydro.hydrotools.tech; Appendix 3). For baseflow, water quality concentrations were determined from linear interpolation of ~monthly samples taken at Matahuru Stream at Myjers Farm Bridge (516_22). For event flow, water quality concentrations were determined from the dataset collected and reported in Hughes (2018). The Hughes (2018) data was sorted into 5 m s^{-1} bins, consisting 0–5, 5–10, 10–15, 15–20, 20–25, and 25+ m s^{-1}, and the mean of each water quality constituent determined for each bin. Event flow water quality concentrations were determined by cross referencing the event flow discharge to the water quality in the relevant discharge bin. The Te Kauwhata WWTP inflow water quality data were determined daily, between 1 July 2016 and 30 June 2020 by linearly interpolating available measurements, and for other periods as the mean value of the interpolated data for a given Julian day. For the Te Kauwhata WWTP, TP was assumed to be DRP, and TN assumed to be apportioned equally as NNN and NH_4.

Water quality (except for temperature) for the minor flows were determined by scaling of the Matahuru water quality dataset (Appendix 3). Scaling factors for TN, TP, DRP, NNN, and NH_4, were determined for Moana, Ohinewai, Onekura, Papaatawhai, and White Streams from the A. Hopkins (Unpub.) dataset. This was achieved by dividing the median value (26 January 2017 through 12 January 2018) collected at Moana, Ohinewai, Onekura, Papaatawhai, and White Streams by the median value (26 January 2017 through 12 January 2018) collected at Matahuru Stream. Scaling factors for TN, TP, DRP, NNN, and NH_4, were also determined for the remaining ungauged minor flows not measured by A. Hopkins. This was achieved by dividing the median value (26 January 2017 through 12 January 2018) across six streams (i.e., Matahuru, Moana, Ohinewai, Onekura,

Papaatawhai, and White Streams) by the median value (26 January 2017 through 12 January 2018) at Matahuru Stream.

Measured DRP and NNN were assumed to correspond in model phosphate (PO_4) and nitrate (NO_3), respectively. PO_4, dissolved organic P (DOP; as DOPL), particulate organic P (POP; as POPL), NH_4, NO_3, dissolved organic N (DON; as DONL), particulate organic N (PON; as PONL), dissolved organic carbon (DOC; as DOCL), particulate organic carbon (POC; as POCL), clay (as suspended solids 1 [SSOL1]), silt (as suspended solids 2 [SSOL2]), cyanobacteria, cyanobacteria internal P (IP_{Cyan}), cyanobacteria internal N (IN_{Cyan}), other-phytoplankton, other-phytoplankton internal P (IP_{Oth}), other-phytoplankton internal N (IN_{Oth}) were determined (directly or indirectly) from measured data. DOP was determined TP-DRP multiplied by 0.217, this was based on the mean proportion of TP-DRP as DOP, at Waikato River at Rangiriri as reported in Gibbs et al. (2014). Consequently, particulate P (i.e., POP, IP_{Cyan}, IP_{Oth}) was determined as TP-DRP multiplied by 1 less 0.217. DON was determined TN-DIN multiplied by 0.363, this was based on the mean proportion of TN-DIN as DON, at Waikato River at Rangiriri as reported in Gibbs et al. (2014). Consequently, particulate N (i.e., PON, IN_{Cyan}, IN_{Oth}) was determined as TN-DIN multiplied by 1 less 0.363.

In the absence of direct chlorophyll *a* measurements in the inflows, this was determined as VSS multiplied by 5.8053, a linear relationship ($R^2 = 0.89$) between VSS and chlorophyll *a* based on measurements collected from the Waikato River at Rangiriri, Ngāruawāhia, Karapiro, and Ohakuri as reported in Gibbs et al. (2014). Chlorophyll *a* was apportioned equally (50:50) to cyanobacteria and other-phytoplankton. This was necessary because only three phytoplankton composition counts were available from Huntly, Mercer, or Rangiriri, all collected in mid-April 2019. Phytoplankton N and P stores were determined as their respective chlorophyll *a* value multiplied by their configured N_Chla_ratio_max and P_Chla_ratio_max values, respectively. PON was determined as particulate N less IN_{Cyan} and IN_{Oth}, and POP was determined as particulate P less IP_{Cyan} and IP_{Oth}. POC was determined as TIN less DIN, multiplied by 7.29; and DOC as DIN multiplied by 7.29 (Abell et al., 2015).

Clay and Silt were determined as 50% each, of inorganic suspended solids (ISS). In the absence of direct measurements of ISS, ISS was determined as TSS multiplied by 0.769, based on the mean proportion of TSS as ISS at Waikato River at Rangiriri (Gibbs et al., 2014). VSS was determined as TSS multiplied by 0.231 (i.e., 1 – 0.769). TSS was determined as Turbidity multiplied by 1.788, a linear relationship ($R^2 = 0.91$) between TSS and Turbidity based on measurements collected at Waikato River at Huntly (1131_77).

The atmospheric deposition flux was input daily by applying concentrations to the rainfall. These concentrations were determined by dividing the average atmospheric deposition of N and P for North Island New Zealand lakes, 6.37 kg N ha^{-1} y^{-1} and 0.34 kg P ha^{-1} y^{-1} (Verburg et al., 2018), by the average annual rainfall recorded over the entire model set-up period (i.e., 1 January 2007 through 30 June 2023). The inorganic portion was determined as that reported in Lake Taupo of 42% of the N flux and 54% of the P flux (Vant & Gibbs, 2006), with 42% of N applied as equally at 21% as NH_4, and 21% as NO_3, and 54% of P applied as PO_4. The remainder of N and P was apportioned equally between the dissolved organic and particulate organic fractions.

In-lake initial conditions

Initial profile conditions for temperature and DO were determined from measured SONDE profiles. As for inflow water quality, measured DRP and NNN were assumed to correspond in model PO_4 and NO_3, respectively. Initial profile conditions for PO_4, DOP, POP, NH_4, NO_3, DON, PON, DOC, POC, clay, silt, cyanobacteria, cyanobacteria internal P (IP_{Cyan}), cyanobacteria internal N (IN_{Cyan}), other-phytoplankton, other-phytoplankton internal P (IP_{Oth}), other-phytoplankton internal N (IN_{Oth}) were determined from measured data. Temperature was initialised as that modelled on a hydrological only model simulation run from 1 June 2016 through 31 June 2017. All other parameters were initialised (as a homogenous water column) from the mean of the data collected on 24 April 2017 and 29 June 2017.

DOP was determined TP-DRP multiplied by 0.311, this was based on the mean proportion of TP-DRP as DOP, from monthly data collected over 12 months in the upper turbid reaches of Lake Wivenhoe (M. Prentice, unpub.). Consequently, particulate P (i.e., POP, IP_{Cyan}, IP_{Oth}) was determined as TP-DRP multiplied 1 less 0.311. DON was determined TN-DIN multiplied by 0.520, this was based on the mean proportion of TN-DIN as DON, at Waikato River at Rangiriri as reported in Gibbs et al. (2014) but multiplied by 1.43. This was based on the difference in DOP factor (0.311) observed in lake by Prentice (unpub.) and the DOP factor (0.217) observed by Gibbs et al. (2014) in the Waikato River. Consequently, particulate N (i.e., PON, IN_{Cyan}, IN_{Oth}) was determined as TN-DIN multiplied by 1 less 0.520. POC and DOC which were determined as an approximate equilibrium value based on previous simulation.

Chlorophyll *a* was apportioned as 39.6% Cyanobacteria and 60.4% other-phytoplankton, based on median fractions of the total biovolume 5 years either side of the initialisation date. This was decided on based on the lack of data near the model initialisation date and the erratic nature of the phytoplankton community. Phytoplankton N and P stores were determined as their respective chlorophyll *a* value multiplied by their configured N_Chla_ratio_max and P_Chla_ratio_max values, respectively. PON was determined as particulate N less IN_{Cyan} and IN_{Oth}, and POP was determined as particulate P less IP_{Cyan} and IP_{Oth}. Clay and Silt were determined as 90% and 10%, respectively, of inorganic suspended solids (ISS), respectively.

3.2.3 Model calibration and validation

The model was calibrated (1 July 2017 through and 30 June 2019) from measurements of lake height, temperature, DO, DRP, TP, NH_4, NO_3, TN, and chlorophyll *a*. Model calibration fit was quantified statistically by way of; model fit using Peason correlation (R), and model accuracy using root mean squared error (RMSE) and mean absolute error (MAE). Lake height was calibrated using hourly data derived from the lake height gauging station (Site 3 [326_6]). In addition, lake height data extracted to coincide with (Site 3 [326_6]), was compared with data extracted at the hypothetical Site 5 (Hypothetical Site: Wind N), to determine the degree of wind set up. Temperature was calibrated using hourly data derived from the LimnoTrack monitoring station (Site 2 [326_58]) at the surface (0.05 m) and the bottom (~ 0.05 m above lakebed), and ~monthly data from the regular monitoring program (Site 1 [326_4]) at the surface (0 m), and the bottom (1.2 m). DO was calibrated using data collected as part of the regular monitoring program (Site 1 [326_4]) at the surface (0 m) and the bottom (1.2 m). These methods of DO calibration were necessitated upon discovery that the LimnoTrack (Site 2 [326_58]) DO data is unusable, likely owing to biological fouling. DRP, TP, NH_4, NO_3, TN, ISS (i.e., SSOL1+SSOL2), chlorophyll *a*, and Secchi depth were calibrated using data collected as part of the regular monitoring program. As AEM3D does not explicitly simulate Secchi depth, Secchi depth was determined as Kd (PAR) multiplied by a Secchi coefficient of 1.05, in turn determined as the mean value for turbid lakes as reported in Koenings and Edmundson (1991). For

comparison, T and DO data was extracted from the model at the same height as that measured in situ, and other parameters extracted at 0.2 m depth. The model was validated, following the same logic as the model calibration, across the 24-month period immediately following the calibration period.

3.2.4 Model scenario simulations

Model simulations were initialised on 1 June 2017, permitting a 30-day spin-up period, and a four-year simulation period from 1 July 2017 through 30 June 2021. All scenarios were initialised per the height and initial conditions used for the model configuration. Scenarios which involved raising the water level were increased during the 30-day spin-up period (1 June 2017 through 30 June -2021) to or near their target water level. This was achieved by enabling the maximum discharge of 6.4 m^3 s^{-1} from the Te Onetea inflow (under criteria of the LWWFCS per Grainger (2025); Figure 4) and shutting off of the NOCG outflow during this 30-day period. Model simulations were analysed within the context of the four hydrological years, to best capture inter-annual variability in hydrological and water quality regimes.

To best recreate the hydrological regime and lake water level under the simulated scenarios in this study, scenario inflows and outflows were driven by a daily automated-iterative water balance that solved for lake height. Inflows from the Matahuru, the ungauged catchment, Te Kauwhata WWTP, and the Fish Pass Culvert outflow were input as described for the model calibration. The Te Onetea inflow and the NOCG outflow, however, were input as a scenario-driven value within the context of the LWWFCS per Grainger (2025) (Figure 4). These values were determined from the mean observed value meeting the LWWFCS criteria, between 1 July 2017 and 30 June 2021 (Table 5). It is acknowledged that method does not consider more subjective aspects such as decisions around holding water back in the event of a bloom, or pre-emptive withdrawal in anticipation of a future rainfall, etc. However, this method was considered to capture well the mean hydrological regime within the system based on the more objective criteria under criteria the LWWFCS (see Figure 4).

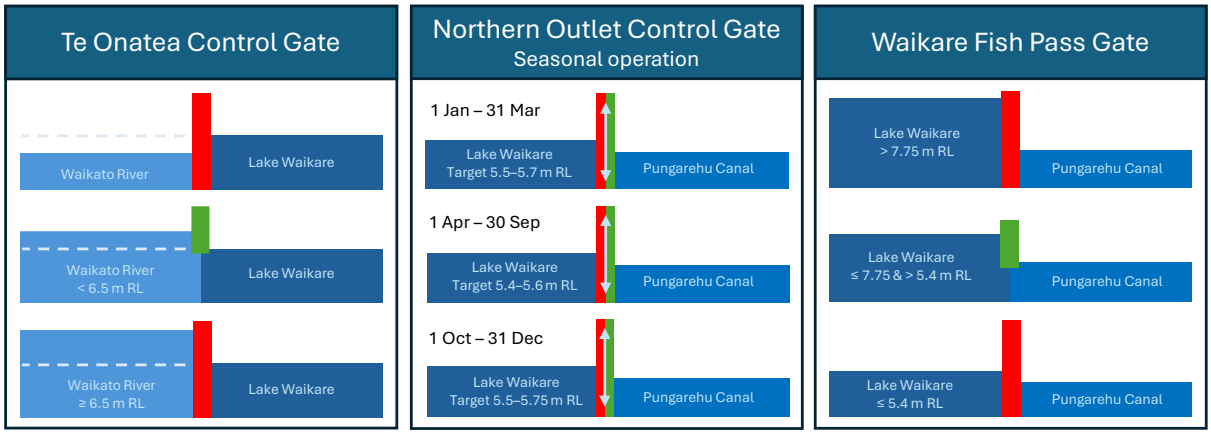

Figure 4: Operating regime for Te Onetea, the Northern Outlet Control Gate (NOCG), and the Waikare Fish Pass Gate. Reference level, RL, is Moturiki Datum (MD) (adapted from Grainger (2025)). Red denotes gate is closed, green denotes gate is open, red-green with arrow denotes gate is conditionally opened and closed to maintain the lakes target water level (considerations might include, for example, water quality, forecast heavy rainfall, low flow in the Whangamarino, etc.)

Table 5 Average discharge rates ($m^3 s^{-1}$; 2 decimal places) for Te Onetea and NOCG for the period 1 July 2017 through 30 June 2021.

	January through March ($m^3 s^{-1}$)	April through September ($m^3 s^{-1}$)	October through December ($m^3 s^{-1}$)
Te Onetea Inflow Average	2.14	4.72	2.97
NOCG Outflow			
Above Waikare Max WL	---------- 11.99* ----------		
Between Waikare Min & Max WL	0.77	5.43	1.24
Below Waikare Max WL	0.00	0.00	0.00

* Annual composite mean applied across all three periods.

Model scenarios included variations to 1) the lakes minimum and maximum water level, 2) the lakes catchment nutrient loading, and 3) Te Onetea's inflow discharge rate, described as below:

1. **Variations to the lakes minimum and maximum water level**. This included three scenarios relating to changes in the minimum and maximum water levels stipulated under the LWWFCS per Grainger (2025). Scenarios included:
    a. Current conditions: Both the minimum and maximum water levels set as that under the LWWFCS.
    b. Raising the maximum water level: The minimum water level set as that under the LWWFCS, and the maximum water level increased by 1 m.
    c. Raising the minimum and maximum water level: Both the minimum and maximum water level increased by 1 m.
2. **Variations to the lakes catchment nutrient loading**. This included two scenarios relating to the water quality derived from the Matahuru and the remaining catchment-derived flows (i.e., all flows except for Te Onetea and the Te Kauwhata WWTP). Scenarios included:
    a. Current loading: N, P, and TSS boundary conditions for each flow determined as described in the calibrated model.
    b. Reduced loading: N, P, and TSS boundary conditions for each flow determined by scaling the Matahuru and the remaining catchment-derived flows. Reductions represent a potential degree of reduction in the losses of N and P from land resulting from mitigation actions based (Monaghan et al., 2021) and (McDowell et al., 2021) predicted for 'Matahuru Stm at Waiterimu Road Below Confluence' using the Freshwater Scenario Builder (freshwater-scenario-builder.co.nz/rivers; Input – Table 6; Output – Table 7).
3. **Variations to Te Onetea's inflow discharge rate (i.e., Variations in flushing rate per Te Onetea inflow)**. This included two scenarios relating to discharge rates entering via Te Onetea, under the gate opening conditions of the LWWFCS per Grainger (2025). N.b. where gates were closed discharge was zero (and there was zero outflow discharge). Scenarios included:
    a. Average discharge rate: Te Onetea inflow discharge rate is set as the mean observed rate across the 4-year study, determined from all days meeting the gate opening conditions under the LWWFCS per Grainger (2025).
    b. Maximised discharge rate: The Te Onetea inflow discharge is set to 6.4 $m^3 s^{-1}$.

Table 6 Scenario builder input as default scenario.

	Current		Scenario		
	Land area (%)	Load contribution (%)	Mitigation effectiveness (%)	Land area (%)	Load contribution (%)
Nitrogen					
Dairy	32	63	57	32	48
Sheep and beef	63	37	27	63	50
Short-rotation crop	0	0	30	0	0
Perennial crop	0	0	15	0	0
Forestry	2	0	0	2	0
Native vegetation	3	0	0	3	0
Urban	0	0	0	0	0
Other	0	0	0	0	0
Phosphorus					
Dairy	32	40	53	32	37
Sheep and beef	63	58	49	63	60
Short-rotation crop	0	0	50	0	0
Perennial crop	0	0	50	0	0
Forestry	2	1	30	2	1
Native vegetation	3	1	0	3	1
Urban	0	0	0	0	0
Other	0	0	0	0	0

Table 7 Scenario builder output as default scenario.

	Current (mg L^{-1})	Scenario (mg L^{-1})	% Reduction (%)
Nitrogen	1.34	0.733	45.3%
Phosphorus	0.083	0.041	50.6%

In total, 12 scenarios were simulated, including all possible iterations of that described above (and outlined in Table 8). It is noted that Scenario 1.1 (see Table 8) may be considered a baseline control scenario in which other scenarios may be compared.

Table 8 Summary table of scenarios.

Scenario	Waikare water level (as increase in min and max)	Waikare catchment nutrient loading	Te Onetea inflow discharge
1.1 (Baseline)	Current	Current	Average (2.1, 4.7, 3.0 $m^3 s^{-1}$)*
1.2	Current	Current	Maximum (6.4 $m^3 s^{-1}$)
1.3	Current	Reduced	Average (2.1, 4.7, 3.0 $m^3 s^{-1}$)*
1.4	Current	Reduced	Maximum (6.4 $m^3 s^{-1}$)
2.1	0 and 1 m	Current	Average (2.1, 4.7, 3.0 $m^3 s^{-1}$)*
2.2	0 and 1 m	Current	Maximum (6.4 $m^3 s^{-1}$)
2.3	0 and 1 m	Reduced	Average (2.1, 4.7, 3.0 $m^3 s^{-1}$)*
2.4	0 and 1 m	Reduced	Maximum (6.4 $m^3 s^{-1}$)
3.1	1 and 1 m	Current	Average (2.1, 4.7, 3.0 $m^3 s^{-1}$)*
3.2	1 and 1 m	Current	Maximum (6.4 $m^3 s^{-1}$)
3.3	1 and 1 m	Reduced	Average (2.1, 4.7, 3.0 $m^3 s^{-1}$)*
3.4	1 and 1 m	Reduced	Maximum (6.4 $m^3 s^{-1}$)

*First value denotes discharge for Jan–Mar; second value denotes discharge for Apr–Sep, third value denotes discharge for Oct–Dec

3.2.5 Model scenario output

For scenario testing, TP, TN, Kd(PAR), Clay (as SSOL1), Silt (as SSOL2), ISS (as TSS), cyanobacteria, other-phytoplankton, total phytoplankton (as chlorophyll *a*) were stipulated to output. All variables were output hourly at S1 (326_4) at 0.2 m depth. Data was converted to daily mean, and—to best capture inter-annual variability in hydrological and water quality regimes—analysed and presented within the context of the four hydrological years. To identify changes across scenarios, results are presented as:

1. Box plots with outliers removed. N.b., analogous plots are presented as appendices with outliers in place per Seaborn's default boxplot method where lower bound outliers are defined as Q1 – 1.5 × IQR and the upper bound as Q3 + 1.5 × IQR (see Appendix 9; Appendix 11; Appendix 13).
2. A heat matrix presenting percentage change relative to the baseline scenario 1.1.

4 RESULTS

4.1 Model performance

4.1.1 Hydrodynamics

Simulations agreed well with daily measurements of lake height at Site 3 (326_6; Figure 5). The model calibration was a strong fit as represented by a high R-value (0.985), with high model accuracy as represented by a low RMSE (0.02) and MAE (0.01; Table 9). The model validation returned similarly strong values, with a high R-value (0.993), and low RMSE (0.02) and MAE (0.01; Table 9). It is likely that the lake water level calibration may have been stronger, if not for the horizontal variation in lake height between the upper and lower reaches on the lake reaching 20.5 cm and the 90th percentile being 2.5 cm (Figure 6).

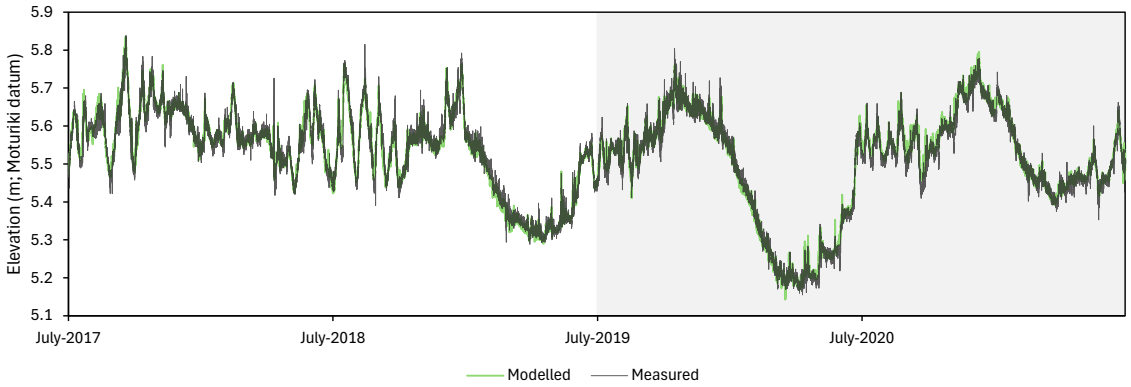

Figure 5: Measured vs modelled lake level (as Height, Moturiki datum) at Site 3 (326_6), during the calibration and validation periods. Calibration period 1 July 2017 through 30 June 2019 (light grey), Validation 1 July 2019 through 30 June 2021 (mid grey). Data are hourly measurements. Modelled and measured data is hourly.

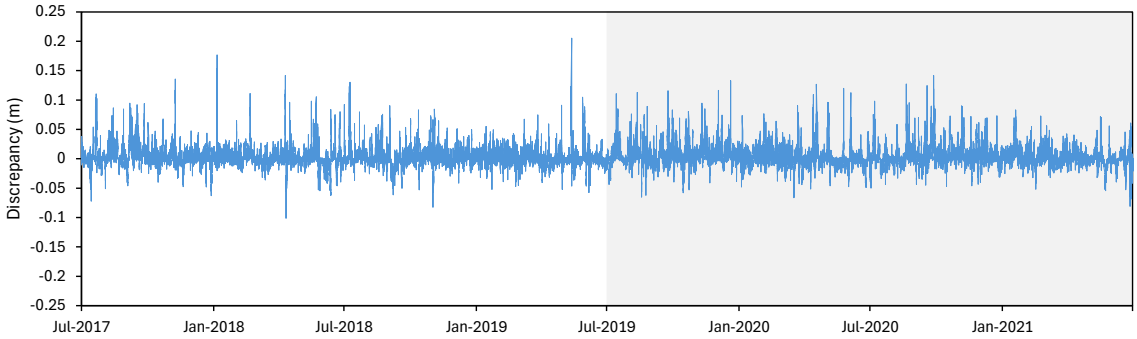

Figure 6: Modelled lake level at Site 3 (326_6) and Site 5 (Hypothetical station; Wind N), as the discrepancy between the two sites (i.e., Site 3 [m] less Site 5 [m]) over the 4-year calibration and validation period. Data is hourly.

Simulations of lake temperature agreed well with monthly field measurements at Site 326_4 (Figure 7a,b) and hourly Profiler data at Site 326_58 (Figure 8a,b) in the surface and bottom waters, and well captured the diurnal stratification pattern in the lake. The temperature calibration—per monthly data—was a strong fit as represented by a high R-value (surface: 0.975; bottom: 0.984), and high model accuracy as represented by a low RMSE (surface: 1.34; bottom: 1.09) and MAE (surface: 1.05; bottom: 1.00; Table 9). The temperature calibration—per high-resolution hourly data—was an even stronger fit as represented by a high R-value (surface: 0.988; bottom: 0.992), and low RMSE (surface:

0.81; bottom: 0.71) and MAE (surface: 0.58; bottom: 0.55; Table 9). Temperature validation using the monthly field measurements and hourly profiler data returned similarly strong values (Table 9).

Table 9 Lake height and temperature performance statistics of the Lake Waikare model. Statistics include Pearson correlation (R), root mean squared error (RMSE), and mean absolute error (MAE). Calibration period 1 July 2017 through 30 June 2019, Validation 1 July 2019 through 30 June 2021. Statistics are based on comparisons to the hour, at either an hourly or monthly resolution as noted. 'Height' compared at Site 3 (326_6), 'Temp – Monthly' at Site 1 (326_4), and 'Temp – Hourly' at Site 2 (326_58).

	Calibration			Validation		
	R	RMSE	MAE	R	RMSE	MAE
Height – Hourly	0.985	0.02	0.01	0.993	0.02	0.01
Temp. – Monthly						
Surface	0.975	1.34	1.05	0.970	1.80	1.37
Depth	0.984	1.09	1.00	0.988	0.79	0.69
Temp. – Hourly						
Surface	0.988	0.81	0.58	0.981	0.87	0.61
Depth	0.992	0.71	0.55	0.988	0.71	0.54

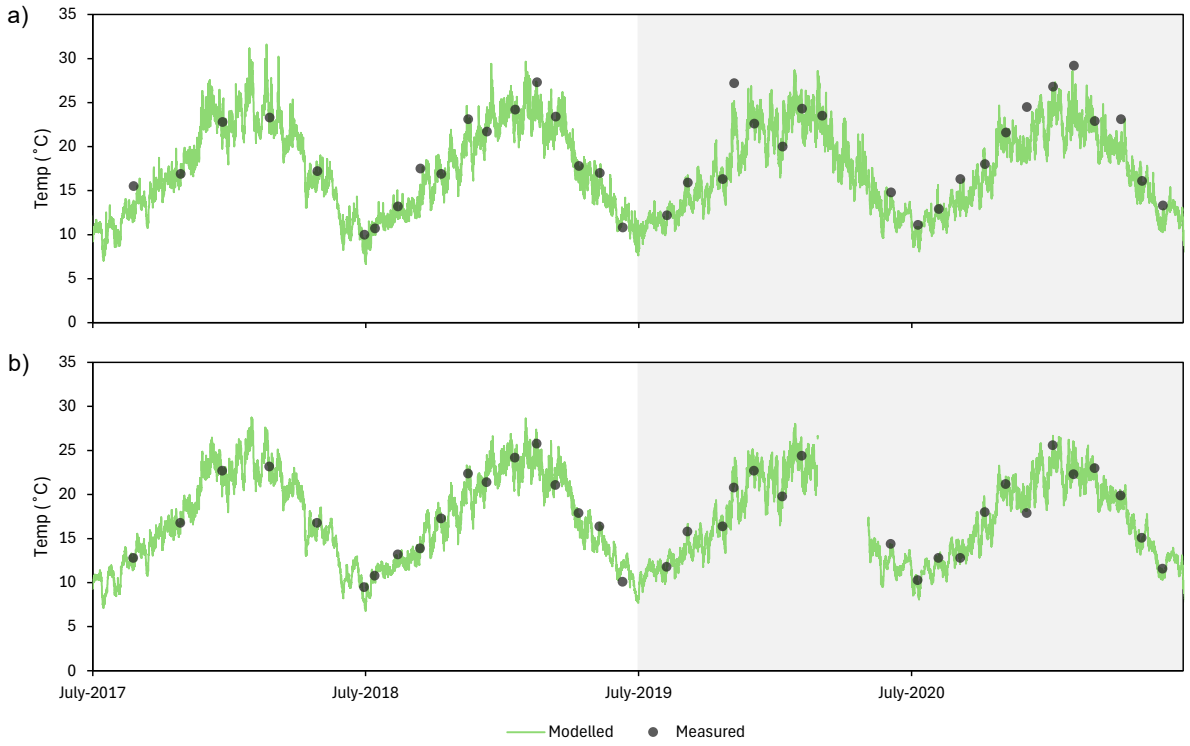

Figure 7: Measured vs modelled Temperature (Temp) at the Lake Waikare regular monitoring Site 1 (326_4), during the calibration and validation periods, at a) 0.0 m depth, and f) 1.2 m depth. Calibration period 1 July 2017 through 30 June 2019 (light grey), Validation 1 July 2019 through 30 June 2021 (mid grey). Modelled data is hourly, and measured data is on the hour.

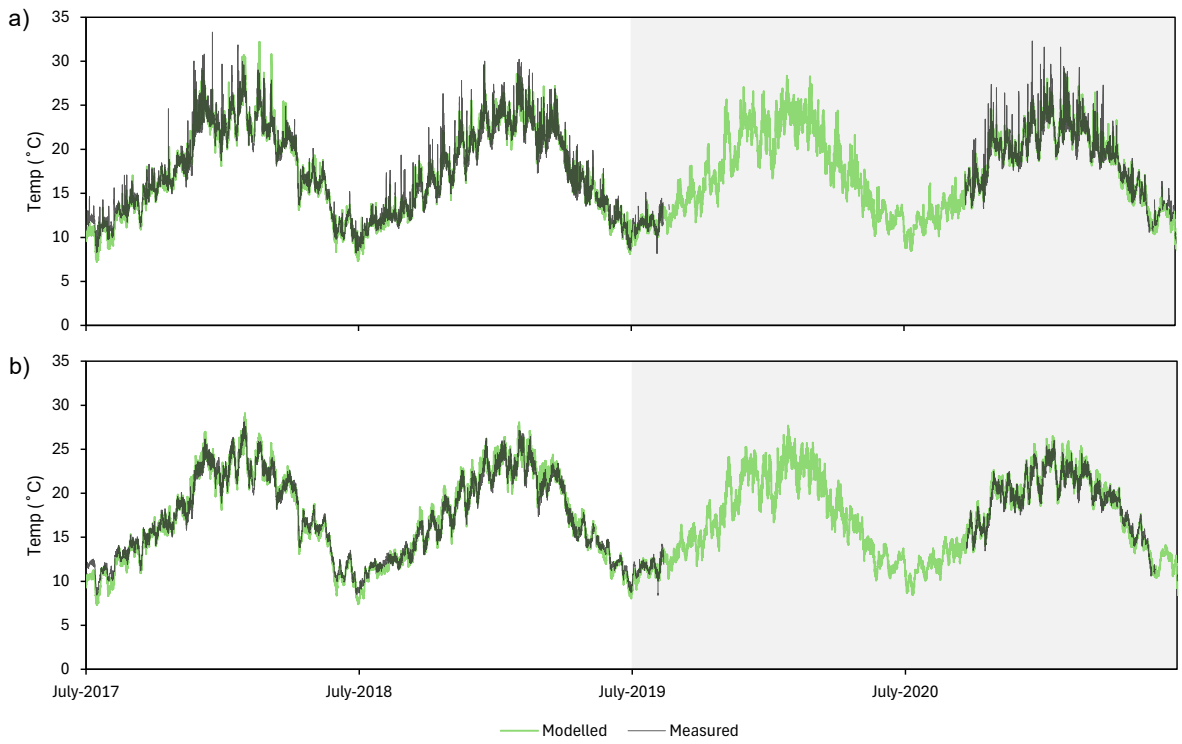

Figure 8: Measured vs modelled Temperature (Temp) at the Lake Waikare monitoring buoy Site 2 (326_58), during the calibration and validation periods, at a) 0.0 m depth, and f) 0.1 m from the lakebed. Calibration period 1 July 2017 through 30 June 2019 (light grey), Validation 1 July 2019 through 30 June 2021 (mid grey). Modelled and measured data is hourly.

4.1.2 Water quality

Simulations of DO agreed sufficiently well with monthly field measurements at Site 326_4 in the surface and bottom waters (Table 9; Figure 9a,b), and except for sporadic elevated values well captured the seasonal pattern in the lake. Specifically, model calibration in terms of R-value, agreed well at depth (0.789), but not at the surface (0.287; Table 9). Model calibration, in terms of RMSE and MAE, agreed less well with both surface (Table 9), in large part due to the sporadic elevated values (Figure 9a,b). DO validation returned similar R, RMSE, and MAE values to the calibration (Table 9).

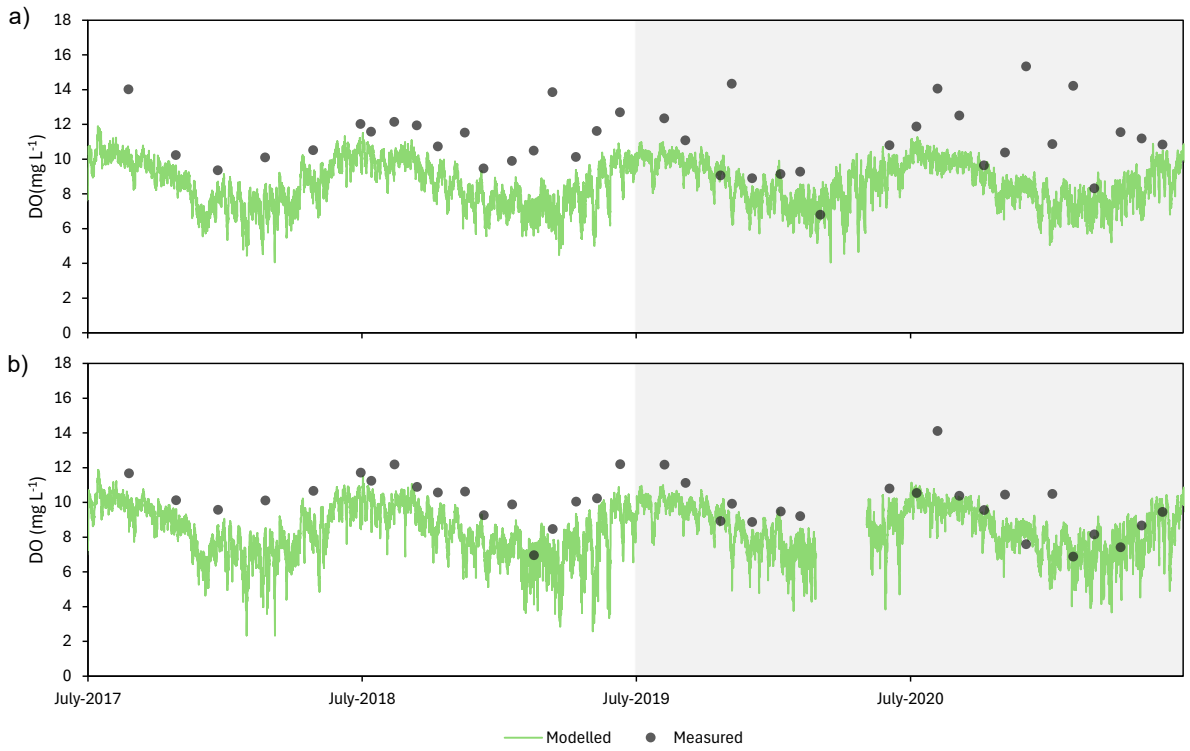

Figure 9: Measured vs modelled dissolved oxygen (DO) at the Lake Waikare regular monitoring Site 1 (326_4), during the calibration and validation periods, at a) 0.0 m depth, and f) 1.2 m depth. Calibration period 1 July 2017 through 30 June 2019 (light grey), Validation 1 July 2019 through 30 June 2021 (mid grey). Modelled data is hourly, and measured data on the hour.

Table 10 Dissolved oxygen performance statistics of the Lake Waikare model. Statistics include Pearson correlation (R), root mean squared error (RMSE), and mean absolute error (MAE). Calibration period 1 July 2017 through 30 June 2019, Validation 1 July 2019 through 30 June 2021. Statistics are based on comparisons to the hour, at either an hourly or monthly resolution as noted. As compared at Site 1 (326_4).

Depth	Calibration			Validation		
	R	RMSE	MAE	R	RMSE	MAE
0 m	0.287	2.93	2.52	0.070	3.43	2.54
1.2 m	0.789	2.27	2.09	0.535	2.03	1.52

Simulations of lake P as TP (Figure 10a) and DRP (Table 11; Figure 10b) agreed sufficiently well with monthly field measurements, although the simulations typically underestimated DRP throughout the majority of the year and overestimated a DRP peak from May 2018 through July 2018. Specifically, model calibration agreed well with measured data in terms of R-value (TP = 0.497; DRP = 0.593) and for TP per RMSE (0.042) and MAE (0.033; Table 11), but less so for DRP per RMSE (0.004) and MAE (0.004; Table 11; Figure 9a,b). TP validation returned similar values to the calibration in terms of all three metrics, however DRP saw a decline in R-value but returned similar values in terms of RMSE and MAE (Table 11).

Table 11 Phosphorus, nitrogen, and inorganic suspended solids, chlorophyll *a* , and Secchi depth performance statistics for the Lake Waikare model. Statistics include Pearson correlation (R), root mean squared error (RMSE), and mean absolute error (MAE). Calibration period 1 July 2017 through 30 June 2019, Validation 1 July 2019 through 30 June 2021. Statistics are based on modelled daily means, and measured samples. As compared at Site 1 (326_4).

	Calibration			Validation		
	R	RMSE	MAE	R	RMSE	MAE
Total Phosphorus	0.497	0.042	0.033	0.571	0.052	0.039
Dissolved Reactive P	0.593	0.004	0.004	-0.074	0.004	0.004
Total Nitrogen	0.504	1.17	0.89	0.486	2.35	1.98
Ammonium	-0.205	0.02	0.01	0.036	0.22	0.06
Nitrate	0.635	0.17	0.08	0.799	0.22	0.09
Inorganic SS	0.660	23.6	18.4	0.898	18.4	13.1
Chlorophyll *a*	0.342	69.3	52.2	0.093	233.8	153.4
Secchi depth	0.238	0.11	0.08	0.473	0.05	0.04

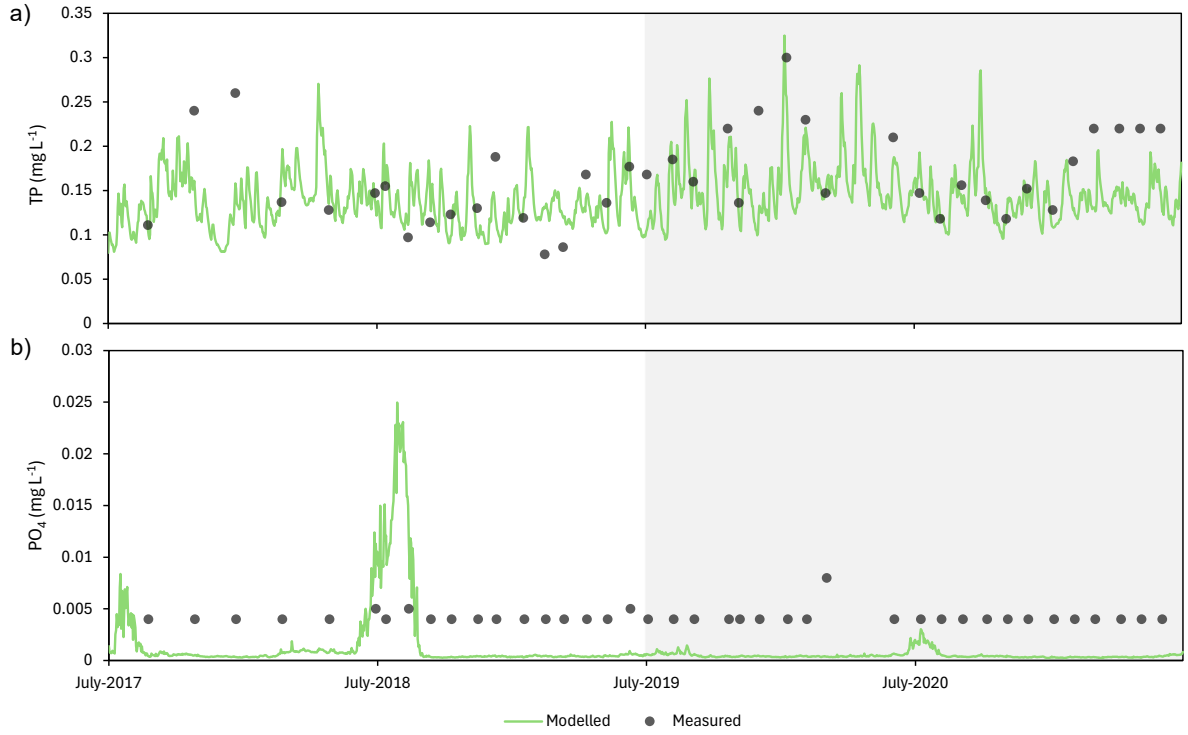

Figure 10: Measured vs modelled total phosphorus (TP) and dissolved reactive phosphorus (DRP) at Site 1 (326_4), during the calibration and validation periods, with a) surface water TP, and b) surface water DRP. Measured data determined as that 326_6 as part of WRC sampling program, at Modelled data as that extracted at the same point at 0.2 m depth. Calibration period 1 July 2017 through 30 June 2019 (light grey), Validation 1 July 2019 through 30 June 2021 (mid grey). Modelled data is a daily mean. N.b. potentially erroneous measured TP values (same value four samples in succession) at the end of the validation period; DRP mostly below detection limit (0.004 mg L^{-1}).

Simulations of lake N as TN (Figure 11a), NH_4 (Figure 11b), and NO_3 (Figure 11c), largely agreed well with monthly field measurements (Table 11). In particular, model calibration for TN and NO_3 agreed well with measured data in terms of R-value (TN = 0.504; NO_3 = 0.635) and for RMSE (TN = 1.17; NO_3 = 0.017) and MAE (TN = 0.89; NO_3 = 0.01; Table 11; 0.004; Table 11). On the other hand, model calibration for NH_4 agreed well with measured data in terms of RMSE (0.02), or MAE (0.01; Table 11), but not R-value (-0.205; Table 11). TN, NH_4, and NO_3 validation returned similar values to the calibration in terms of all three metrics (Table 11).

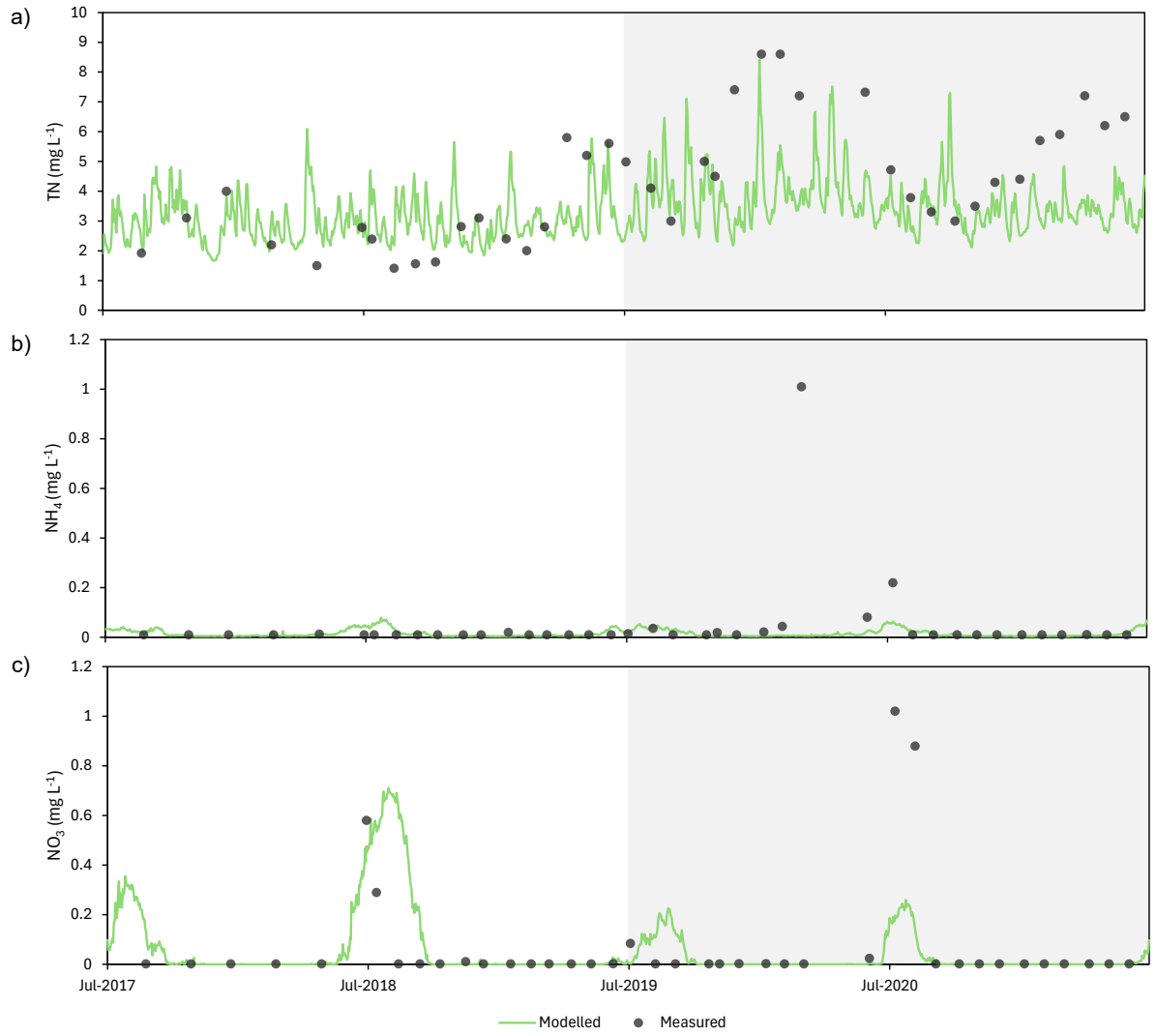

Figure 11: Measured vs modelled total nitrogen (TN), ammonium (NH_4), nitrate (NO_3) at Site 1 (326_4), during the calibration and validation periods, with a) surface water TN, b) surface water NH_4, and d) surface water NO_3. Measured data determined as that 326_6 as part of WRC sampling program, at Modelled data as that extracted at the same point at 0.2 m depth. Calibration period 1 July 2017 through 30 June 2019 (light grey), Validation 1 July 2019 through 30 June 2021 (mid grey). Modelled data is a daily mean.

Model simulations for ISS agreed well with monthly field measurements (Table 11; Figure 12), as evidenced by a high R-value (0.660), and low RMSE (23.6) and MAE (18.0). For chlorophyll *a*, model simulations agreed moderately well with monthly field measurements (Table 11; Figure 13), as represented by a low R-value (0.342), and moderate RMSE (69.3) and MAE (52.2). Cyanobacteria (Appendix 6), other-phytoplankton (Appendix 7), and chlorophyll *a* (Appendix 8) exhibited spatial variation, with periods when concentrations were notably higher in the southern basin than in the larger northern basin. For Secchi depth, model simulations agreed moderately well with monthly field measurements (Table 11; Figure 14), as represented by a low R-value (0.238), yet low RMSE (0.11) and MAE (0.08). ISS and Secchi depth validation saw an improved values, however chlorophyll *a* saw a reduction primarily coinciding with the largest measured bloom on record in the lake.

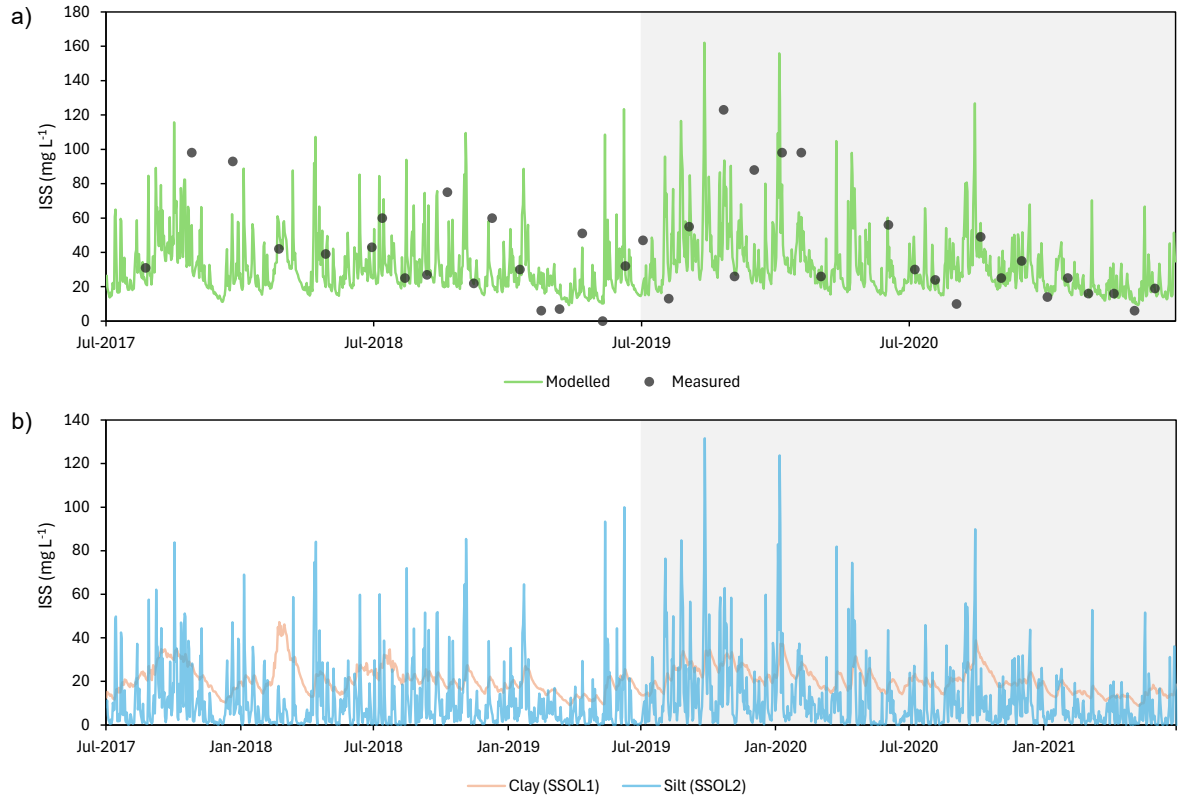

Figure 12: a) Measured vs modelled inorganic suspended solids (ISS), at Site 1 (326_4), during the calibration and validation periods, and b) the breakdown of the modelled clay and silt subgroups. Measured data determined as that Site 1 (326_4) as part of WRC sampling program, and Modelled data as that extracted at the same point at 0.2 m depth. Calibration period 1 July 2017 through 30 June 2019 (light grey), Validation 1 July 2019 through 30 June 2021 (mid grey). Modelled data is a daily mean.

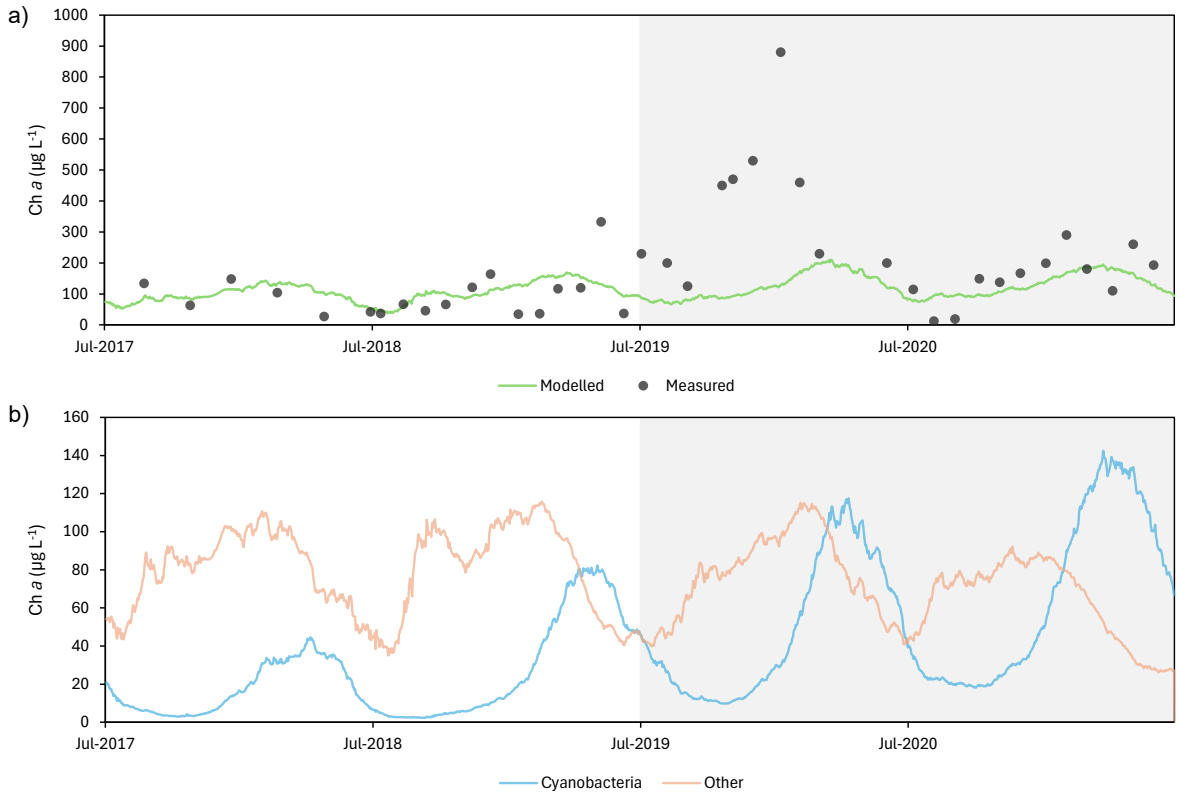

Figure 13: a) Measured vs modelled chlorophyll *a* (Chl a) at Site 1 (326_4), during the calibration and validation periods, and b) the breakdown of the phytoplankton assemblage as cyanobacteria and other. Measured data determined as that Site 1 (326_4) as part of WRC sampling program, and Modelled data as that extracted at the same point at 0.2 m depth. Calibration period 1 July 2017 through 30 June 2019 (light grey), Validation 1 July 2019 through 30 June 2021 (mid grey). Modelled data is a daily mean.

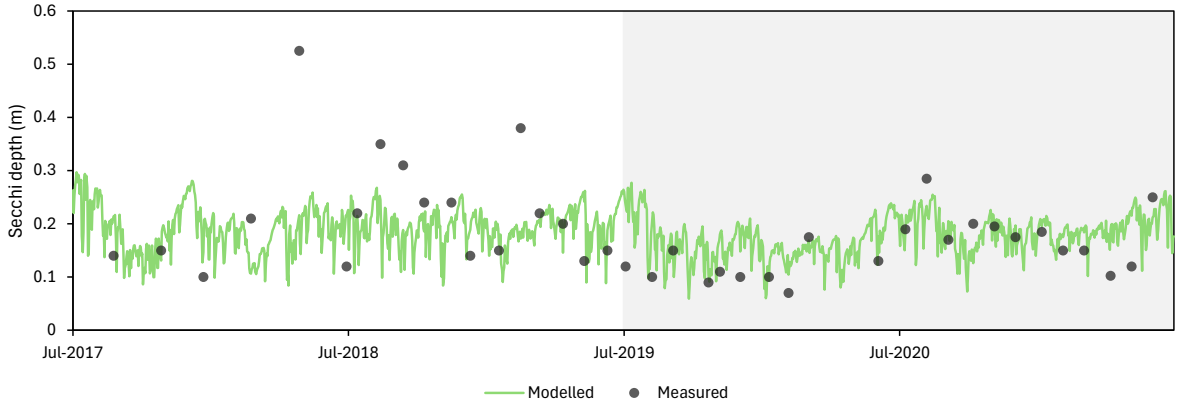

Figure 14: Measured vs modelled Secchi depth, at Site 1 (326_4), during the calibration and validation periods. Measured data determined as that Site 1 (326_4) as part of WRC sampling program, and Modelled data as that extracted at the same point at 0.2 m depth. Calibration period 1 July 2017 through 30 June 2019 (light grey), Validation 1 July 2019 through 30 June 2021 (mid grey). Modelled data is a daily mean.

4.2 Model output

4.2.1 Management measures applied in isolation only

Raising the minimum and maximum water level in the lake (Scenario 3.1) proved to be more effective in improving water quality than the maximum water level only (Scenario 2.1), reducing catchment

nutrient loading (Scenario 1.3), maximising Te Onetea inflow discharge rate (Scenario 1.2; Figure 15; Figure 16; Figure 17; Table 12). Raising the water maximum water level only (Scenario 2.1) was the second most effective, while reducing catchment nutrient loading (Scenario 1.3), and maximising Te Onetea inflow discharge rate (Scenario 1.2) were comparable in showing little improvement (Figure 15; Figure 16; Figure 17; Table 12).

Improvements in water quality were observed across all measures (Figure 15a-c; Figure 16a-c; Figure 17b; Table 12), except for cyanobacteria concentration (Figure 17a; Table 12) which increased despite these improvements, and total phytoplankton concentration which remain relatively unchanged (Figure 17c). Increases in cyanobacteria were most pronounced where catchment nutrient loading was reduced (Scenario 1.3) and minimum and maximum water level was raised (Scenario 3.1; Figure 17). However, increases were small where only the maximum water level was raised (Scenario 2.1) and zero where Te Onetea inflow discharge rate was maximised (Scenario 1.2; Figure 17).

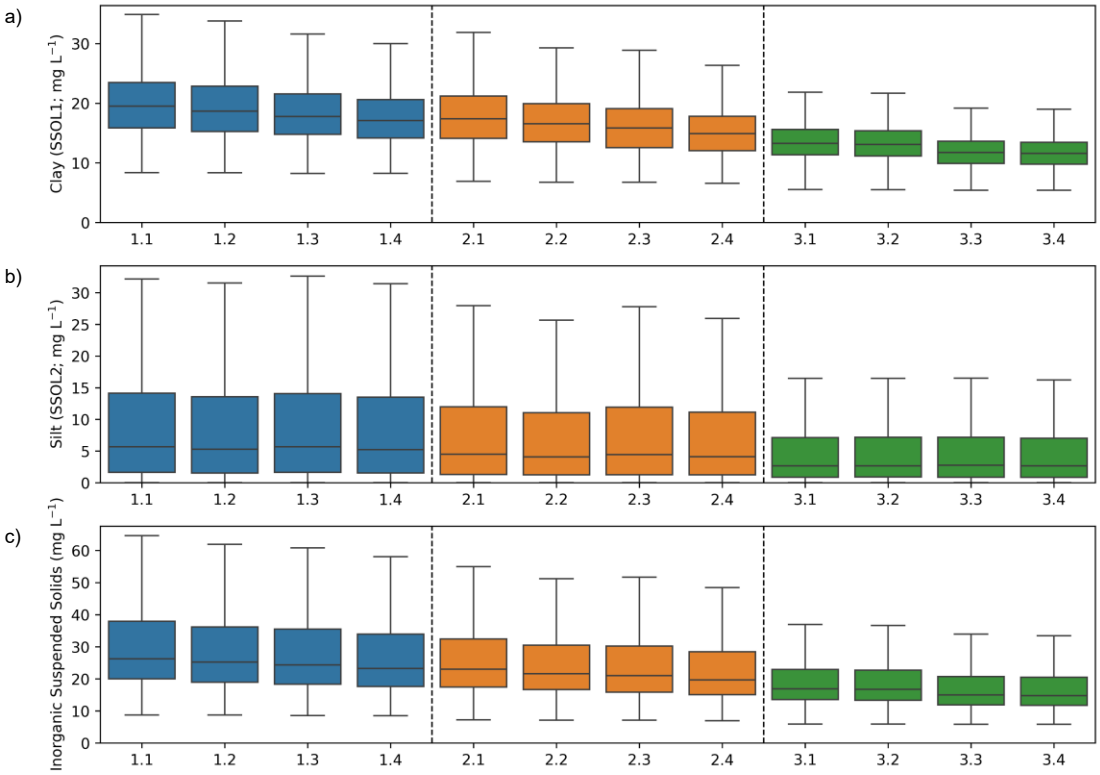

Min & Max WL increase	Current	Current	Current	Current	0 & 1 m	0 & 1 m	0 & 1 m	0 & 1 m	1 & 1 m	1 & 1 m	1 & 1 m	1 & 1 m
Catchment loading	Current	Current	Reduced	Reduced	Current	Current	Reduced	Reduced	Current	Current	Reduced	Reduced
Te Onetea inflow rate	Average	Maximum	Average	Maximum	Average	Maximum	Average	Maximum	Average	Maximum	Average	Maximum

Figure 15: Simulated a) Clay (SSOL1), b) Silt (SSOL2), and c) Inorganic Suspended Solids, as box plots—with outliers removed—of daily mean values across the simulation period of four limnological years (1 July 2017 through 30 June 2021) for the twelve scenarios as described in the table below panel 'c'. The box represents the interquartile range (IQR), spanning from the first quartile (Q1) to the third quartile (Q3), with the line within the box denoting the median value. The whiskers extend from the quartiles to the minimum and maximum values that lie within 1.5 times the IQR, excluding outliers. N.b. variable vertical scale; outliers removed; for equivalent figure with outliers included see Appendix 9, and for equivalent figure as a daily time series see Appendix 10.

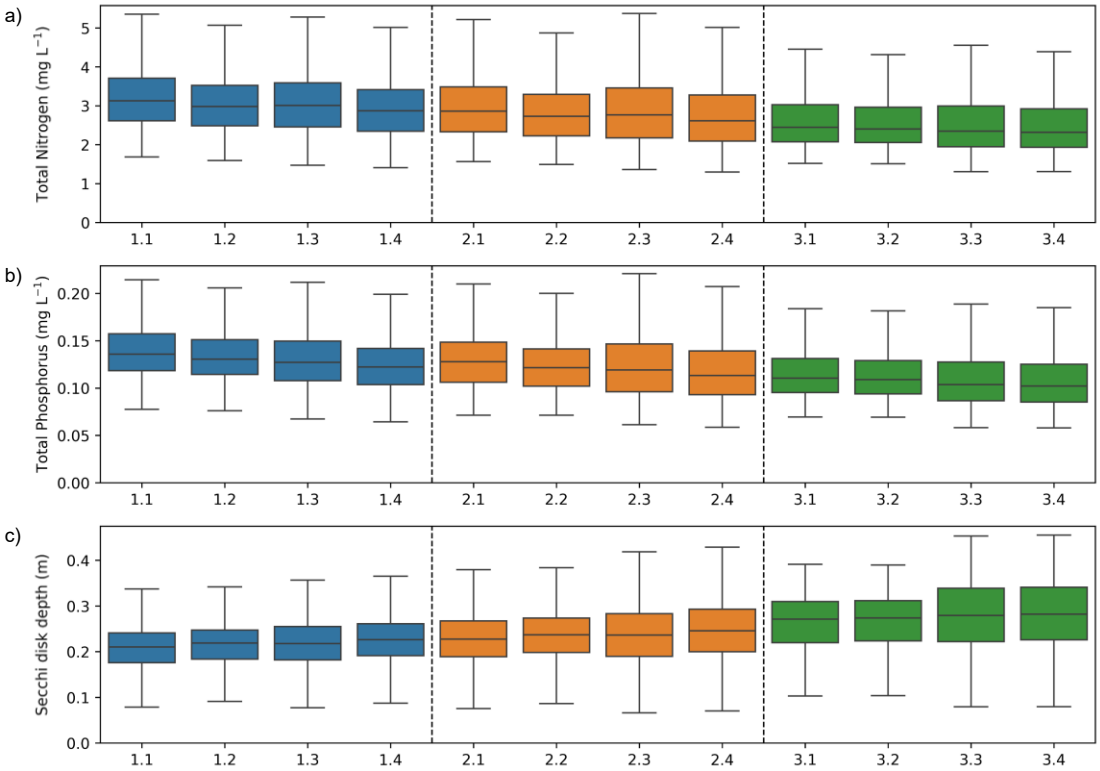

Min & Max WL increase	Current	Current	Current	Current	0 & 1 m	0 & 1 m	0 & 1 m	0 & 1 m	1 & 1 m	1 & 1 m	1 & 1 m	1 & 1 m
Catchment loading	Current	Current	Reduced	Reduced	Current	Current	Reduced	Reduced	Current	Current	Reduced	Reduced
Te Onetea inflow rate	Average	Maximum	Average	Maximum	Average	Maximum	Average	Maximum	Average	Maximum	Average	Maximum

Figure 16: Simulated a) total nitrogen, b) total phosphorus, and c) Secchi disk depth, as box plots—with outliers removed—of daily mean values across the simulation period of four limnological years (1 July 2017 through 30 June 2021) for the twelve scenarios as described in the table below panel 'c'. The box represents the interquartile range (IQR), spanning from the first quartile (Q1) to the third quartile (Q3), with the line within the box denoting the median value. The whiskers extend from the quartiles to the minimum and maximum values that lie within 1.5 times the IQR, excluding outliers. N.b. variable vertical scale; outliers removed; for equivalent figure with outliers included see Appendix 11, and for equivalent figure as a daily time series see Appendix 12.

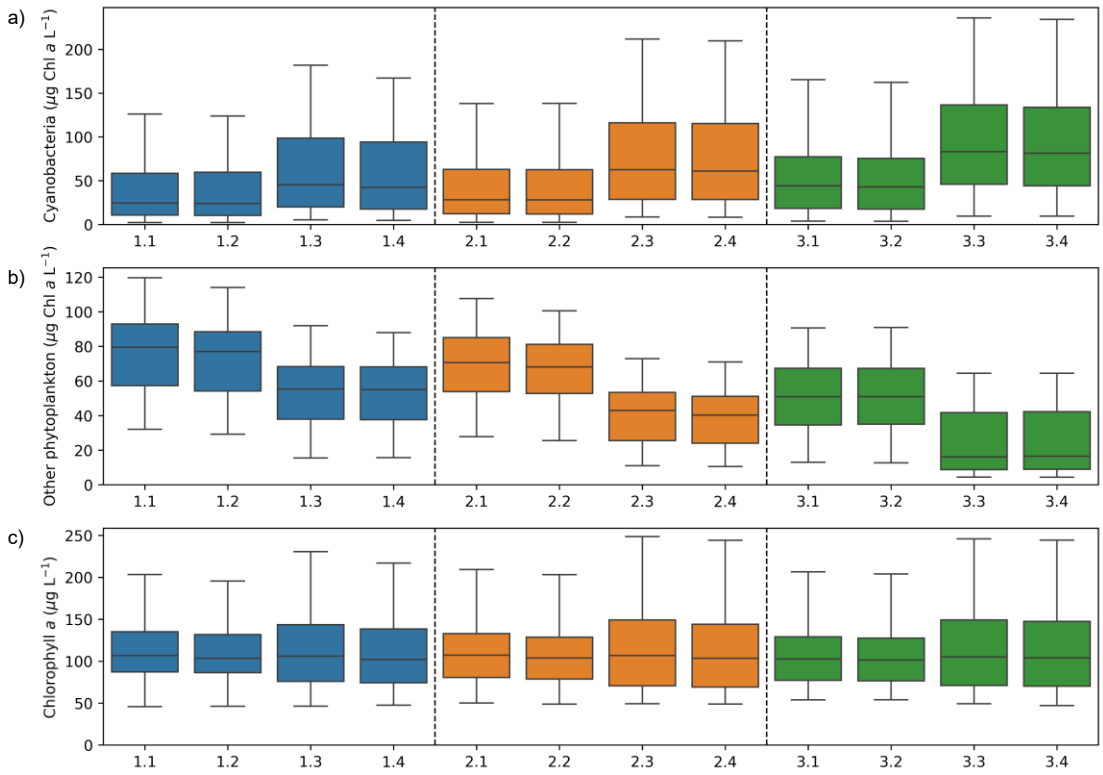

Min & Max WL increase	Current	Current	Current	Current	0 & 1 m	0 & 1 m	0 & 1 m	0 & 1 m	1 & 1 m	1 & 1 m	1 & 1 m	1 & 1 m
Catchment loading	Current	Current	Reduced	Reduced	Current	Current	Reduced	Reduced	Current	Current	Reduced	Reduced
Te Onetea inflow rate	Average	Maximum	Average	Maximum	Average	Maximum	Average	Maximum	Average	Maximum	Average	Maximum

Figure 17: Simulated a) cyanobacteria, b) other-phytoplankton, and c) chlorophyll *a*, as box plots—with outliers removed—of daily mean values across the simulation period of four limnological years (1 July 2017 through 30 June 2021) for the twelve scenarios as described in the table below panel 'c'. The box represents the interquartile range (IQR), spanning from the first quartile (Q1) to the third quartile (Q3), with the line within the box denoting the median value. The whiskers extend from the quartiles to the minimum and maximum values that lie within 1.5 times the IQR, excluding outliers. N.b. variable vertical scale; outliers removed; for equivalent figure with outliers included see Appendix 13. and for equivalent figure as a daily time series see Appendix 14.

Table 12 Heatmap of percentage changes in median water quality parameters for each scenario relative to baseline (i.e., Scenario 1.1)

	Scenario											
	1.1	1.2	1.3	1.4	2.1	2.2	2.3	2.4	3.1	3.2	3.3	3.4
Scenario description												
Min & Max WL increase	Current	Current	Current	Current	0 & 1 m	0 & 1 m	0 & 1 m	0 & 1 m	1 & 1 m	1 & 1 m	1 & 1 m	1 & 1 m
Catchment loading	Current	Current	Reduced	Reduced	Current	Current	Reduced	Reduced	Current	Current	Reduced	Reduced
Te Onetea inflow rate	Average	Maximum	Average	Maximum	Average	Maximum	Average	Maximum	Average	Maximum	Average	Maximum
Scenario result												
Clay (SSOL1)	N/A	-4.1%	-8.7%	-12.3%	-10.8%	-14.9%	-19.0%	-23.6%	-31.8%	-32.8%	-40.0%	-40.5%
Silt (SSOL2)	N/A	-7.0%	0.0%	-8.8%	-21.1%	-28.1%	-22.8%	-28.1%	-52.6%	-52.6%	-52.6%	-52.6%
Inorganic suspended solids	N/A	-3.8%	-7.3%	-11.5%	-12.2%	-17.6%	-19.8%	-24.8%	-35.5%	-36.3%	-42.7%	-43.5%
Total nitrogen	N/A	-4.8%	-3.8%	-8.3%	-8.6%	-12.8%	-11.8%	-16.3%	-22.0%	-23.3%	-24.9%	-25.9%
Total phosphorus	N/A	-7.1%	-7.1%	-14.3%	-7.1%	-14.3%	-14.3%	-21.4%	-21.4%	-21.4%	-28.6%	-28.6%
Secchi disk depth	N/A	4.8%	4.8%	9.5%	9.5%	14.3%	14.3%	19.0%	28.6%	28.6%	33.3%	33.3%
Cyanobacteria	N/A	0.0%	87.5%	75.0%	16.7%	16.7%	162.5%	154.2%	83.3%	79.2%	245.8%	237.5%
Other-phytoplankton	N/A	-2.5%	-30.4%	-30.4%	-10.1%	-13.9%	-45.6%	-49.4%	-35.4%	-35.4%	-79.7%	-79.7%
Total phytoplankton	N/A	-3.7%	-0.9%	-4.7%	0.0%	-2.8%	0.0%	-3.7%	-3.7%	-5.6%	-1.9%	-2.8%

4.2.2 Management measures applied in isolation and combination

No single management strategy was shown to improve water quality by more than 26% for TN, 29% for TP, 33% for Secchi disk depth, and 6% for chlorophyll *a*, respectively. However, given the hypertrophic nature of the lake, such improvements are by no means trivial and equate to reductions of up to 0.810 mg L^{-1} for TN, 0.034 mg L^{-1} for TP, 5.3 µg L^{-1} for chlorophyll *a*, and improvements of 0.07 m for Secchi disk depth. Increasing the minimum and maximum water level in the lake alongside other management measures (Scenarios 3.2–3.4) proved to be more effective than increasing the minimum and maximum water level alone (Scenarios 3.1) and all other combinations (Scenarios 1.2–1.4 and 2.2–2.4; Figure 15; Figure 16; Figure 17; Table 12). This additional benefit, however, varied from negligible to small-moderate. For example, increasing the minimum and maximum water level alongside maximising Te Onetea inflow discharge rate (Scenario 3.2) provided little-to-no additional benefit, while increasing the minimum and maximum water level alongside reducing catchment nutrient loading (Scenario 3.3) provided a small-to-moderate additional benefit. Similarly, increasing the minimum and maximum water level alongside both maximising Te Onetea inflow discharge rate and reducing catchment nutrient loading (Scenario 3.4), provided little-to-no additional benefit than increasing the minimum and maximum water level alongside only reducing catchment nutrient loading (Scenario 3.3).

Improvements in water quality were observed across all measures (Figure 15a-c; Figure 16a-c; Figure 17b; Table 12), except for cyanobacteria concentration (Figure 17a; Table 12) which increased despite these improvements, and total phytoplankton concentration which remain relatively unchanged (Figure 17c). Increases in cyanobacteria were most pronounced where the minimum and maximum water level was increased by 1 m, and catchment nutrient loading was reduced, which was associated with the greatest reduction in TP concentrations and improvement in Secchi depth.

5 DISCUSSION

The aim of this study was to apply a process-based modelling approach to investigate the effects of changes in the hydrodynamic regime (as lakes minimum and maximum water level, and Te Onetea inflow discharge rate), both in isolation and in combination with hypothetical reductions in catchment nutrient loading, on water quality in Lake Waikare. The study also aimed to contribute to the identification of adaptive management strategies that could mitigate potential conflicts and maximise the overall benefits to both Lake Waikare and the broader flood protection scheme. The twelve scenarios investigated in this study provided valuable insights into the potential impacts of modifying minimum and maximum lake levels, catchment nutrient loading, and Te Onetea inflow discharge rate, both independently and in combination. Scenario testing also revealed that broad-scale improvements in water quality, such as increased Secchi disk depth and small reductions in N and P concentrations, may lead to greater cyanobacterial dominance in the lake.

5.1 Interpretating scenario simulations

The scenario simulations offer insights into the effects of various plausible management strategies that cannot be assessed in situ. Interpretation of management strategy outcomes should be interpreted with the following caveats and the calibration limitations in mind.

5.1.1 Model caveats

The simulation period (1 July 2017 through 30 June 2021) coincided with a relative dry period, especially in the latter two years. As a result, the number of days Te Onetea was opened to discharge into Lake Waikare, according to criteria in the LWWFCS (Figure 4), may have been reduced. Combined with lower catchment inflows, this likely prevented the lake from reaching or maintaining typical annual water levels. Despite this, the relative difference between the three water level scenarios was well controlled.

The impact of increasing the Te Onetea flow rate was constrained by the LWWFCS. These constraints resulted in average daily inflow discharge values of 1.33 and 1.94 $m^3\ s^{-1}$ for scenarios 1.1 (Base height, current catchment, current Te Onetea discharge) and 1.4 (Base height, current catchment, maximum Te Onetea discharge), respectively. As a result, the scenario involving increased Te Onetea inflow discharge only yielded modest improvements of 5%, 7%, and 4% for TN, TP, and chlorophyll *a*, respectively. These improvements are substantially lower than those reported in Cooke and Cox (2015), where even the lowest discharge scenario (5 $m^3\ s^{-1}$) produced 39%, 33%, and 42% improvements for TN, TP, and chlorophyll *a*, respectively. This discrepancy likely stems from our application of the increased discharge rate under real-world constraints, whereas Cooke and Cox (2015) applied a hypothetical constant discharge rate of 5 $m^3\ s^{-1}$. We consider a constant 5 $m^3\ s^{-1}$ inflow discharge rate an impractical scenario given the role Lake Waikare plays in the wider flood protection scheme. However, there is scope to further explore scenarios where the current flood protection restrictions do not apply (i.e., more water flushed through the system), to better understand the benefits of increased flow rate and flushing on water quality improvements in the lake.

The extent of the lake was clipped to 5.6 m Moturiki Datum, reflecting its standard maximum operational level. This decision was based on uncertainties surrounding the lake's flooding extent (e.g., stopbanks), unknown sediment conditions in potential flood zones, the complexity of adjusting catchment inflows for a reduced catchment area, and the potential inclusion of adjacent lakes under higher water levels. Although this clipping may slightly underestimate wind-induced turbulence, due

to reduced shallow areas in potential flood areas, it was considered the most conservative approach for minimising additional uncertainty in the scenario simulations.

5.1.2 Model calibration

Developing a coupled hydrodynamic-ecological model, with confidence in its ability to capture and represent specific lake, requires considerable time and effort spent on model calibration. The time and effort involved in model calibrations is typically related to; data availability, the state of knowledge, and summarising complex biogeochemical or ecological aspects in more general terms.

The model was able to well represent temperature, evidenced by strong model fit and accuracy, and importantly the intermittent diurnal stratification patterns in the lake. This performance was only achievable through generation of a long-term wind dataset representative of on lake conditions (necessitated by limited on-site wind speed data), and the treatment of the near-infrared (NIR) extinction coefficient as a calibratable parameter. These approaches were informed by an extensive calibration effort and a sensitivity analysis examining the interaction between wind forcing which affects mixing depth and NIR extinction which influences vertical heat distribution. To address the generation of a long-term wind speed data set, various statistical transformations were applied to the long-term NIWA dataset in an attempt to replicate simulated temperature profiles produced using the two-year window of measured on-site wind data. However, standard transformation methods typically used for off-site wind datasets failed to replicate the water temperature dynamics forced by local wind conditions. A more targeted correction was found to be effective by adjusting the mean and standard deviation of wind speeds for each hour of the day, and redistributing these values based on empirical relationships with the two-year on-site dataset (see Section 3.2.2 Model set-up: Meteorology). Wind direction was not scaled, thus limiting the model's ability to simulate wind-driven horizontal heterogeneity. To address the unknown extent of NIR extinction in the lake, the Kd(NIR) was treated as a calibratable parameter and, following sensitivity analysis, increased from 1 to 7.5. This adjustment was supported by remote sensing data (M. Allan, pers. comm.) suggesting elevated NIR attenuation, and that NIR extinction would reasonably be expected to increase with PAR extinction; which Secchi disk depth readings in the lake indicate is typically 0.1–0.2 m. This increase in the NIR coefficient reduced excessive heat penetration below 0.5 m and, when combined with improved wind forcing, enabled the model to simulate the shallow, diurnal thermocline structure observed in situ.

DO was moderately well represented in the model. This was largely due to a lack of depth-resolved data, with the automated profiler data unusable likely due to biological fouling, and the monthly monitoring program lacking the frequency to capture the intermittent nature of diurnal stratification, which typically peaks later in the day than the ~1300 hrs sampling time. Additionally, the model's limited ability to reproduce fine-scale surface processes such as oxygen generation from whitecapping, commonly observed in the lake, may have further contributed to the discrepancy.

Nitrogen (excluding NH_4) and P dynamics were relatively well represented in the model, as evidenced by a moderate to strong model fit and adequate model accuracy (Table 11). However, several factors likely limited a stronger fit, including data resolution and unmeasured system processes. For N and P, temporal and spatial irregularities in nutrient loading, particularly for DRP, NH_4, and NO_3, likely arose from the monthly resolution of nutrient inflow data for the Te Onetea and Matahuru streams, assumptions around inflows from ungauged catchments, and the simplified representation of atmospheric deposition. For P, DRP as measured in situ is a poor proxy for PO_4 which is output in silico. Although often conflated, DRP can overestimate true PO_4 concentrations by up to three orders of magnitude, with the discrepancy being non-linear and system-dependent (Hudson et al., 2000).

This mismatch, alongside measured DRP concentrations mostly being below the detection limit, likely explains the lower simulated PO_4 concentrations relative to DRP observations used in model calibration and validation. For N, nitrogen fixation was not modelled due to its complexity, the lack of supporting observational data, and the high degree of uncertainty its inclusion can introduce. Although the approach taken for estimating N and P inputs from ungauged catchments and atmospheric deposition was robust given available data, additional in situ measurements would have improved model performance.

The model was able to well represent ISS, but only moderately well represent the phytoplankton community. ISS was separated into two size classes representing clay and silt, and when combined with the statistical transformations applied to wind speed data (used to replicate wind-induced turbulence), was able to reproduce a strong fit for ISS in the lake. Phytoplankton was divided into two functional groups representing cyanobacteria and other-phytoplankton, but the model was only able to adequately reproduce total biomass in the lake. This limitation likely stems from insufficient data to describe the temporal dynamics of phytoplankton inputs from the Te Onetea inflow; the calibration-validation period coinciding with the largest recorded bloom at the site (dominated by *Monoraphidium* spp.); limited understanding of the infrequent bloom behaviour observed in situ, especially for cyanobacteria and *Monoraphidium* spp.; and the need to group dozens of species, many with little or no consistent seasonality, into two simplified functional groups. Despite these constraints, we are confident that the calibration applied to the two phytoplankton groups effectively capture a representative mean biomass for the lake.

5.2 Scenario simulations

No single management strategy—whether applied individually or in combination—was shown to improve water quality by more than 26% for TN, 29% for TP, 33% for Secchi disk depth, and 6% for chlorophyll *a*, respectively. Therefore, no strategy was effective in improving water quality sufficiently for the system to meet the national bottom line under the National Policy Statement for Freshwater Management 2020 (NPS-FM 2020). Despite this, given the hypertrophic nature of the lake, such changes are by no means trivial and equate to reductions of up to 0.810 mg L^{-1} for TN, 0.034 mg L^{-1} for TP, 5.3 µg L^{-1} for chlorophyll *a*, and improvements of 0.07 m for Secchi disk depth.

Hydrological modification through altering the lake level height provided the greatest overall improvement in water quality among all management measures applied individually. The most substantial benefit occurred when both minimum and maximum water levels were raised by one meter (average of 16.9% improvement across all variables). This was followed in effectiveness by increasing the maximum water level alone (average of 6.3% improvement across all variables), reducing catchment nutrient loading (average of 3.8% improvement across all variables), and, lastly, maximising Te Onetea inflow discharge rate (average of 3.6% improvement across all variables). Raising lake levels reduced wind-induced resuspension of particulate matter from the lakebed. As a result, concentrations of suspended solids, and the associated bound N and P in the water column decline, leading to increased Secchi disk depth and reduced availability of particulate nutrients for decomposition and mineralisation. Furthermore, relatively modest improvements from reducing catchment nutrient loading further support the idea that internal dynamics, shaped by lake level, are the dominant drivers of water quality. These results underscore the extent of the N and P legacies in the lake, accumulated over nearly a century, and how they continue to influence water quality.

Hydrological modification through raising lake levels, when combined with other measures, provided additional benefits, particularly when paired with reducing catchment nutrient loading. Specifically,

the combination of raising both minimum and maximum water levels, reducing catchment nutrient loading, and maximising Te Onetea inflow discharge rate resulted in the greatest overall improvement in water quality. However, adding the maximising Te Onetea inflow discharge rate to the combination of lake level increases and catchment nutrient loading reductions provided little additional benefit. This suggests that effective long-term management of the lake will require addressing both internal processes by raising lake levels and external inputs through reducing catchment nutrient loading.

Despite overall improvements in water quality, all management strategies were associated with elevated cyanobacterial biomass, albeit while total phytoplankton biomass remained relatively stable. This shift appears to be driven by the reduction in suspended solids, and their associated bound N and P, in the water column, leading to greater light penetration (as indicated by increased Secchi disk depth) and reduced availability of particulate nutrients for decomposition and mineralisation. Further, increasing the lake water level or reducing catchment loading leads to lower in-lake concentrations of bioavailable N and P derived from catchment-derived inflows (particularly during the wet season when the phytoplankton assemblage is dominated by other-phytoplankton). The competitive advantage of cyanobacteria under improved light conditions and lower N and P availability is reflected in the model configuration of the two phytoplankton groups, with cyanobacteria configured as less competitive under extremely low light conditions, but more efficient under low P conditions. This is supported by a body of literature showing that cyanobacteria are ill adapted under low light conditions, and hence are configured in ecological models as such (e.g., Ghane & Boegman, 2023; Özkundakci et al., 2011), yet possess a suite of phosphorus acquisition strategies that give them a competitive advantage in phosphorus-depauperate conditions (Burford et al., 2023). These strategies include the ability to store P in access as polyphosphate bodies (Xiao et al., 2020), switch to high-affinity phosphorus uptake (Xiao et al., 2023) and to access dissolved organic phosphorus through the production of phosphatases (Xiao et al., 2023). Although the shift from low- to high-affinity phosphorus uptake or the use of DOP under low-phosphate conditions is unable to be explicitly parameterised in AEM3D, these two aspects were indirectly represented by assigning cyanobacteria a higher maximum phosphorus uptake rate and a lower half-saturation constant compared to the other-phytoplankton group. Despite this, the increases in cyanobacteria and reductions in the other-phytoplankton group must be interpreted with respect to the following: 1) each group represents group of which encapsulates multiple species, and 2) that the success of each group lies in their parameterisation (as outlined previously in this paragraph). Nevertheless, management activities that result in broad-scale improvements in water clarity and nutrient availability may in fact lead to an unintended shift towards greater cyanobacterial dominance in the lake.

5.3 Other findings

The annual nutrient budget calculated over 10 hydrological years (2013/14 through 2022/23) from the model's boundary conditions was 278.8 N t y^{-1} for TN and 29.5 P t y^{-1} for TP. This budget includes all external sources—Matahuru catchment, Te Onetea inflow, Te Kauwhata WWTP, the ungauged catchment, and atmospheric deposition—except potential nitrogen fixation by the phytoplankton community (Appendix 15). Our results align closely with the annual N and P loadings reported by Elliot (2015), with values of 384.1 t N y^{-1} and 22.5 t P y^{-1}, respectively, based on measured data, and 197.1 t N y^{-1} and 14.7 t P y^{-1}, respectively, based on modelled data. In contrast, our nutrient budget differs substantially from annual N and P loadings reported by Cooke and Cox (2015), with values of 578 t N y^{-1} and 96 t P y^{-1}, respectively. The discrepancy appears to be primarily related to differences in assumptions around the ungauged catchment. In our study N and P loading from ungauged catchments was estimated to be of 103.3 t N y^{-1} and 14.5 t P y^{-1} (Appendix 15), whereas Cooke and Cox (2015) calculated 363 t N y^{-1} and 74 t P y^{-1}, respectively. This difference likely arises from two key differences. First, Cooke and Cox (2015) derived nutrient concentrations for the ungauged

catchment by applying ratio factors of 2.2 for TN and 4.4 for TP to Matahuru Stream load-flow relationships (c.f., ratio factors of 1.42 for TN and 2.20 and TP in our study, through comparing the median Matahuru concentration and the median 'ungauged' volumetric mean concentration described in the methods). The factors in Cooke and Cox (2015), however, were based on a single Matahuru Stream measurement collected during an event in November 2014 versus the mean of three spot measurements at three other inflows collected during same event. These three measurements were significantly higher than those used in this study derived from approximately fortnightly collected annual data during 2017 and 2018 (A. Hopkins, Unpub.). This difference likely stems from the sites sampled in Cooke and Cox (2015) exhibiting disproportionately high nutrient concentrations relative to other locations, and nutrient levels at the sampled sites being coincidently elevated in November 2014, possibly contributing to an overestimation of TN and TP loadings derived from the ungauged catchment by factors of approximately ~1.5 and ~2.0, respectively. Second, we assume that Cooke and Cox (2015) included the surface area of the lake when calculating the surface area of ungauged catchment. This assumption is based on their catchment area calculations the Matahuru Stream portion being 51% of the total catchment, and the ungauged catchment being 49%. Our calculations show that that the Matahuru Stream catchment is 50.5% of the total catchment area, 16.4% as the lake, and 33.1% ungauged catchment; contributing to a further overestimation of TN and TP loadings from the ungauged catchment by a factor of ~1.5 in Cooke and Cox (2015).

Model simulations revealed substantial horizontal variation in lake height between the upper and lower reaches of Lake Waikare, with a maximum difference of 20.5 cm and a 90th percentile difference of 2.5 cm. These discrepancies reflect the influence of wind setup and inflows from the Matahuru inflow. These findings have practical implications for the accuracy of lake height (and therefore volume) measurements, as well as for inflow and outflow discharge rates based on gauging station–flow rate relationships. They also support our approach in constructing the daily water balance for the lake, in which we defined the measured water level as the 3-day mean of midnight lake height readings, and calculated the residual term in the water balance as a 15-day mean. This approach was adopted because using daily residuals without smoothing resulted in highly variable positive and negative residuals, and would have resulted in unrealistic daily volumes (and associated nutrient and sediment load) being added to or removed from the system daily.

5.4 Implications and future work

This study presented a set of scenarios, designed within the constraints of current hydrological management regimes (Figure 4; Grainger (2025)), to assess the effects of modifying the hydrological regime, specifically water levels in the lake and inflows from Te Onetea, and reducing nutrient loads from the catchment, both independently and in combination. The findings provide a foundational framework for future research to build upon, enabling; 1) exploration of a wider range of scenarios, 2) consideration of the logistics and practicalities in running specific scenarios, 3) investigation of the impact of plausible future climates, and the complex interactions among these three factors, and 4) investigation of the spatial variation in TSS and phytoplankton community.

In exploring a wider range of scenarios, future work could examine a wider variety of prescribed water level changes. This study assessed the impact of raising both the minimum and maximum lake levels by 1 m, showing that such an increase outperformed even the most optimistic land use change scenarios within the catchment. Future research could evaluate scenarios that restore the lake closer to its historical mean lake level (~1 m greater than present), and lake level fluctuation (2.36 m greater than present; Reeves et al., 2002)

In considering the logistics and practicalities in running specific scenarios, future work might consider three factors as described below. First, the lake grid might be broadened to include the lake's potential flooding extent. In this study, the grid was clipped at the lake's boundary corresponding to its target full supply level (i.e., 5.6 m Moturiki datum). Second, adjustments might be made to the Fish Pass Culvert outflow rate. In this study, outflow was determined using a polynomial relationship derived from measured discharge and lake level data. This approach resulted in a non-linear increase in outflow as water levels rise, due to increasing hydraulic head. Instead, future work might consider engineering modifications to the structure to reduce outflow under elevated lake levels. Third, assumptions around Te Onetea's operating regime might be revised, for example, that it remains closed when the Waikato River exceeds 6.5 m Moturiki datum, and that its maximum inflow discharge rate is 6.4 $m^3 s^{-1}$. In this study, the current operational conditions were applied; however, future simulations could explore engineering or management changes that allow for greater flow through the gate. If such restrictions were relaxed, the impact of increasing Te Onetea's discharge rate might be more pronounced than observed in the current scenario testing.

In investigating the impact of plausible future climates, future work might apply downscaled outputs from global climate models of Coupled Model Intercomparison Project Phase 6 (CMIP6; see Eyring et al., 2016). Unlike its predecessor CMIP5, CMIP6 provides data at hourly resolution, which, when dynamically downscaled (i.e., transformed into high-resolution, regionally specific data; Chapman et al., 2023), offers meteorological input for simulating future climate scenarios within the lake model, thus enabling robust stress-testing of hypothetical hydrological changes under plausible future climates. Given recent research suggesting that climate warming will lead to a higher frequency of extreme weather events such as flooding (Eccles et al., 2019; Stott, 2016), such scenario testing could yield valuable insights to inform long-term planning for the LWWFCS.

In investigating the spatial variation in TSS and phytoplankton community, future work might benefit from the application of remotely sensed TSS and chlorophyll *a* data (Allan, 2016). This data could be used to calibrate and validate the model on a spatial scale, thereby enabling scenario testing on a spatial scale. In this current study the limited time periods during which on-lake wind speed existed were used to statistically transform wind speed data from an adjacent NIWA site (see 'Methods: Modelling: Model set-up: Meteorology'). The approach allowed diurnal stratification of the lake to be captured, something not achievable using the raw NIWA data or conventional statistical transformations (see 'Discussion: Interpretating scenario simulations: Model calibration'). However, the method could not be applied to wind direction. We therefore acknowledge that investigation of the spatial extent of TSS and the phytoplankton community would require either the use of the limited periods of on-lake wind speed data, or the application of an adequate statistical transformation method for both wind speed and wind direction.

5.5 Conclusions

This study found that no single simulated management strategy for Lake Waikare, whether implemented individually or in combination, led to improvements in water quality exceeding 26% for TN, 29% for TP, 33% for Secchi disk depth, and 6% for chlorophyll *a*, respectively. Consequently, no strategy was effective in improving water quality for the system to meet the national bottom line under the NPS-FM 2020. However, given the hypertrophic nature of the lake, such improvements are by no means trivial and equate to reductions of up to 0.810 mg L^{-1} for TN, 0.034 mg L^{-1} for TP, 5.3 µg L^{-1} for chlorophyll *a*, and improvements of 0.07 m for Secchi disk depth. Scenario testing revealed, hydrological modification through increasing the minimum and maximum lake level height to provide the greatest overall improvement in water quality among management measures applied individually. This benefit was enhanced when combined with optimizing land use and increasing the

Te Onetea discharge rate. Scenario testing also provided valuable insights into the potential impacts of modifying minimum and maximum lake levels, catchment land use, and the discharge rate from Te Onetea, both independently and in combination. In addition, scenario testing helped to demonstrate the relative influence of the hydrological regime and catchment land use as key drivers of water quality decline in the lake, thereby aiding the identification of targeted management strategies. Interestingly, scenario testing also revealed that management activities that result in broad-scale improvements in water quality may in fact lead to an unintended shift towards greater cyanobacterial dominance in the lake.

6 ACKNOWLEDGEMENTS

We thank Mathew Allan and Michael Pingram for initiating the study, and the Waikato Regional Council for funding. We thank Areka Hopkins for supplying water quality data for Matahuru, Moana, Ohinewai, Onekura, Papaatawhai, and White streams. We thank David Hamilton and Kohji Muraoka for modelling advice. We thank Mafalda Bapista for providing phytoplankton data for Lake Waikare. We thank Steven Cornelius for discussions around lake height and discharge gauging. We thank Grant Tempero, Josh Smith, and Mafalda Bapista for providing thorough and insightful manuscript reviews. Waikato Regional Council provided bathymetric data, and flow and water quality data, and would like to thank the environmental data team and in particular Debbie Eastwood for providing all requested data. MetService provided meteorological data.

7 REFERENCES

Abell, J., McBride, C., & Hamilton, D. (2015). *Lake Rotorua Treated Wastewater Discharge: Environmental Effects Study* (ERI Report 80). U. o. W. Environmental Research Institute, Hamilton, New Zealand.

Allan, M. (2016). *Remote sensing of Waikato lakes* (ERI Report 93). U. o. W. Environmental Research Institute, Hamilton, New Zealand.

Bird, R. E., & Hulstrom, R. L. (1981). *A Simplified Clear Sky Model for Direct and Diffuse Insolation on Horizontal Surfaces* (SERI/TR-642-761). C. Solar Energy Research Institute, USA.

Bruce, L. C., Hamilton, D., Imberger, J., Gal, G., Gophen, M., Zohary, T., & Hambright, K. D. (2006). A numerical simulation of the role of zooplankton in C, N and P cycling in Lake Kinneret, Israel [Article]. *Ecological Modelling*, *193*(3-4), 412–436.

Burford, M. A., Anusuya, W., Man, X., J., P. M., & and Hamilton, D. P. (2023). Understanding the relationship between nutrient availability and freshwater cyanobacterial growth and abundance. *Inland Waters*, *13*(2), 143-152.

Chan, T. U., & Hamilton, D. P. (2001). Effect of freshwater flow on the succession and biomass of phytoplankton in a seasonal estuary. *Marine and Freshwater Research*, *52*(6), 869–884.

Chapman, S., Syktus, J., Trancoso, R., Thatcher, M., Toombs, N., Wong, K. K.-H., & Takbash, A. (2023). Evaluation of Dynamically Downscaled CMIP6-CCAM Models Over Australia. *Earth's Future*, *11*(11), e2023EF003548.

Chung, S. W., Hipsey, M. R., & Imberger, J. (2009). Modelling the propagation of turbid density inflows into a stratified lake: Daecheong Reservoir, Korea [Article]. *Environmental Modelling and Software*, *24*(12), 1467-1482.

Cooke, J., & Cox, T. (2015, 16-18 September, 2015). *Lake Waikare Water Quality Modeling: Using a New Model to Investigate Flushing Strategies* Water New Zealand Annual Conference,

Dean-Speirs, T., Neilson, N., Reeves, P., & Kelly, J. (2014). *Waikato region shallow lakes management plan: Volume 2* (Waikato Regional Council Technical Report 2014/59). H. Waikato Regional Council, New Zealand.

Eccles, R., Zhang, H., & Hamilton, D. (2019). A review of the effects of climate change on riverine flooding in subtropical and tropical regions. *Journal of Water and Climate Change*, *10*(4), 687-707.

Elliot, S. (2015). *Modelling Nutrient Loads in the Waikato and Waipa River Catchments: Development of catchment-scale models* (NIWA Client Report HAM2015-089). H. National Institute of Water & Atmospheric Research Ltd, New Zealand.

Eyring, V., Bony, S., Meehl, G. A., Senior, C. A., Stevens, B., Stouffer, R. J., & Taylor, K. E. (2016). Overview of the Coupled Model Intercomparison Project Phase 6 (CMIP6) experimental design and organization. *Geosci. Model Dev.*, *9*(5), 1937-1958.

Fischer, H. B., List, E. J., Koh, R. C. Y., Imberger, J., & Brooks, B. W. (1979). *Mixing in Inland and Coastal Waters*. Academic Press. New York, USA.

Ghane, A., & Boegman, L. (2023). The dissolved oxygen budget of a small Canadian Shield lake during winter. *Limnology and Oceanography*, *68*(1), 265-283.

Gibbs, M., Albert, A., Croker, G., Duggan, I., & Ovenden, R. (2014). *Waikato River Bioassay Study 2013-14 - Assessment of nutrient limitation* (NIWA Client Report HAM2014-072). H. National Institute of Water & Atmospheric Research Ltd, New Zealand, Hamilton, New Zealand.

Grainger, N. (2025). Lake Level Managment. In D. Özkundakci, Grainger, N., Dean-Speirs, T. (Ed.), *Hidden gems of the Waikato – the history, ecology and management of the Waikato lakes; Ō Tātou Roto - He Taonga Tuku Iho*. Waikato Regional Council and Te Tumu Whakaora Taiao – The Environmental Research Institute (The University of the Waikato). Hamilton, New Zealand.

Hipsey, M. R., Bruce, L. C., Boon, C., Busch, B., Carey, C. C., Hamilton, D. P., Hanson, P. C., Read, J. S., de Sousa, E., Weber, M., & Winslow, L. A. (2019). A General Lake Model (GLM 3.0) for linking with high-frequency sensor data from the Global Lake Ecological Observatory Network (GLEON). *Geoscientific Model Development*, *12*(1), 473-523.

Hodges, B., & Dallimore, C. (2013). *Estuary, Lake and Coastal Ocean Model: ELCOM v3. 0 Science Manual*.

Hodges, B., & Dallimore, C. (2018). *Aquatic Ecosystem Model: AEM3D. v1.0 User manual*. In Hydronumerics.

Hodges, B. R., Imberger, J., Saggio, A., & Winters, K. B. (2000). Modeling basin-scale internal waves in a stratified lake. *Limnology and Oceanography*, *45*(7), 1603–1620.

Hudson, J. J., Taylor, W. D., & Schlindler, D. W. (2000). Phosphate concentrations in lakes. *Nature*, *406*, 54–56.

Hughes, A. (2018). *Matahuru Stream water quality monitoring - data report*.

Koenings, J. P., & Edmundson, J. A. (1991). Secchi disk and photometer estimates of light regimes in Alaskan lakes: Effects of yellow color and turbidity. *Limnology and Oceanography*, *36*(1), 91-105.

Lawrence, L., & Ridley, G. (2018). *Lake Waikare and Whangamarino Wetland Catchment Management Plan: Part One - Catchment Background*.

León, L. F., Imberger, J., Smith, R. E. H., Hecky, R. E., Lam, D. C. L., & Schertzer, W. M. (2005). Modeling as a tool for nutrient management in Lake Erie: A hydrodynamics study. *Journal of Great Lakes Research*, *31*, 309–318.

Leonard, B. P. (1991). The ULTIMATE conservative difference scheme applied to unsteady one-dimensional advection. *Computer Methods in Applied Mechanics and Engineering*, *88*(1), 17-74.

Luo, L., Hamilton, D., & Han, B. (2010). Estimation of total cloud cover from solar radiation observations at Lake Rotorua, New Zealand. *Solar Energy*, *84*(3), 501-506.

McDowell, R. W., M., M. R., Chris, S., Andrew, M., Les, B., F., B. D., Seth, L., Peter, P., Raphael, S., & and Depree, C. (2021). Quantifying contaminant losses to water from pastoral land uses in New Zealand III. What could be achieved by 2035? *New Zealand Journal of Agricultural Research*, *64*(3), 390-410.

Monaghan, R., Andrew, M., Les, B., Chris, S., David, B., Esther, M., & and McDowell, R. (2021). Quantifying contaminant losses to water from pastoral landuses in New Zealand I. Development of a spatial framework for assessing losses at a farm scale. *New Zealand Journal of Agricultural Research*, *64*(3), 344-364.

Myers, D. R. (2012). *Bird Clear Sky Model*. https://www.nrel.gov/grid/solar-resource/clear-sky.html

Özkundakci, D., Hamilton, D. P., & Trolle, D. (2011). Modelling the response of a highly eutrophic lake to reductions in external and internal nutrient loading. *New Zealand Journal of Marine and Freshwater Research*, *45*(2), 165-185.

Pettyjohn, W. A., & Henning, R. (1979). *Preliminary estimate of ground-water recharge rates, related streamflow and water quality* (Ohio State University Water Resources Center Project Completion Report Number 552). O. S. U. Water Resources Center, Ohio, United States of America.

Prentice, M., & Özkundakci, D. (2024). *Ōhau Channel diversion wall: 7-year review — Water quality review and modelling* (ERI Report 169, a client report prepared for Bay of Plenty Regional Council). D. o. H. Environmental Research Institute – Te Tumu Whakaora Taiao, Engineering, Computing & Science, University of Waikato, Hamilton, New Zealand.

QGIS.org. (2023). *QGIS Geographic Information System*. In QGIS Association. http://www.qgis.org

Reeves, P., Craggs, R., Stephens, S., de Winton, M., & Davies-Colley, R. (2002). *Environmental Changes at Lake Waikare, North Waikato. Wave climate, water quality and 'biology'* (NIWA Client Report EVW02235). H. National Institute of Water & Atmospheric Research Ltd, New Zealand.

Romero, J. R., Antenucci, J. P., & Imberger, J. (2004). One- and three-dimensional biogeochemical simulations of two differing reservoirs [Article]. *Ecological Modelling*, *174*(1-2), 143-160.

Stott, P. (2016). How climate change affects extreme weather events. *Science*, *352*(6293), 1517-1518.

Vant, B., & Gibbs, M. (2006). *Nitrogen and Phosphorus in Taupō Rainfall* (Technical Report 2006/46). W. R. Council.

Verburg, P., Schallenberg, M., Elliott, S., & McBride, C. G. (2018). Lake Nutrient budgets. In D. P. Hamilton, K. J. Collier, J. M. Quinn, & C. Howard-Williams (Eds.), *Lake restoration handbook: A New Zealand perspective*. Springer.

Xiao, M., Burford, M. A., Prentice, M. J., Galvanese, E. F., Chuang, A., & Hamilton, D. P. (2023). Phosphorus storage and utilization strategies of two bloom-forming freshwater cyanobacteria. *Proceedings of the Royal Society B: Biological Sciences*, *290*(2003), 20231204.

Xiao, M., Hamilton, D. P., Chuang, A., & Burford, M. A. (2020). Intra-population strain variation in phosphorus storage strategies of the freshwater cyanobacterium Raphidiopsis raciborskii. *FEMS Microbiology Ecology*, *96*(6), fiaa092.

8 APPENDICES

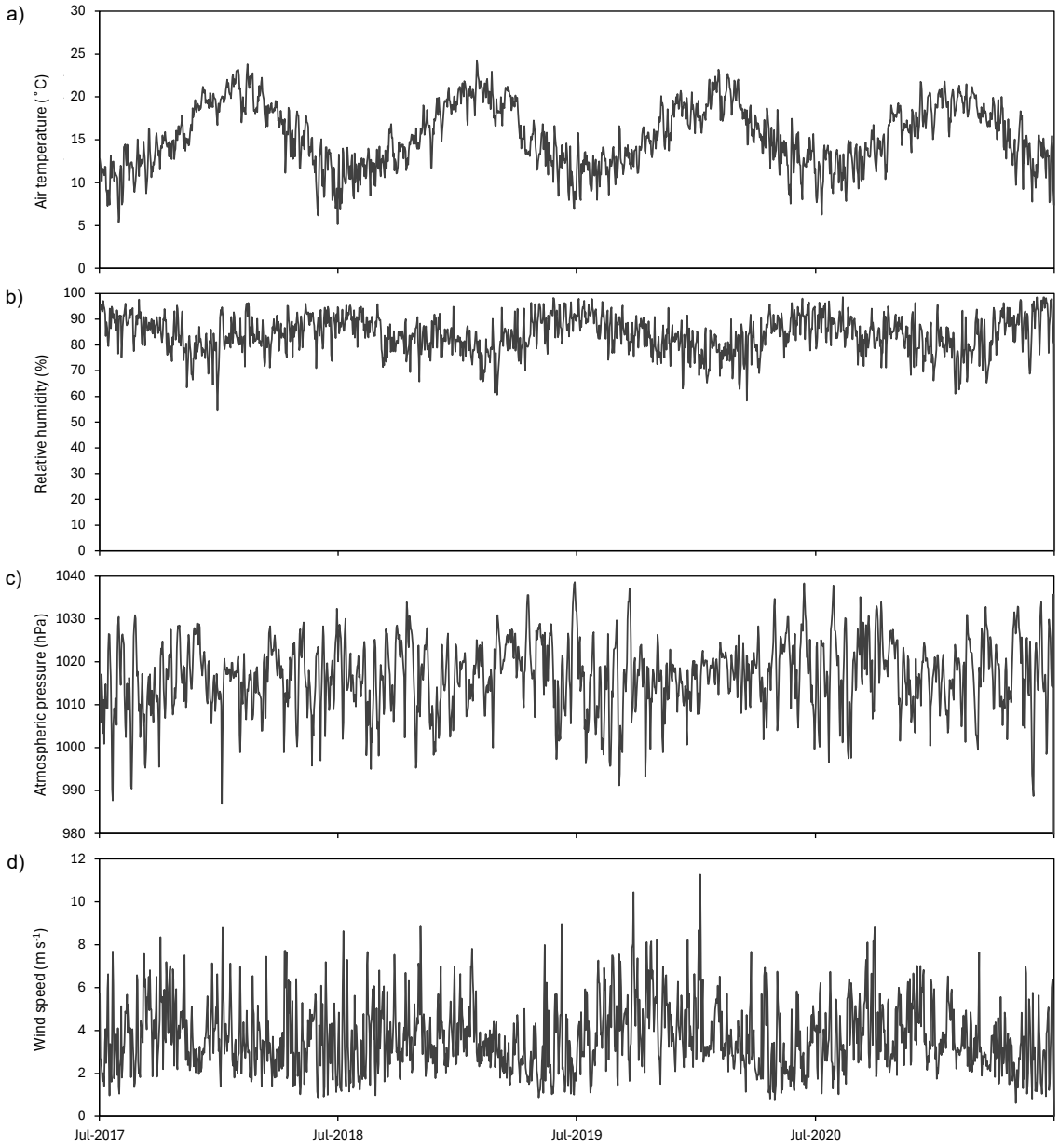

Appendix 1: Model meteorological data summaries as daily mean a) air temperature, b) relative humidity, c) atmospheric pressure, d) wind speed. N.b. Air temperature, relative humidity, and wind speed are presented as daily data but input in the model hourly.

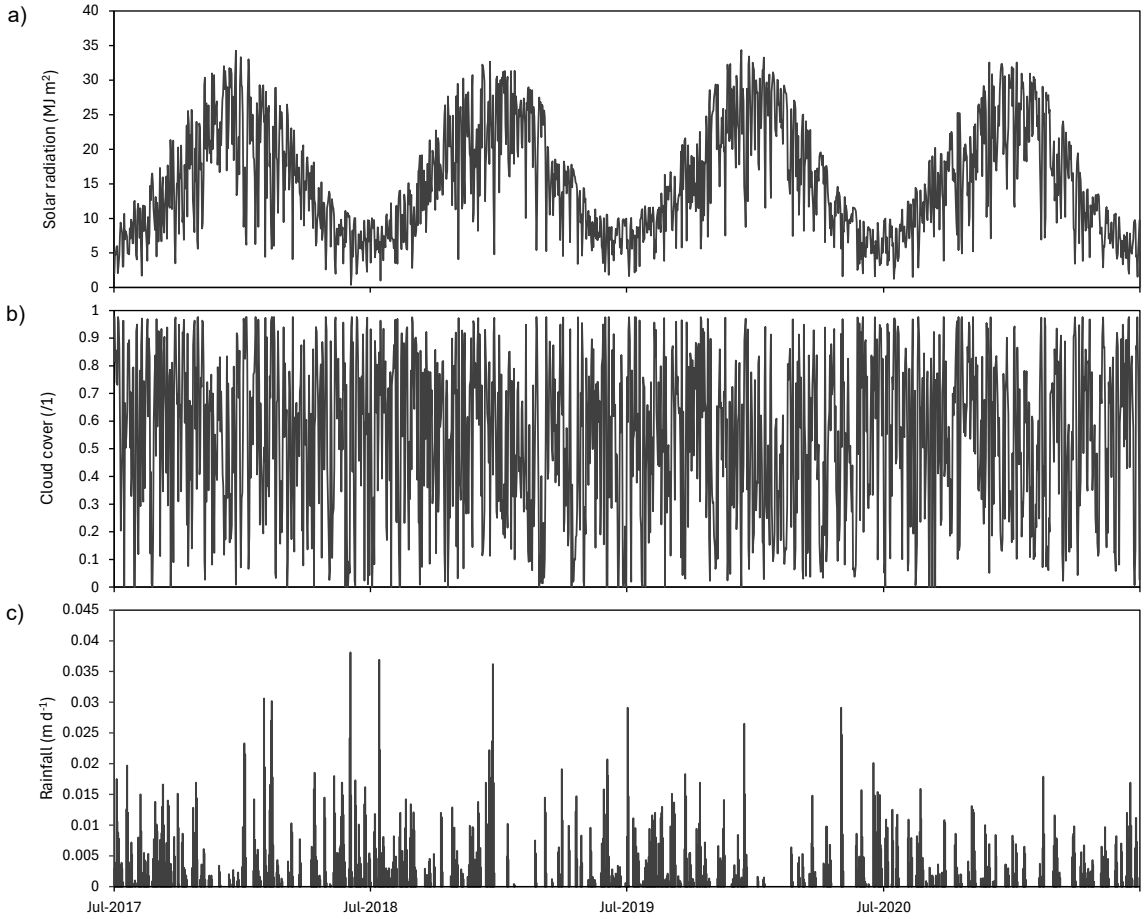

Appendix 2: Model meteorological data summaries as daily mean solar radiation, daily mean cloud cover, and daily total rainfall. N.b. Solar radiation is presented as daily data but input in the model hourly.

Appendix 3 Inflow and outflow discharge and water quality summaries, as mean values across the 4-year simulation period.

BC Number	BC Name	Discharge	Temp	DO	NH_4	NO_3	TN	PO_4	TP	ISS	Chl a
		($m^3 s^{-1}$)	(˚C)	($mg L^{-1}$)	($mg L^{-1}$)	($mg L^{-1}$)	($mg L^{-1}$)	($mg L^{-1}$)	($mg L^{-1}$)	($mg L^{-1}$)	($\mu g L^{-1}$)
201	Matahuru	1.37	15.4	8.4	0.08	0.75	1.64	0.02	0.19	115	0.0
202	Te Onetea	1.26	17.0	9.4	0.02	0.50	0.74	0.02	0.05	9	5.9
203	3010120	0.01	15.4	8.4	0.14	0.43	2.19	0.02	0.22	64	0.0
204	3010321	0.02	15.4	8.4	0.14	0.43	2.19	0.02	0.22	64	0.0
205	3010438	0.01	15.4	8.4	0.14	0.43	2.19	0.02	0.22	64	0.0
206	3010615	0.03	15.4	8.4	0.14	0.43	2.19	0.02	0.22	64	0.0
207	3010802	0.01	15.4	8.4	0.14	0.43	2.19	0.02	0.22	64	0.0
208	3010908 – Okekura	0.07	15.4	8.4	0.05	0.38	0.87	0.01	0.09	60	0.0
209	3011077 – Moana	0.04	15.4	8.4	0.07	0.46	1.28	0.02	0.16	41	0.0
210	3011172	0.02	15.4	8.4	0.14	0.43	2.19	0.02	0.22	64	0.0
211	3011273	0.01	15.4	8.4	0.14	0.43	2.19	0.02	0.22	64	0.0
212	3011253	0.01	15.4	8.4	0.14	0.43	2.19	0.02	0.22	64	0.0
213	3010901	0.09	15.4	8.4	0.14	0.43	2.19	0.02	0.22	64	0.0
214	3011044	0.01	15.4	8.4	0.14	0.43	2.19	0.02	0.22	64	0.0
215	3011196	0.03	15.4	8.4	0.14	0.43	2.19	0.02	0.22	64	0.0
216	3011366 – Papaatawai	0.15	15.4	8.4	0.55	0.62	3.41	0.43	1.35	68	0.0
217	3011366 – Ohinewai	0.11	15.4	8.4	0.23	0.35	2.79	0.01	0.24	59	0.0
218	3011365	0.04	15.4	8.4	0.14	0.43	2.19	0.02	0.22	64	0.0
219	3010718	0.03	15.4	8.4	0.14	0.43	2.19	0.02	0.22	64	0.0
220	3010795	0.03	15.4	8.4	0.14	0.43	2.19	0.02	0.22	64	0.0
221	3010771	0.02	15.4	8.4	0.14	0.43	2.19	0.02	0.22	64	0.0
222	3010437 – Whites	0.06	15.4	8.4	0.21	0.02	2.75	0.04	0.57	88	0.0
223	3010422	0.02	15.4	8.4	0.14	0.43	2.19	0.02	0.22	64	0.0
224	3010167	0.03	15.4	8.4	0.14	0.43	2.19	0.02	0.22	64	0.0
225	3010017	0.01	15.4	8.4	0.14	0.43	2.19	0.02	0.22	64	0.0
226	3010113	0.03	15.4	8.4	0.14	0.43	2.19	0.02	0.22	64	0.0
227	Te Kauwhata WWTP	0.01	17.0	9.4	17.43	0.00	17.43	4.57	4.57	18	0.0
228	Residual	-0.30	N/A	N/A	N/A	N/A	N/A	N/A	N/A	N/A	N/A
101	Northern Outlet Control Gate	2.98	N/A	N/A	N/A	N/A	N/A	N/A	N/A	N/A	N/A
102	Fish Pass Culvert	0.30	N/A	N/A	N/A	N/A	N/A	N/A	N/A	N/A	N/A

Appendix 4 Summary of minor flows, including NZReach information and model specific information. N.b. Scaled area relates to the area associated with the specific inflow scaled to include the sub-catchments (i.e., those with areas < 0.5% of Matahuru) not explicitly included in the model.

NZReach			Waikare model				
Number	Area (m^2)	Faction cf. Matahuru	BC Number	BC Name	Area (m^2)	Scaled area (m^2)	Faction cf. Matahuru
3010120	592,200	0.0056	203	3010120	592,200	679,952	0.0064
3010321	1,132,200	0.0106	204	3010321	1,132,200	1,299,970	0.0122
3010438	728,100	0.0068	205	3010438	728,100	835,990	0.0079
3010615	1,884,600	0.0177	206	3010615	1,884,600	2,163,860	0.0204
3010802	536,400	0.0050	207	3010802	536,400	615,884	0.0058
3010908	5,011,200	0.0471	208	3010908_Okekura	5,011,200	5,753,761	0.0541
3011077	2,783,700	0.0262	209	3011077_Moana	2,783,700	3,196,189	0.0301
3011172	1,287,000	0.0121	210	3011172	1,287,000	1,477,708	0.0139
3011273	589,500	0.0055	211	3011273	589,500	676,852	0.0064
3011253	544,500	0.0051	212	3011253	544,500	625,184	0.0059
3010901	5,769,900	0.0543	213	3010901	5,769,900	6,624,885	0.0623
3011044	766,800	0.0072	214	3011044	766,800	880,425	0.0083
3011196	2,130,300	0.0200	215	3011196	2,130,300	2,445,968	0.0230
3011366	18,059,400	0.1699	216	3011366_Papaatawai	10,348,871	11,882,369	0.1118
N/A	N/A	N/A	217	3011366_Ohinewai	7,710,529	8,853,076	0.0833
3011365	2,832,300	0.0266	218	3011365	2,832,300	3,251,991	0.0306
3010718	1,935,900	0.0182	219	3010718	1,935,900	2,222,762	0.0209
3010795	1,747,800	0.0164	220	3010795	1,747,800	2,006,789	0.0189
3010771	1,305,000	0.0123	221	3010771	1,305,000	1,498,375	0.0141
3010655	1,546,200	0.0145	N/A	N/A	N/A	N/A	N/A
3010437	3,861,900	0.0363	222	3010437_Whites	3,861,900	4,434,157	0.0417
3010422	1,472,400	0.0138	223	3010422	1,472,400	1,690,581	0.0159
3010167	2,029,500	0.0191	224	3010167	2,029,500	2,330,232	0.0219
3010017	676,800	0.0064	225	3010017	676,800	777,088	0.0073
3010113	1,701,900	0.0160	226	3010113	1,701,900	1,954,088	0.0184

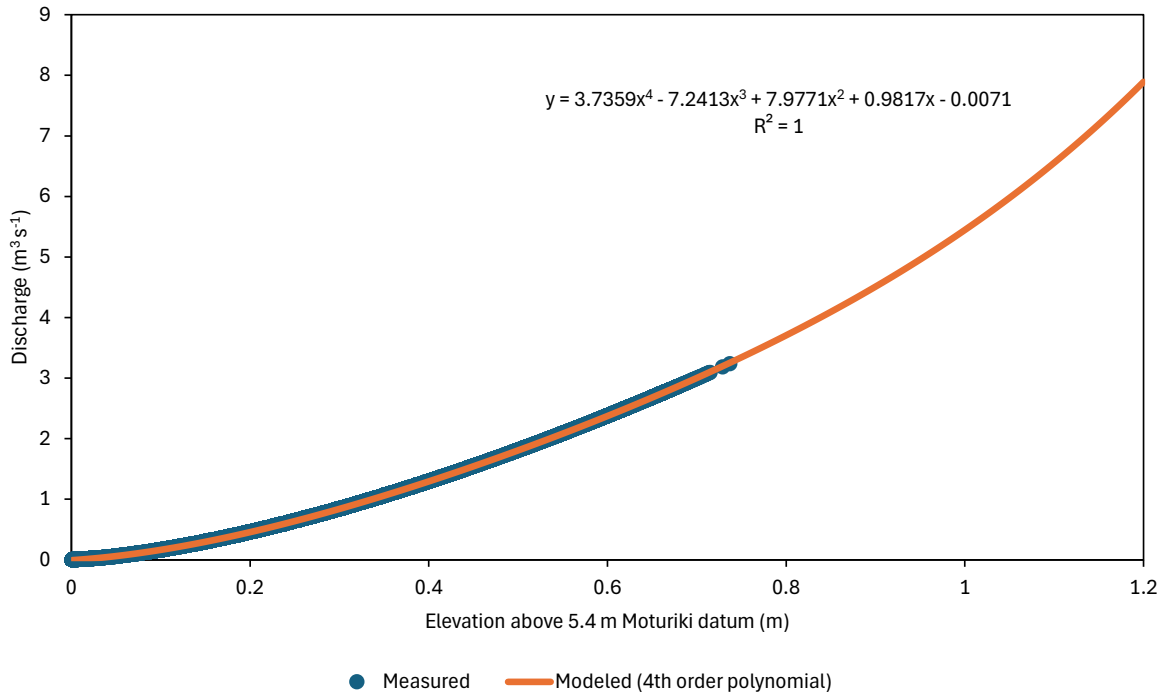

Appendix 5: Fish pass outflow, as measured and modelled (4th order polynomial).

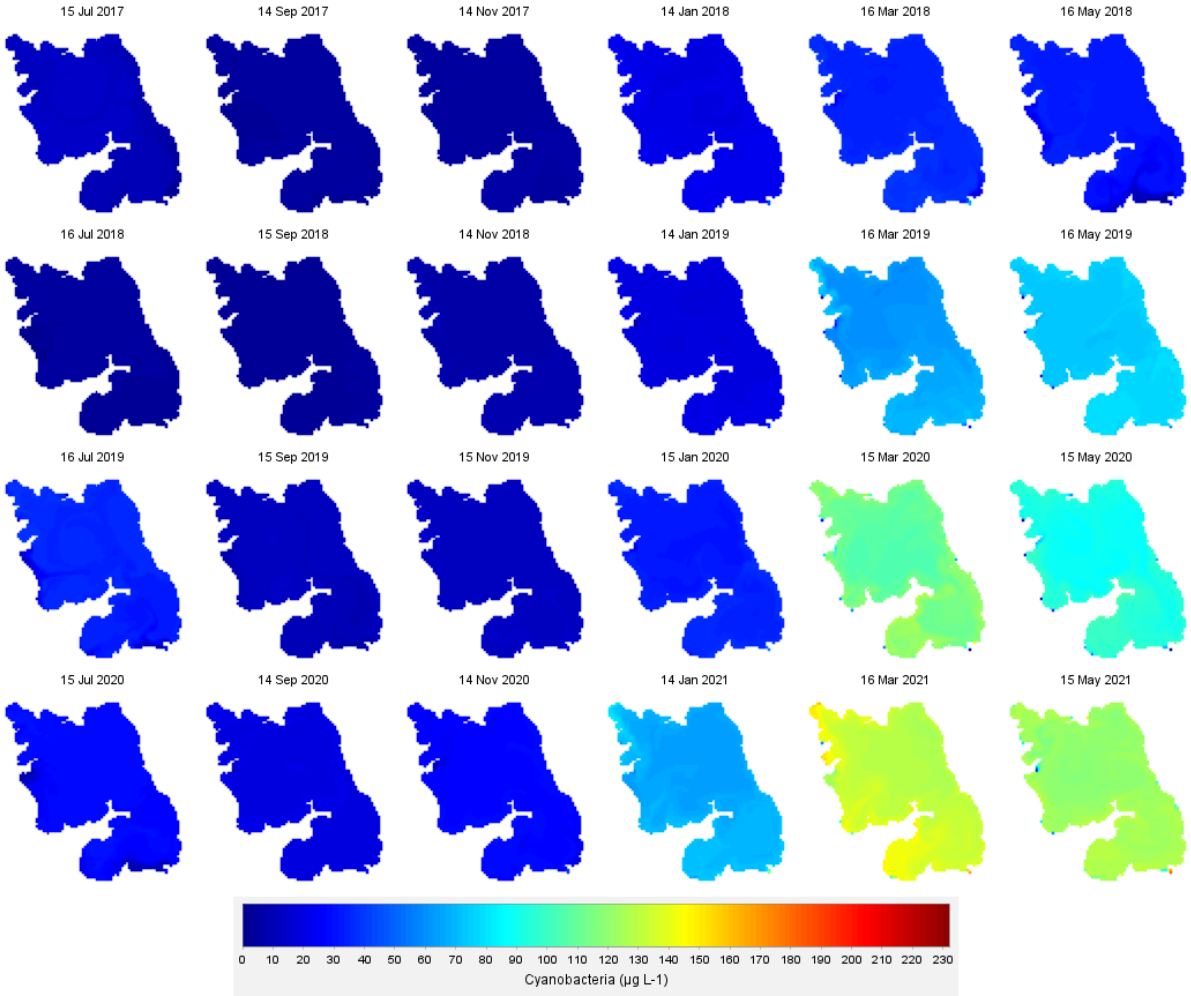

Appendix 6: Modelled surface water (0.1 m below surface) cyanobacteria (µg L^{-1} Chl *a*), during the calibration and validation periods. Calibration period 1 July 2017 through 30 June 2019, validation 1 July 2019 through 30 June 2021. Daily output was extracted at 23:58 on the given day.

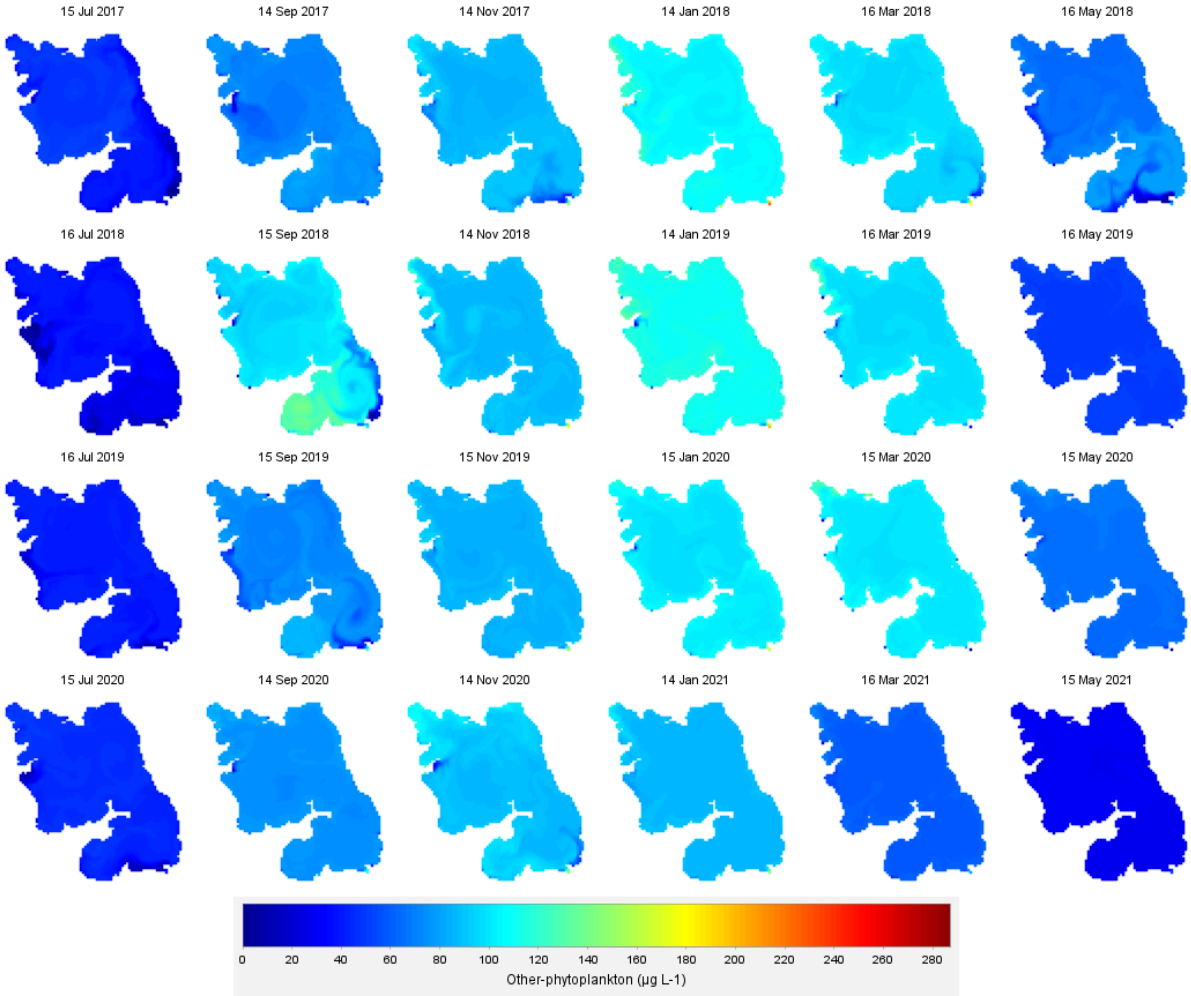

Appendix 7: Modelled surface water (0.1 m below surface) other-phytoplankton (µg L^{-1} Chl *a*), during the calibration and validation periods. Calibration period 1 July 2017 through 30 June 2019, validation 1 July 2019 through 30 June 2021. Daily output was extracted at 23:58 on the given day.

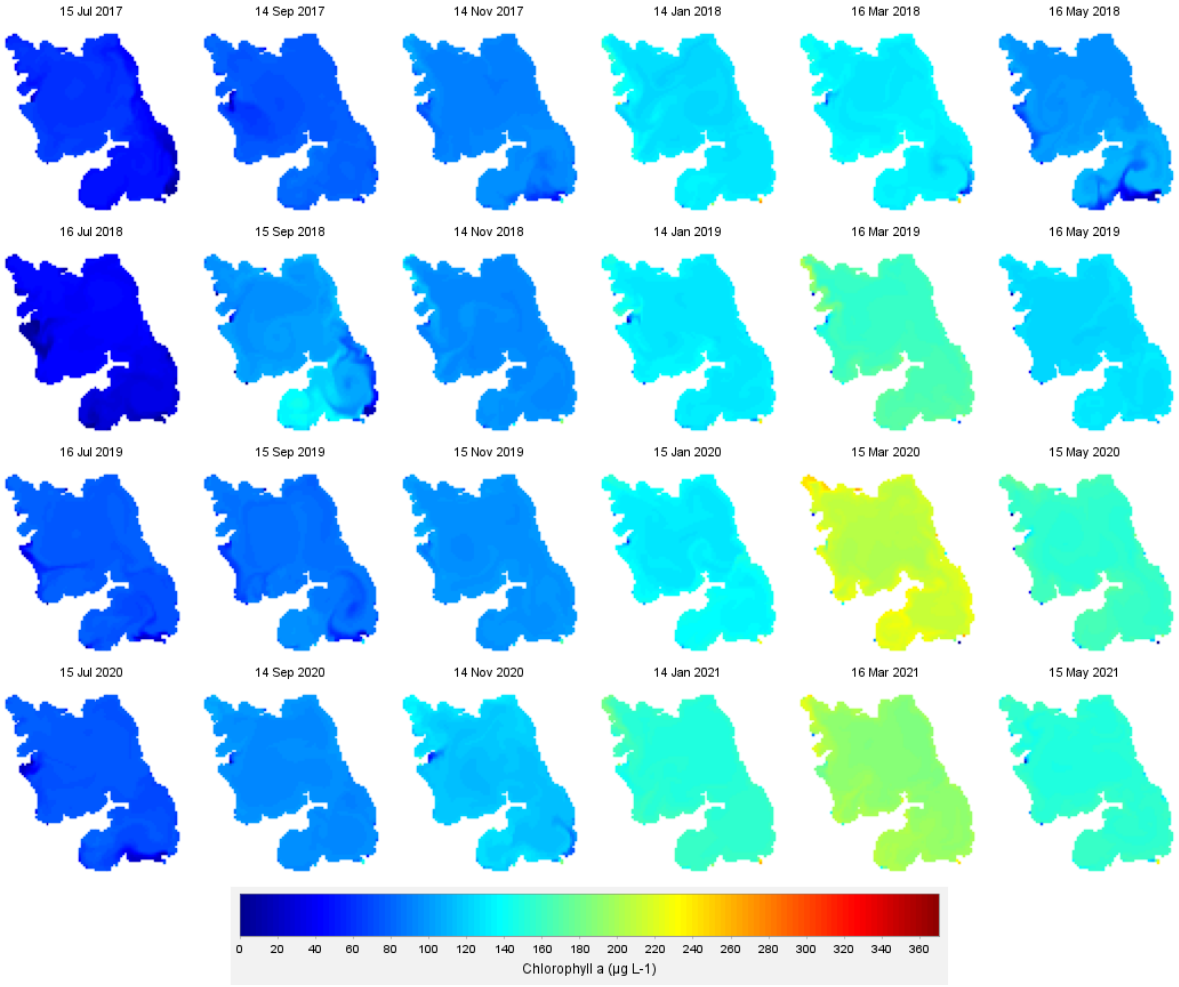

Appendix 8: Modelled surface water (0.1 m below surface) chlorophyll *a* (µg L^{-1}), during the calibration and validation periods. Calibration period 1 July 2017 through 30 June 2019, validation 1 July 2019 through 30 June 2021. Daily output was extracted at 23:58 on the given day.

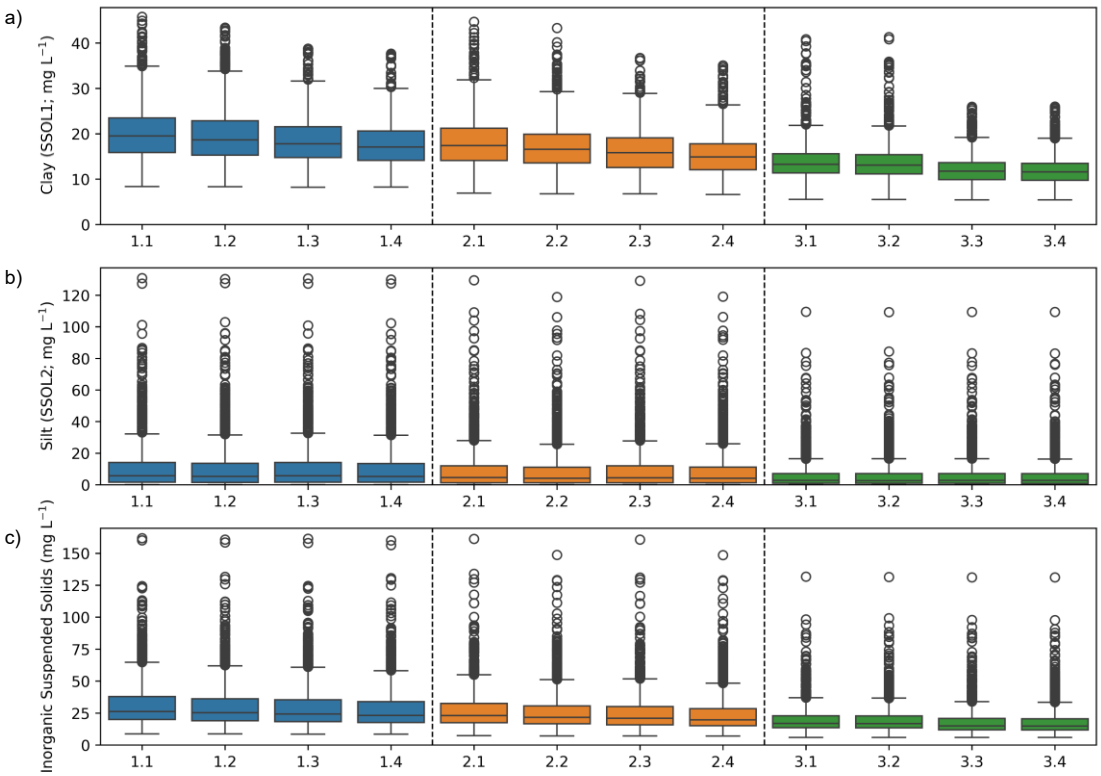

Min & Max WL increase	Current	Current	Current	Current	0 & 1 m	0 & 1 m	0 & 1 m	0 & 1 m	1 & 1 m	1 & 1 m	1 & 1 m	1 & 1 m
Catchment loading	Current	Current	Reduced	Reduced	Current	Current	Reduced	Reduced	Current	Current	Reduced	Reduced
Te Onetea inflow rate	Average	Maximum	Average	Maximum	Average	Maximum	Average	Maximum	Average	Maximum	Average	Maximum

Appendix 9: Simulated a) Clay (SSOL1), b) Silt (SSOL2), and c) Inorganic Suspended Solids, as box plots of daily mean values across the simulation period of four limnological years (1 July 2017 through 30 June 2021) for the twelve scenarios as described in the table below panel 'c'. The box represents the interquartile range (IQR), spanning from the first quartile (Q1) to the third quartile (Q3), with the line within the box denoting the median value. The whiskers extend from the quartiles to the minimum and maximum values that lie within 1.5 times the IQR. N.b. variable vertical scale.

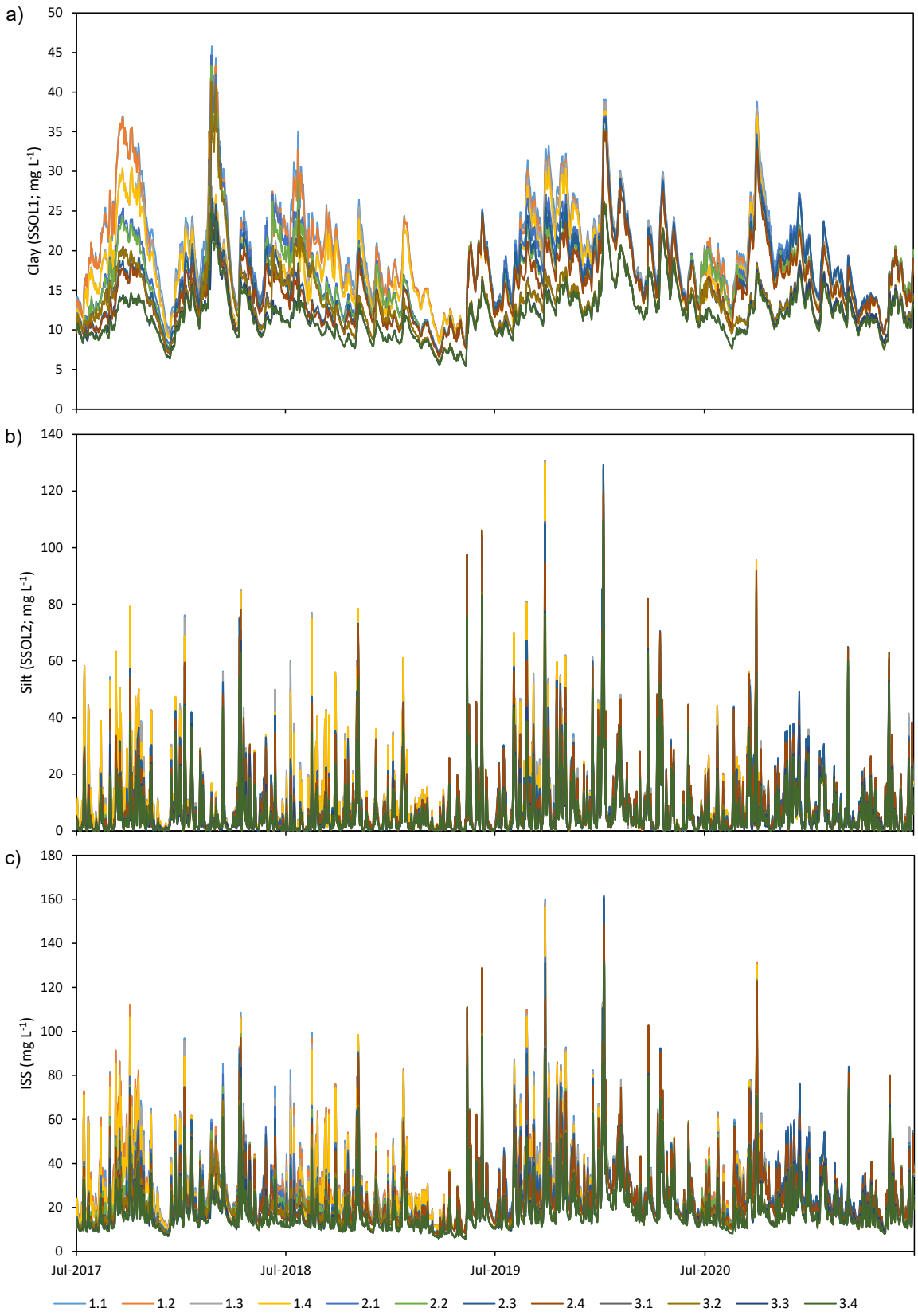

Appendix 10: Simulated a) Clay (SSOL1), b) Silt (SSOL2), and c) Inorganic Suspended Solids, as a time series of daily mean values across the simulation period of four limnological years (1 July 2017 through 30 June 2021) for the twelve scenarios.

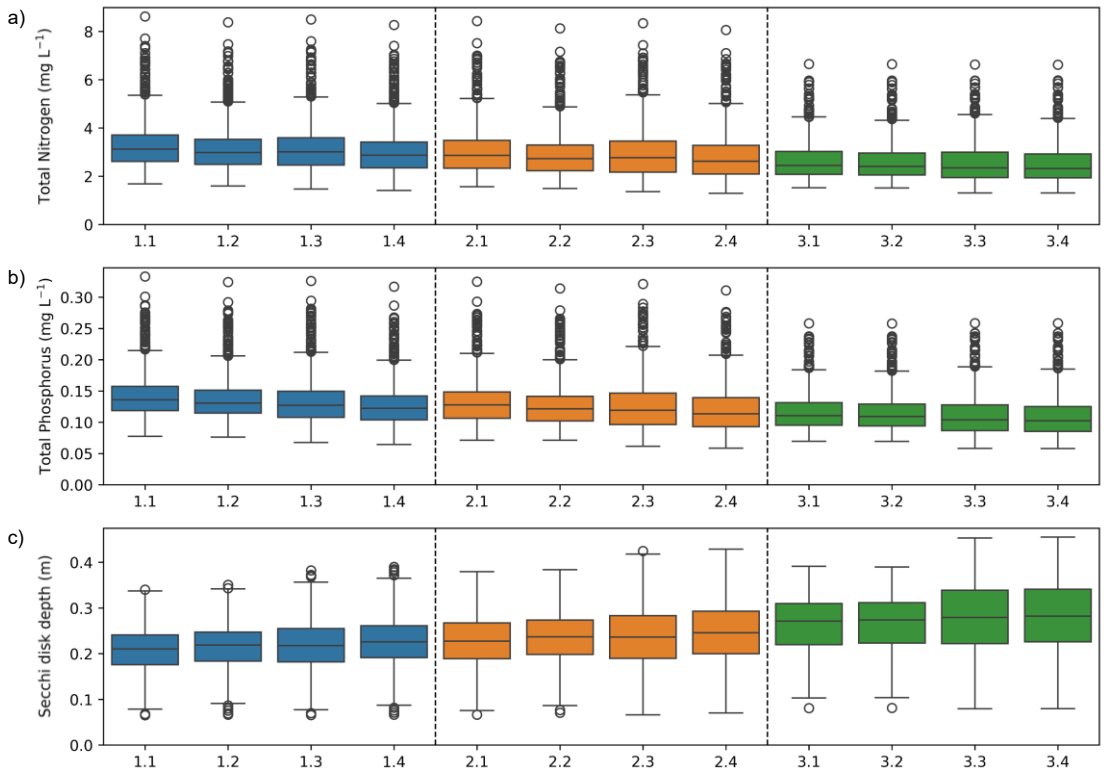

Min & Max WL increase	Current	Current	Current	Current	0 & 1 m	0 & 1 m	0 & 1 m	0 & 1 m	1 & 1 m	1 & 1 m	1 & 1 m	1 & 1 m
Catchment loading	Current	Current	Reduced	Reduced	Current	Current	Reduced	Reduced	Current	Current	Reduced	Reduced
Te Onetea inflow rate	Average	Maximum	Average	Maximum	Average	Maximum	Average	Maximum	Average	Maximum	Average	Maximum

Appendix 11: Simulated a) total nitrogen, b) total phosphorus, and c) Secchi disk depth, as box plots of daily mean values across the simulation period of four limnological years (1 July 2017 through 30 June 2021) for the twelve scenarios as described in the table below panel 'c'. The box represents the interquartile range (IQR), spanning from the first quartile (Q1) to the third quartile (Q3), with the line within the box denoting the median value. The whiskers extend from the quartiles to the minimum and maximum values that lie within 1.5 times the IQR. N.b. variable vertical scale.

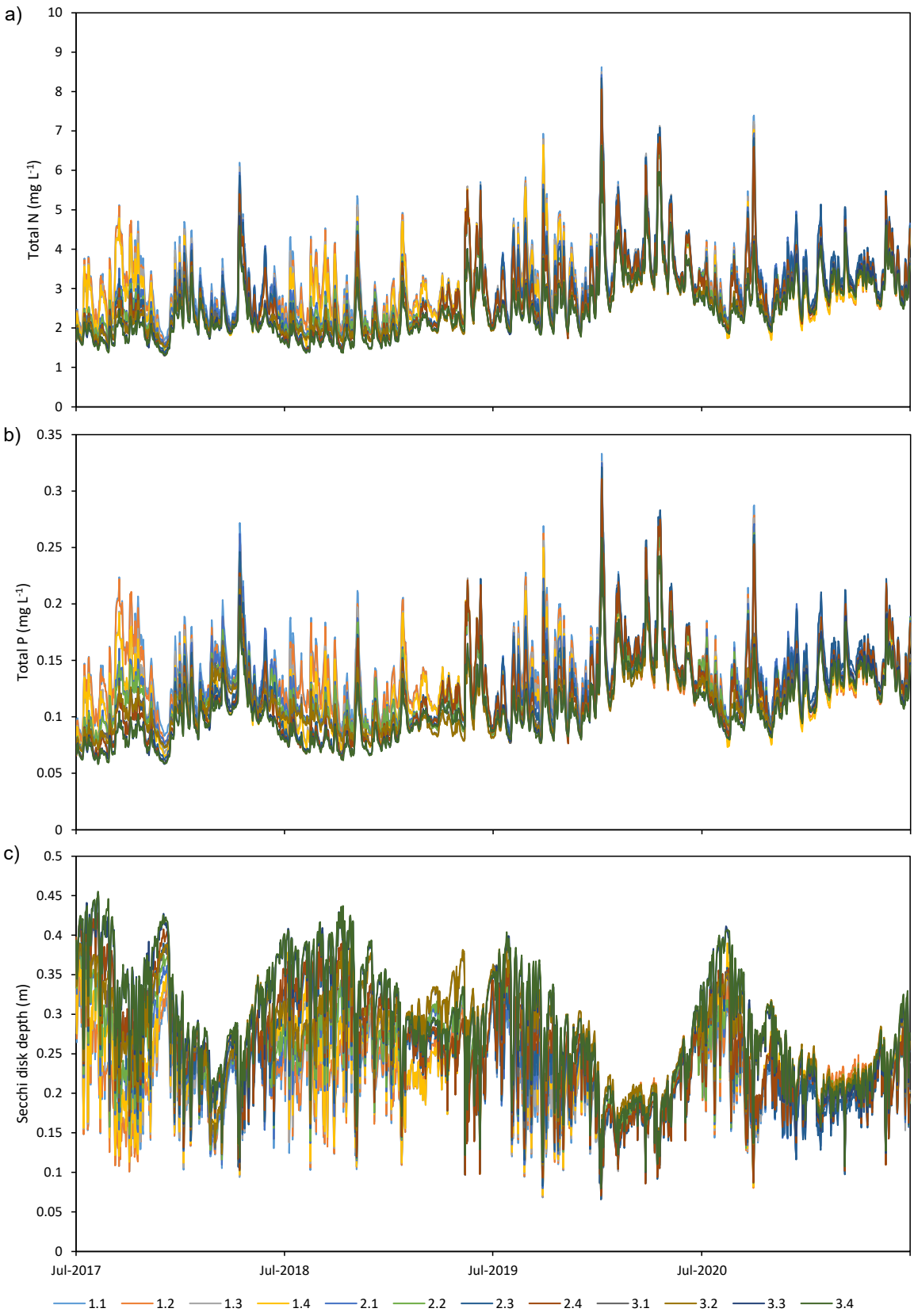

Appendix 12: Simulated a) total nitrogen, b) total phosphorus, and c) Secchi disk depth, as a time series of daily mean values across the simulation period of four limnological years (1 July 2017 through 30 June 2021) for the twelve scenarios.

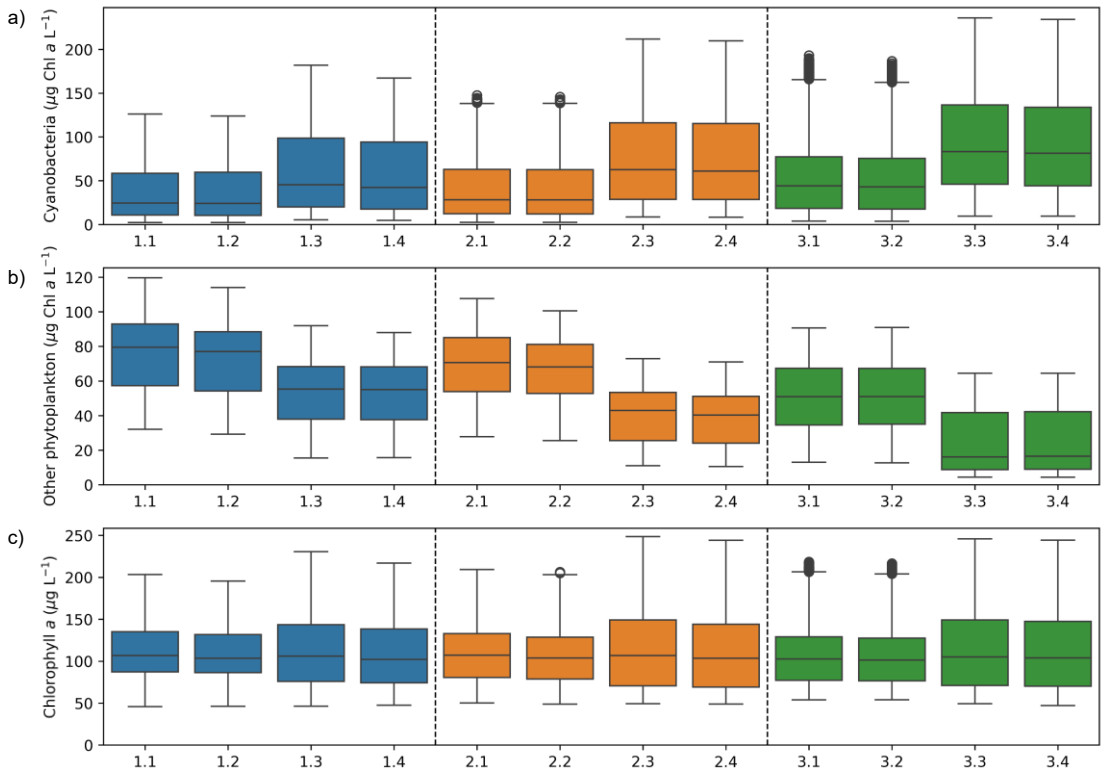

Min & Max WL increase	Current	Current	Current	Current	0 & 1 m	0 & 1 m	0 & 1 m	0 & 1 m	1 & 1 m	1 & 1 m	1 & 1 m	1 & 1 m
Catchment loading	Current	Current	Reduced	Reduced	Current	Current	Reduced	Reduced	Current	Current	Reduced	Reduced
Te Onetea inflow rate	Average	Maximum	Average	Maximum	Average	Maximum	Average	Maximum	Average	Maximum	Average	Maximum

Appendix 13: Simulated a) cyanobacteria, b) other-phytoplankton, and c) chlorophyll *a*, as box plots of daily mean values across the simulation period of 4 limnological years (1 July 2017 through 30 June 2021) for the twelve scenarios as described in the table below panel 'c'. The box represents the interquartile range (IQR), spanning from the first quartile (Q1) to the third quartile (Q3), with the line within the box denoting the median value. The whiskers extend from the quartiles to the minimum and maximum values that lie within 1.5 times the IQR. N.b. variable vertical scale.

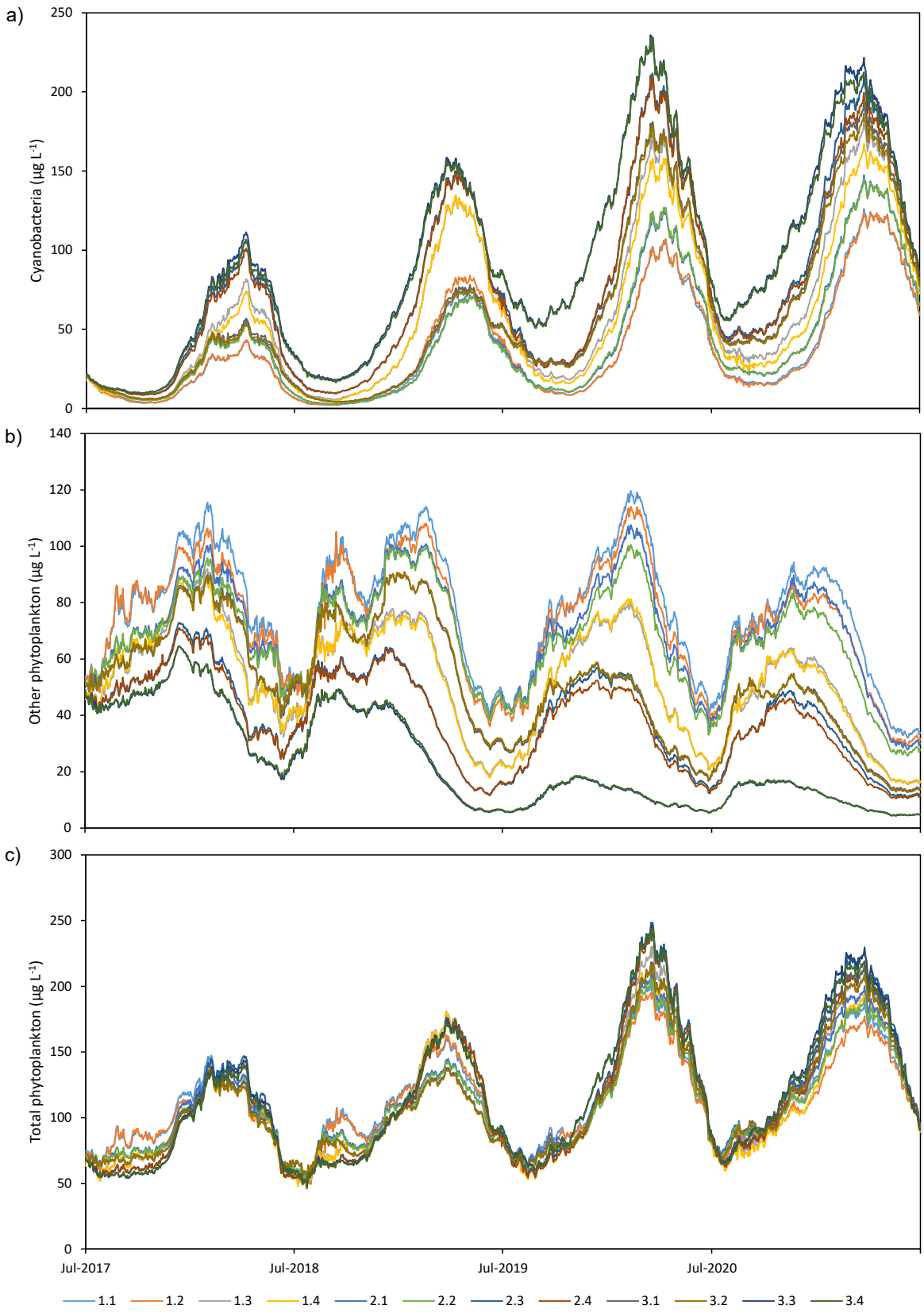

Appendix 14: Simulated a) cyanobacteria, b) other-phytoplankton, and c) chlorophyll *a*, as a time series of daily mean values across the simulation period of four limnological years (1 July 2017 through 30 June 2021) for the twelve scenarios.

Appendix 15 Nutrient budget for Lake Waikare across 10 hydrological years from 2013-14 through 2022-23.

	TP (T year^{-1})		TN (T year^{-1})	
	Mean	Standard deviation	Mean	Standard deviation
Matahuru inflow	10.3	6.1	112.0	53.4
Te Onetea inflow	2.0	1.1	35.8	21.4
Te Kauwhata WWTP inflow	1.5	0.1	5.8	0.8
Ungauged catchment inflows	14.5	8.6	103.3	49.3
Atmospheric deposition	1.2	0.3	22.0	6.0
Total	29.5	15.4	278.8	114.3